Modeling the Impacts of Climate and Land Use Land Cover change on Streamflow and Sediment Yield, and Developing Best Management Practices in the Upper Awash Sub-basin, Ethiopia

Getahun Belachew Bula

A thesis Submitted to the Department of Water Resources Engineering

School of Civil Engineering and Architecture

Presented in Partial Fulfillment of the Requirement for the Degree of Master's in Water Resources Engineering (Specialization in Hydrology and Water Resource Management)

Office of Graduate Studies

Adama Science and Technology University

March, 2023

Adama, Ethiopia

Modeling the Impacts of Climate and Land Use Land Cover change on Streamflow and Sediment Yield, and Developing Best Management Practices in the Upper Awash Sub-basin, Ethiopia

Getahun Belachew Bula

Advisor: Abdulkerim B. Serur (PhD)

A thesis Submitted to the Department of Water Resources Engineering

School of Civil Engineering and Architecture

Presented in Partial Fulfillment of the Requirement for the Degree of Master's in Water Resources Engineering (Specialization in Hydrology and Water Resource Management)

Office of Graduate Studies

Adama Science and Technology University

March, 2023

Adama, Ethiopia

DECLARATION

I declare that this Master's thesis entitled "Modeling the Impacts of Climate and Land Use Land Cover change on Streamflow and Sediment Yield, and Developing Best Management Practices in the Upper Awash Sub-basin, Ethiopia" is my original work. That is, it has not been submitted for the award of any academic degree, diploma or certificate in any other university. All sources of materials that are used for this thesis have been duly acknowledged through citation

Getahun Belachew Bula___	________________________	________________
Name of student	Signature	Date

RECOMMENDATION OF THE ADVISOR

I, the advisor of this thesis, hereby certify that I have read the revised version of the thesis entitled "Modeling the Impacts of Climate and Land Use Land Cover change on Streamflow and Sediment Yield, and Developing Best Management Practices in the Upper Awash Sub-basin, Ethiopia**"** prepared under my guidance by Getahun Belachew Bula submitted in partial fulfillment of the requirements for the degree of Mater's of Science in Water Resources Engineering (Specialization in Hydrology and Water Resource Management). Therefore, I recommend the submission of revised version of the thesis to the department following the applicable procedures.

Abdulkerim B. Serur (PhD)	___________________	_______________________
Major Advisor	Signature	Date

APPROVAL PAGE OF THE M.Sc. THESIS

I, the advisor of the thesis entitled "Modeling the Impacts of Climate and Land Use Land Cover change on Streamflow and Sediment Yield, and Developing Best Management Practices in the Upper Awash Sub-basin, Ethiopia" and developed by Getahun Belachew Bula hereby certify that the recommendation and suggestions made by the board of examiners are appropriately incorporated into the final version of the thesis.

Abdulkerim B. Serur (PhD) ____________________ ____________________

Major Advisor Signature Date

We, the undersigned, members of the Board of Examiners of the thesis by Getahun Belachew Bula have read and evaluated the thesis entitled "Modeling the Impacts of Climate and Land Use Land Cover change on Streamflow and Sediment Yield, and Developing Best Management Practices in the Upper Awash Sub-basin, Ethiopia" and examined the candidate during open defense. This is, therefore, to certify that the thesis is accepted for partial fulfillment of the requirements of the degree of Master of Science in Water Resources Engineering (Specialization in Hydrology and Water Resource Management).

Mesfin Benti (PhD) ____________________ ____________________

Chairperson Signature Date

Mekonen Ayana (PhD) ____________________ ____________________

Internal Examiner Signature Date

Kassa Tadele (Dr.Ing) ____________________ ____________________

External Examiner Signature Date

Final approval and acceptance of the thesis is contingent upon submission of its final copy to the Office of Postgraduate Studies (OPGS) through the Department Graduate Council (DGC) and School Graduate Committee (SGC).

____________________ ____________________ ____________________

Department Head Signature Date

____________________ ____________________ ____________________

School Dean Signature Date

____________________ ____________________ ____________________

Office of Postgraduate Studies, Dean Signature Date

ACKNOWLEDGMENTS

First and foremost, I would like to thank the Almighty God for his priceless mercy throughout my life and for providing the capability to accomplish this study.

Next, I would like to express my sincere gratitude to my adviser Abdulkerim B. Serur (PhD) for his continuous guidance, constructive feedbacks, critical comments and encouragement throughout this work. Besides his valuable advice academically, I learned from him the value of responsibility, punctuality and commitments have for the success of any type of work on time.

I am very grateful to Adama Science and Technology University, Department of Water Resources Engineering for Providing sufficient computer class and Internet access throughout my research work.

I would also like to thank the National Metrological Institute of Ethiopia (NMI) and the Ministry of Water, and Energy (MoWE) for their support in providing necessary data.

Last but not least, my deep thanks go to my father and mother who did their best to bring me up and allow me to be educated, without being educated themselves.

Finally, yet importantly, my thanks go to my friends Gutema Genene, Nebiyu Waliyi, and Israel G/Selassie who helped me in one way or another during the study.

TABLE OF CONTENTS

LIST OF TABLES

LIST OF FIGURES

LIST OF TABLES IN APPENDIX

LIST OF FIGURES IN APPENDEX

LIST OF ACRONYMS AND ABBREVIATIONS

BMPs	Best Management Practices
CN	Curve Number
CORDAID	Catholic Organization for Relief and Development Aid
DEM	Digital Elevation Model
FAO	Food and Agricultural Organization
GHGs	Greenhouse Gases
IGBP	International Geosphere-Biosphere Programme
IPCC	Intergovernmental Panel on Climate Change
ITCZ	Inter Tropical Convergence Zone
LULC	Land Use/ Land Cover
MoWE	Ministry of Water and Energy of Ethiopia
NMI	National Meteorology Institute of Ethiopia
NSE	Nash Sutcliffe efficiency
PBIAS	Percent of Bias
PET	Potential Evapotranspiration
RACMO	Regional Atmospheric climate model
RCM	Regional Climate Model
RCP	Representative Concentration Pathway
SCS	Soil Conservation Service
SRTM	Shuttle Radar Topography Mission
SWAT	Soil and Water Assessment Tool
UNFCCC	United Nations Framework Convention on Climate Change
USDA-ARS	US Department of Agriculture Research Service
WMO	World Health Organization
WXGEN	Weather Generator

ABSTRACT

Climate change and land cover change, as well as its consequences on water resources, have been hot topics in recent years. Understanding the impact of climate change and land use/land cover (LULC) has become a top priority for Awash Basin water management and resources utilization. In this study, SWAT is used to assess the impacts of climate and land use land cover changes on Streamflow and Sediment yield, and the development of best management practices(BMPs) in the Upper Awash Sub-Basin (UASB), Ethiopia. CORDEX-Africa RAMO22T (EC-EARTH) data outputs for UASB were chosen under the representative concentration pathways (RCP4.5) scenario to make mid-term rainfall and temperature projections (2041-2070). The LULC change analyses for three periods (1990, 2005, and 2020) were performed using ERDAS Imagine 2015 with a maximum likelihood classifier. Based on the result obtained (1990-2020), significantly increasing rates were observed in urban/settlement (3.5%), and agriculture (17.8%) and a decreasing rate were observed in forest (3.1%), grassland (9.7%), and shrubland (8,6%). The simulation was done by dividing the watershed into 27 sub watersheds and by assigning a hydrological response unit based on multiple HRU definition. The model performance in simulating streamflow and sediment yield was evaluated through sensitivity analysis, calibration, and validation processes. The results of the model calibration (2002-2006) and validation (2007-2010) showed reliable estimates of monthly streamflow and sediment yield with R^2 = 0.83 &0.85, ENS= 0.78 &0.81 and PBIAS=11.35 &14.1 during the calibration period and R^2=0.77 &0.8, ENS=0.73 &0.78 and PBIAS=8.9 & 12.5 during the validation period respectively. Streamflow increased by 4.8% under LULC change and decreased by 1.26% under the impacts of climate change. The change in sediment was 12.64% under LULC change and 3.28% under the climate change effect. The LULC change had a greater contribution to changes in sediment yield than climate change. Both streamflow and sediment yield increased under combined impacts, with 4.6% for streamflow and 15.54% for sediment yield. During 1989–2019, the combined impacts of climate and LULC played a more important role in alterations of streamflow and sediment than individual impacts. Simulation of sediment yield established nine sub-basins that yielded higher sediments. They were sub-basin ,9,12, 13, 14, 18, 20, 21, 22, and 27. Hence, three BMPs namely filter strips, terracing and reforestation were developed for critical sub-watersheds to reduce the sediment yield and filter strip 5 m wide is the most effective for reducing sediment yield in Upper Awash Sub-basin. The findings of this study, in particular, will provide valuable information for planning and designing sustainable water management approaches that reduce the impact of droughts, floods, and sedimentation in Upper Awash Sub-basin.

Keywords: *Arc SWAT, LULC, Upper Awash Sub-basin, Climate change, Stream flow, Sediment yield, BMPs*

1. INTRODUCTION

1.1 Background

Our world is made up of a range of complex systems that interact on a variety of spatial and temporal scales, with natural and human influences deeply linked. The close link between land use, water, and climate in these systems has sparked widespread worry about the planet's underlying traits and processes (Ding et al., 2018).

Water resource planning and management require an understanding of the hydrologic response of watersheds to physical (land use) and climatic (rainfall and air temperature) change (Vörösmarty et al., 2000). Land cover and climate change have a significant impact on a basin's hydrologic responses. However, depending on the nature and intensity of the changes as well as basin features, responses differ from basin to basin. Furthermore, the cumulative effects of the alterations have an offsetting or synergistic effect on a basin's hydrologic responses (Kabite et al., 2020). The hydrologic cycle is affected by climate and land-use change via changing hydrological responses such as streamflow, surface runoff, base-flow, and evapotranspiration (Teklay et al., 2021). Anthropogenic interferences in the form of land use/land cover change alter the balance between rainfall, evaporation, and runoff response in a watershed, modifying hydrological processes. This means that understanding the effects of LULC and climate change on river flow and soil erosion is critical for effective and long-term monitoring and planning of land resources. Land use and land cover (LULC) dynamics in general, and the conversion of natural vegetation cover to cultivated land in particular, are major human-induced concerns in Ethiopia that have contributed to increased soil erosion and altered the country's hydrological balance (Negese, 2021).

In recent decades, climate change has an impact on natural and human systems on all continents and throughout oceans. Impacts are a result of climate change that has been observed, regardless of its source, indicating the vulnerability of natural and human systems to climate change (Meyer et al., 2014). Global population growth and demand, as well as climate change, are putting pressure on water resources. Ethiopia's precipitation patterns, rainfall variability, and temperature will be affected by climate change, thereby increasing the frequency and severity of floods and droughts. The supply of clean drinking water is likely to diminish as a result of increasing evaporation and increased variability in rainfall events. Quantitative evaluation of land use land cover change and climate change's hydrological consequences at the watershed scale will aid in comprehending the possible water resource problem, better planning, decisions, and the development of appropriate water management methods (Simane et al., 2016).

The lack of suitable soil conservation measures and poor land use management are two of the most serious risks to sustainable agriculture and watershed management around the world. Best management practices (BMPs) approaches are cost-effective ways to improve basin health and agricultural land productivity while reducing environmental impact (Uniyal et al., 2020). Agricultural and structural-based BMPs are commonly used for reducing soil loss within the critical sediment parts of the watershed. To minimize substantial erosion from the upper catchment and limit sediment delivery, (BMPs) must be implemented.

For many years, hydrological models have been a useful tool in water resource management, and they are typically used to predict the effects of projected land use/land cover and climate change scenarios, as well as to assess management techniques (Legesse et al., 2010). A process-based hydrological model can be used to explore the combined effects of land cover and climate change on hydrological processes (Zhou et al., 2013). The best possibilities for integrated modeling method are hydrological models (Soil and Water Assessment Tool; SWAT). Because they can forecast hydrologic responses to spatially and temporally varied inputs (precipitation and land cover). Therefore, in this study SWAT model was applied to assess the impacts of climate change and land use land cover changes on streamflow and sediment yield, development of BMPs in the Upper Awash River Basin in Ethiopia.

1.2 Statement of the Problem

The rapid land use/land cover changes caused by the clearing of the forest for agricultural, urbanization and industrialization are presumed to adversely affect the hydrologic response of the Ethiopian’s River Basins (Gashaw et al., 2018; Tesfa, 2018). This is shown by reduced streamflow during dry periods and increased flash floods in wet seasons. In addition, the climatic change from time to time, has a direct impact on the hydrology of the catchment (Shiferaw et al., 2018).

The Awash River is one of the country's river basins, and it is under severe stress as a result of fast population increase, urbanization, industrialization, and agricultural development. As a result of changes in land use/cover and climate change, the basin's hydrological pattern shifts. According to Getahun and Gebre (2015) and Mulu et al. (2022), Awash River basin is highly vulnerable to recurrent flood due to extensive land use change and intensified rainfall.

A combined study of climate change and LULC can provide information about watersheds that can be used to make decisions about water and land resource development and management (Randhir and Tsvetkova, 2011). Different researches were conducted on the separate impacts of climate change and land use land cover change in the basin. But, separate studies of LULC change or climate change do not provide complete information about the combined effects of climate and LULC changes on streamflow and sedimentation of water bodies. Also, few researchers conducted research on combined impacts, and they didn't develop BMPs or evaluate the effectiveness of the BMPs for the basin. As a result, it is critical to assess the effects of both climate and LULC changes on streamflow, sediment yield, and establish BMPs in the catchment.

With poor land management, the upper Awash sub-basin is extensively exploited for grazing and cultivation (Sufiyan, 2014). In this sub-basin, poor land management leads to uncontrolled soil erosion and degradation, this results to significant silt transport in streams and river systems. As a result, developing the watershed management practice is paramount to alleviate sedimentation problem in the area.

1.3 Objectives of the Study

1.3.1 General objective

The general objective of the study was to Model the Impacts of Climate and Land Use Land Cover change on Streamflow and Sediment Yield, and Developing Best Management Practices in the Upper Awash Sub-Basin in Ethiopia.

1.3.2 Specific objectives

In order to meet the general objective of the study, the following specific objectives are set to:

- Assess spatiotemporal variations of LULC change of upper Awash sub-basin (1990 to 2020)
- To evaluate the performance of the SWAT hydrologic model in simulating streamflow and sediment yield in the Upper Awash Sub-Basin
- Evaluate combined impact of CC and LULC on stream flow and sediment yield
- To develop best watershed management practices to alleviate sedimentation problem in the study area

1.4 Research Questions

- How spatiotemporal variations of LULC change look like in the study area?
- How well does the SWAT hydrologic model performs in simulating streamflow and sediment yield in the study area?
- How to evaluate combined implication of changing both climate and LULC on streamflow and sediment yield?
- Which watershed management practices is best for alleviating the problem of sedimentation in the study area?

1.5 Significance of the Study

The Awash basin has a high rate of land use, land cover, and climate change. Quantitative estimates of climate and LULC change's hydrologic effects are also necessary for comprehending and resolving potential water resource management issues such as water supply for domestic and industrial water use, power generation, and agriculture, as well as future water resource planning, design, and management, and environmental protection. This shift and its impact were evaluated using semi-distributed models, which allowed the watershed to obtain critical information. As a result, evaluating the impact of land use, land cover, and climate change on watershed hydrology response might encourage policymakers and experts to maintain water management and consumption in the catchment.

1.6 Scope and Limitation of the Study

This study is focused on determining the impact of Climate and LULC on the streamflow and sediment yield due to historical Climate and LULC change in the Upper Awash Sub-basin. It also includes identifying the best management practice to minimize sediment production in the upper Awash Sub-basin. An approach, based on land surface features mainly responsible for erosion, which includes slope and soil type is also used in this study by dividing the catchment into sub-watersheds to assess the sub-watersheds contributing maximum sediments. The dynamically downscaled regional climate data from the EC-EARTH output of CORDEX-Africa downscaled with the RCP 4.5 scenario was used to project future rainfall and temperatures from 2041 to 2070. SWAT model also applied to simulate streamflow and sediment yield over the basin in this specific study.

The followings are the limitations the study:

- The study is limited from investigating future LULC and Climate change impacts on streamflow and sediment.
- The climate variables used in this study for rainfall and temperatures projection are CORDEX-Africa results, which are not an ensemble or single RCM output and only RCP4.5, which may affect the outcome.

1.7. Thesis Organization

This thesis contains five chapters organized as follows. Chapter one gives a general introduction to the study with its background, objective and research questions are also discussed in this chapter. Chapter two describes reviewed literature about the subject matter and it gives a scientific review on facts this study is mainly based on. Chapter three describes materials and methods adopted for the study including brief description of the study area location, the available hydrological meteorological and spatial data used for this study and as well as how data are analyzed. Chapter four discussed the result of the study and the last chapter five ends with research conclusion and recommendations based on the study conducted to indicate direction for future studies.

2. LITERATURE REVIEW

2.1. Overview of Climate Change

Climate change is a change in the state of the climate that; can be identified by changes in the mean and/or the variability of its properties and that perseveres for an extended period, typically decades or longer (IPCCII,2007). In the context of global climate change, most of Africa has also experienced a significant warming trend over the past decades and the trend is expected to continue in the future (Hulme et al, 2011; Mango et al, 2015).

According to IPCCII (2007) findings, developing countries, such as Ethiopia will be more vulnerable to climate change. Because of the less flexibility to adjust the economic structure and is largely dependent on agriculture, the impact of climate change has far reach implication in Ethiopia. Upward trends in annual air temperature and downward trends in annual rainfall have been observed over Ethiopia between 1948 and 2006 (Jury et al., 2013), whereas (World Bank, 2008) reported that Ethiopia will see further warming of 0.7°C and 2.3°C by the 2020s and between 1.4°C and 2.9°C by the 2050s (Belay et al., 2016). The changes in both temperature and precipitation exhibit remarkable regional variability (Belay et al., 2016).

2.2 General Circulation Model (GCM)

General Circulation Models, or GCMs, depict the physical processes that occur in the atmosphere, ocean, cryosphere, and land surface IPCC (2014). Additionally, the most sophisticated techniques now in use for predicting how the global climate system will respond to rising greenhouse gas concentrations (Rahman, 2019). Simpler models have also been used to provide estimates of the global or regional average of the climate response, but only GCMs, possibly in conjunction with regional models, have the potential to provide the geographically and physically consistent estimates of regional climate change that are necessary for impact analysis.

2.3. Downscaling Methods

GCM represent climate in a horizontal resolution between 250 and 600km which is more global representation that would be quit coarse for regional impact assessment (Alerts et al., 2004; IPCC, 2013; IPCC, 2007). However, the hydrological effects and adaptation to changing climate in river basins are mainly taking place at local to regional scales that lie within just one or a few GCM grid-cells. For instance, climate change impact assessment on the future runoff may require daily rainfall scenario at regional or at catchment scales (IPCC, 2013). Finer the resolution over which the information is given, the more adequate, usable, or richer it is (Charron, 2014; IPCC, 2007). This implies that, the use of GCM outputs directly may mask the reality for impact assessment at regional or catchment scales. Therefore, downscaling techniques into local meteorological variables is essential to assess climate change impact in detail as compared with direct use GCM outputs (IPCC, 2007). Dynamical and Statistical Downscaling Methods (SDSM) are the two types of downscaling techniques used mostly in literatures.

2.3.1. Statistical downscaling approach.

Statistical downscaling procedures build statistical relationships between large-scale climate information (predictors) and regional variables (predicted) (Wilby et al.,2004). It involves the creation of empirical correlations between local and large-scale atmospheric variables across time. Future local climate variables are predicted using future global climatic variables predicted by GCMs. These SD techniques, according to (IPCC, 2001), can be divided into three groups: weather categorization, regression models, and weather generators (Wilby et al., 2004). As a result, a GCM should be able to accurately reproduce a suitable predicator that is pertinent to the predicted. the predicate of interest significantly corresponds with the data already available from GCM simulation archives have a steady relationship with the expected (time invariant).

Advantages of statistical downscaling are that it is computationally inexpensive and efficient. This allows many different emissions scenarios and GCM pairings. Also the disadvantages of statistical downscaling are that high quality observed data may be unavailable for many areas and it assumes that relationships between large and local-scale processes will remain the same in the future

2.3.2. Dynamical downscaling approach

Dynamical downscaling (DD) implies the application of regional climate models (RCMs) for limited regions with boundary conditions based on GCM simulations. Dynamical downscaling is implemented to nest a fine-resolution regional climate model (RCM) driven by boundary conditions from the GCM (Guo and Wang, 2016; Wang et al., 2017; Liang et al., 2019). Computationally, dynamical downscaling is time-consuming. Many collaborative projects are now using dynamical downscaling to generate climate simulations for model inter-comparisons and effect assessments.

Dynamical downscaling has been used to give regional climate projections since the end of the 1980s (Dickinson et al., 1989) and it has become a well acknowledged and widely utilized method for producing climate change information at the regional scale. The Coordinated Regional Climate Downscaling Experiment (CORDEX) is a multi-model regional climate change projection study that is being coordinated internationally (Giorgi et al., 2009). Under the auspices of the World Climate Research Program (WCRP), CORDEX (Coordinated Regional Climate Downscaling Experiment) is an initiative to downscale different GCM outputs that participated in the Coupled Model Intercomparison Project Phase 5 (CMIP5) data archive (Taylor et al., 2012) on 25Km and 50Km grid spacing for 14 regions of the globe.

2.4. Evaluation of Regional Climate Model Simulations of Climate Variables

The complexity and diversity of the processes that need to be represented make it difficult to accurately and consistently simulate the climate over the African continent using GCMs and RCMs (Laprise et al., 2013). The annual mean rainfall variability over the Ethiopian highlands was overstated by the models. According to studies from Endris et al. (2013) for the Ethiopian highlands, simulation results from CORDEX-Africa models accurately represented the shape of the monthly rainfall distribution and the yearly rainfall anomaly, but they overstated the mean monthly rainfall quantity. The model simulation outputs of rainfall data are assessed using statistical approaches like bias, coefficient of variation (CV), and correlation coefficient (Correl.). These statistical methods are the most frequently used standards for assessing the effectiveness of model simulations, including in Ethiopia (e.g., Haile and Rientjes, 2015). According to (NMSA, 1996) classification; the degree of rainfall variability is less with (CV <20%), moderately variable (CV ranges between 20 to 30%) and highly variable (CV >30%).Correlation coefficient (Correl.) was used to evaluate the linear relationships between the observed and model output datasets with a value of one representing perfect relationships.

2.5. Climate Change Scenarios

2.5.1 Shared socioeconomic pathways (SSPs)

The Shared Socioeconomic Pathways (SSPs) are an essential part of the new generation of climate scenarios. The shared socio-economic pathways (SSPs), which forecast future socio-economic circumstances around the world and related GHG emissions (O'Neill et al., 2013). They include narrative and quantitative components of socio-ecological systems, such as demographic, political, social, cultural, institutional, lifestyle, economic, and technological variables and trends, and they outline conceivable alternative states of human and natural societies at a macro scale. They also cover how humans affect ecosystems and ecosystem services like biodiversity and the quality of the air and water. The regional and sectoral scenarios can be added to the global SSPs.

2.5.2 Representative concentration pathways (RCPs)

To provide a variety of potential futures for the evolution of atmospheric composition, climate experts have established a set of scenarios called as Representative Concentration Pathways (RCPs) (Moss et al., 2008).

Four typical concentration pathways are defined for effect assessment studies in the IPCC Fifth Assessment Report (AR5, 2014). The terms RCP2.6, RCP4.5, RCP6.0, and RCP8.5 are derived from the likely range values of radiative forcing in 2100, which are, respectively, +2.6, +4.5, +6.0, and +8.5 W/m2. Here is a summary of the four pathways:

Table 2.1: Summary of representative concentration pathways

Name	Description	Publication-IA Model
RCP2.6	Peak in radiative forcing at 3W/m^2 (490ppm CO_2equiv.) before 2100 and then declines to 2.6 3W/m^2 by 2100.	(Van Vuurentet al., 2007a; Van Vuurent et al. 2006)-IMAGE
RCP4.5	Pathway without overshoot to 4.5W/m ^{2} (650 ppm CO_2equiv.) at stabilization after 2100	(Clarke et al. 2007; Smith and Wgley 2006)-GCAM
RCP6.0	Pathway without overshoot to 6.0W/m^2 (850 ppm CO_2equiv.) at stabilization after 2100	(Fujinoet al. 2006; Hijioka et al. 2008)-AIM
RCP8.5	Rising pathway leading to 8.5W/m^2 (1370 ppm CO_2equiv.) in 2100	(Riahet al. 2011)-MESSAGE

Source: (Vuuren et al., 2011).

2.5.3. Comparisons of SRES with SSPs and RCP climate scenarios

Radiative forcing estimates from the four RCP scenarios used in CMIP5 range from 2.6 to 8.5 Watt per m^2 at 2100, a greater range than the three SRES scenarios used in CMIP3 (IPCC, 2013). Unlike the RCP scenarios, the SRES scenarios do not anticipate any type of strategy to combat climate change. RCPs describe radiative forcing paths and, in contrast to the Special Report on Emission Scenarios, are not exclusively tied to socio-economic assumptions (SRES). A wide variety of socio-economic and technical development scenarios could lead to any one radiative forcing pathway (Van Vuuren et.al., 2011).

2.6. Impact of Climate Change on Temperature and Precipitation

2.6.1. Global climate change impact on temperature and precipitation

The global temperature and precipitation have changed rapidly over the last century due to anthropogenic increases of greenhouse gases *(*GHGs) in the atmosphere (for example, burning of fossil fuels, like coal, petroleum and natural gasses and widespread deforestation) (Gemeda and Sima, 2015). According to the Intergovernmental Panel on Climate Change (IPCC), increasing concentrations of GHGs, specifically carbon dioxide, would cause global surface temperatures to rise by 1.4 to 5.8°C by 2100 years.

African countries are more affected by climate change because of their reliance on agriculture as well as their lower financial, technical, and institutional capacity to adapt (Rose, 2015).The most significant climatic change that has occurred in Africa has been a long-term reduction in rainfall in the semi-arid regions of West Africa.

2.6.2. Climate change impacts on temperature and precipitation in Ethiopia and Awash Basin

Ethiopia contributes very little to global greenhouse gas emissions, but it is affected by the negative effects of climate change brought on by rich countries' carbon-intensive development pathways over the last century. Temperatures across the country could rise by 0.5 to 3.6 degrees Celsius by 2070, according to the government's First National Communications to the UNFCCC.

Rainfall is a valuable resource, especially for developing nations, and its fluctuation has a significant impact on social and economic life (Zarough et al., 2014), as agriculture is their primary source of income. Flooding can arise from excessive rainfall intensity, whereas drought can result from a lack of it. Ethiopia was severely impacted by both a rainy and dry year in 2007 (Bedassa et al., 2015). According to the author, Ethiopia experienced severe failure in 2009 during the main rain season in most parts of the country (JJAS), which was the most severe in the last 30 years. In 2007 and 2006, the country had severe floods; 2007 was one of the worst flood years in East Africa. Crop failure and starvation happened as a result of such climate hazards in the country, while catastrophic flooding induced by rainfall wreaked havoc on many people across eastern Africa in 2007.

For example, according to research conducted by CORDAID (2012) in Dire Dawa, the following are the main flooding incidents that occurred in the recent three decades and resulted in significant loss of human life and property: - in May 1984, 42 people were destroyed, and property worth 10 million birr was lost; in August 2006, 256 people were destroyed, 244 people went missing, 10,000 people were displaced, and 1827 households in 17 rural kebeles were negatively impacted; in April 2010, no human life or live animals were lost as a result of the early warning system's implementation, but property worth 28 million birr was lost.

Kebede et al. (2013) used large-scale atmospheric output variables from CGCM3.1 global circulation model and the regional model REMO with statistical downscaling method to assess temperature and precipitation change projection over all Baro Akobo river basins. The investigator used GCM outputs based on Special report on emission scenario (SRES) to assess the future precipitation and temperature for a period of 2011 to 2050 with A1B and B1 climate scenarios. The author suggested that, the result of downscaled precipitation reveals that precipitation does not verify a systematic increase or decrease in all future time horizons for both A1B and B1 scenario unlike that of maximum temperature. However, the result of REMO A1B and B1 scenario suggested similar trend for maximum temperature (+1.3°C) and (24%) for rainfall during a time range of 2011 to 2050s. The assessment of the investigation was done based on GCM models of horizontal resolution 250-600km at regional scale which may not address local scale.

2.7. RS and GIS Application in Hydrological Systems and LULC Change Analysis

The science (and to some extent, art) of learning about the earth's surface without actually being in contact with it is known as remote sensing, according to Canada Centre for Remote Sensing (CCRS) (1999). To do this, energy that is reflected or released is sensed, recorded, processed, examined, and put to use. Analyzing change is crucial for maintaining and monitoring the earth's natural resources. Monitoring shifting agricultural, estimating deforestation, and other environmental changes are a few examples of its use (Jingan et al., 2005).

There are only roughly 157 different land cover categories, and no research location will have all of them, according to the modified United Nations Educational Scientific and Cultural

Organization (UNESCO, 1976) classifications scheme. Therefore, using the Classification method, it will be essential to divide pixels into a smaller number of closely related classes based on spectral similarity (Oumer, 2009). The categorization of remotely sensed pictures for various applications involves two main strategies: supervised classification and unsupervised classification.

In supervised classification, the computer program is trained to understand that particular sorts of pixels correspond to particular types of land cover. In this method, the software divides the pixels into groups based on comparable sample signatures, with information from the fieldwork and prior knowledge of the area serving as crucial inputs. The desired number of groups or clusters will be entered into the software during unsupervised categorization (Oumer, 2009). The pixels are then grouped by the software in decreasing brightness order based on comparable spectral properties.

2.7.1 Drivers of LULC Change in Ethiopia and Awash River Basin

According to Bronstert et al. (2002) throughout the entire history of mankind, intense human utilization of land resources has resulted in significant changes on the land-use and land-cover. The fast population growth and desire for a higher standard of living in Ethiopia have put enormous strain on the country's natural resources. The requirement for arable land, grazing land, fuel wood, and settlement areas has increased in tandem with the increase in the human population in order to meet the local demand for food, energy, and cattle population. According to numerous studies a number of variables have influenced Ethiopia's land cover from its initial state. The growth of cultivated land at the expense of grasslands is one example of these human activities. According to Gebrehiwet (2004), the impact of population pressure has resulted in a decline in natural vegetation and an increase in agricultural land cover. Hadgu (2008), the expense of woods and shrub land, open space and settlements are growing Hedlund and Tekle (2000), conversion of natural pastures and forests to croplands has resulted in their decline Kassa (2003).

According to the majority of these research (Amsalu et al. 2007; Hurni & Zeleke, 2001), population pressure is one of the main factors influencing changes in land use and land cover through the removal of vegetation and forests for agricultural and urban expansion. And also Shiberu and Kifle (1998), Badege (2001), and MoARD and WB (2007) also concluded that the dominant mixed farming practices in the highlands of Ethiopia without appropriate and integrated land management practices were major driving forces of vegetation cover loss and land degradation. Tessema et al.

(2020) conduct a research on modelling land use dynamics in the Kesem sub-basin, Awash River basin and conclude that the major driving forces of land use land cover were population density and over-use of land. The population size has played a fundamental role in the dynamics of LULC in the study basin. Besides the alarming rate population growth, the study basin has been a center for both the agricultural and industrial revolution in recent years due to the proximity to the urban centers of the country including Addis Ababa (Chakma & Shawul, 2019).

2.8. Climate and LULC Change Impacts on Streamflow and Sediment Yield

Zhang et al. (2022) studied the Impacts of Land Use and Cover Change (LUCC) and Climate Change on Discharge and Sediment Load in the Hunhe River Basin, Northeast China Using SWAT hydrological model and found that the combined impact of LUCC and climate change decreased the annual discharge and sediment load by 22.65% and 31.51%, respectively. And also minor changes in annual discharge (+0.08%) and sediment load (−1.33%) were caused by LUCC, and climate change led to a pronounced decrease in annual discharge (−22.69%) and sediment load (−30.61%). In general, they conclude that climate change rather than LUCC dominated the hydrological alterations in the Hunhe River Basin.

Watershed temperatures, nutrients, and other elements affecting streamflow and water quality change through time and space. According to Ahearn et al. (2005), Ficklin et al. (2014), Kaushal et al. (2014), and Kharel et al. (2016), the two main factors affecting water quantity and quality in watersheds and waterways are climate change and LULC change. Local hydrological processes are altered by climate change, and this has an effect on water quality and streamflow both directly and indirectly. Changes in LULC have an impact on hydrological processes such interception, infiltration, and evapotranspiration, which modify surface and subsurface flows as a result.

In a watershed, erosion and sedimentation are closely tied to organic processes that are primarily fueled by precipitation and runoff. Topography, soil type, catchment area, climate (precipitation, wind, temperature, etc.), plant cover, human-influenced soil erosion, forest fires, and river discharge are some of the contributing elements that affect sediment output in a watershed (Francipane et al. 2015). Erosion and sediment transport processes are sensitive to changes in climate and land cover and to a wide range of human activities because of their close links to land cover, land use, and the hydrology of a river basin (Walling 2009).

Mekonnen and Tadele (2012) analyzed the combined effects of land use and climate change on soil erosion and stream flow in the Upper Gilgel Abay River catchment using SWAT hydrological model. The result showed that the combined effect of trend-based land use and climate change (2011–2025) will increase the average annual sediment load by 29 % and significantly affects soil erosion compared with other scenario. The study conducted by Mitiku et al. (2023) examining the impacts of climate variabilities and land use change on hydrological responses of Awash River basin reported that the effects of both climate and land use changes will likely to increase the river flow and possibly cause flooding in the upper Awash River basin.

2.9. Hydrologic Models

2.9.1 Hydrologic model concepts

Hydrological modeling is a powerful technique of hydrological systems investigation for both the research hydrologist and practicing water resources engineers involved in the planning and development of an integrated approach for the management of water. The goal of utilizing a model is to establish baseline characteristics when data isn't available and to mimic difficult to calculate long-term effects (Lenhart et al., 2002).

2.9.2 Classification of hydrologic models

For studying hydrologic processes and hydrologic responses to land use and climatic changes, mathematical models and geospatial analysis tools are required (Dilnesaw, 2006). They are classified as, Lumped, Semi-distributed, Distributed Models. The parameters in Lumped Models are not spatially variable within the basin and do not represent physical aspects of hydrologic processes. The basin response is simply assessed at the outlet, with no consideration for adjacent sub-basins. The effect of geographic variability on model parameters is assessed by determining effective values for the entire basin using specific methodologies. By dividing the basin into a number of smaller sub-basins, semi-distributed models allow parameters to change in space to some extent. When compared to other models, the fundamental advantage of semi-distributed models is that they have a more identifiable physically based structure and require less input data. Some hydrological models, such as SWAT, HEC-HMS, and HBV, fall into the semi-distributed category. In a distributed model, parameters can fluctuate in space at a resolution that is normally set by the user. Data about the spatial distribution of parameter variations, as well as computational tools, are combined in a distributed modeling approach. The parameterization of this model usually necessitates a substantial amount of data.

2.9.3 Criteria for model selection

There are a number of factors that can be used to select the best hydrological model for a given problem. Because each project has its own set of objectives and needs, these criteria are always project-specific. Furthermore, some criteria are dependent on the user. There are four common, fundamental selection criteria that must always be answered among the various project-dependent selection criteria (Cunderlik., 2003):

- Required model outputs important to the project and therefore to be estimated by the model (Does the model predict the variables required by the project such as long-term sequence of flow?),
- Hydrologic processes that need to be modelled to estimate the desired outputs adequately (Is the model capable of simulating single-event or continuous processes?),
- Availability of input data (Can all the inputs required by the model be provided within the time and cost constraints of the project?),
- Price (Does the investment appear to be worthwhile for the objectives of the project?).

2.10. Soil and Water Assessment Tool Model

SWAT was created by (Arnold et al. 1998) to forecast how various management techniques would affect water quality, sediment output, and pollution loading in watersheds. This model has not let us down, as it has shown to be a useful tool for analyzing water resource and nonpoint-source pollution issues at a variety of scales and in a variety of environmental contexts around the world. The model was created to be utilized with watersheds that are not gauged (Arnold et al. 1998; Chaubey et al. 2010). SWAT is capable of modeling both local and big areas (Gitau et al. 2008) accurately). Due to its ability to function on a daily, monthly, or annual time step, the SWAT model is adaptable. The internet offers a variety of SWAT models that may be downloaded for free. They are categorized according on the operating system that they use. There is the MWSWAT, which utilizes the Map Window interface, and the QSWAT, which operates on the QGIS platform. Anyone can use MWSWAT and QSWAT because map windows and QGIS are both free resources. The Arc SWAT, which utilizes the ArcGIS platform, is the last option.

However, ArcGIS is a commercial product, which restricts how the Arc SWAT can be used. Therefore, the SWAT model application was calibrated and verified in various regions of Ethiopia (Kassa, 2009; Setegn et al., 2009; Getachew and Melesse, 2012; Tesfahunegn et al., 2012; Shawul et al., 2019; Choto and Fetene, 2019). These studies have already demonstrated that the SWAT model was evaluated in some regions of Ethiopia with a sufficient level of accuracy in gauged catchments.

2.11. Best Management Practices (BMPs)

BMPs are defined as the soil and water conservation practices including social and cultural actions which have been recognized as the effective and practical ways for the environmental protection (Sharpley et al., 2006). BMPs are commonly designed with the purpose of ensuring the efficient use of agricultural chemicals; enhancing soil cover; reducing the velocity of surface runoff, and improving the management of livestock waste (Cestti et al., 2003). Troeh et al. (2004) stated that soil and water conservation methods are usually classified into two as vegetative and mechanical practices. Vegetative practices ensure denser vegetative cover for a longer period. Crop rotation, efficient use of fertilizers, and narrow row spacing can be given as examples of vegetative practices. These practices provide both improved product yield and erosion control. The mechanical practices of soil conservation are a methods of soil protection which includes various engineering techniques and structures such as Basin leaching, Pan breaking, Sub soiling, Contour terracing, and Contour trenching. Novotny (2003), on the other hand, categorized BMPs under three categories as structural, vegetative, and management.

In humid regions, the terraces are functioning as the structures improving the quality of water by reducing the rill erosion, avoiding the formation of gullies, and permitting the settling of sediment from the surface runoff. Contouring or the contour farming is plowing and the crops are planted so that field contours across the slope. Contouring is used for both erosion control in humid regions and for increasing soil moisture by decreasing runoff losses in sub-humid regions (Novotny, 2003; Troeh et al., 2004).

2.11.1. Land management practice effect on soil erosion

Physical, agronomic, and vegetative SWC measures have a direct impact on the entire on-site and off-site impacts of runoff and soil erosion (Shiferaw & Holden, 1999; Nyssen et al., 2007). As a result, SWC measures play a critical role in reducing runoff, soil erosion, and sediment yield in the Ethiopian highlands (Vancampenhout et al., 2006; Nyssen et al., 2007; Tilahun et al., 2013). Over the last three decades, Ethiopia's government has launched and implemented a huge soil and water management (SWM) initiative to limit the damage caused by erosion, flooding, and sedimentation (Shiferaw and Holden, 1998; Herweg and Ludi, 1999; Mitiku et al., 2006). Sufficient surface cover can control splash-eroded soil while regulating its velocity with physical and vegetative measures to reduce soil transportation by surface runoff (Nyssen et al., 2008). The fundamental principle of reducing soil erosion by water is to reduce runoff as much as possible (Mitiku et al., 2006; Nyssen et al., 2010).

2.11.2. Best management practices to alleviate sediment yield

Several studies have been conducted around the world, notably in Ethiopia, to assess the efficiency of various BMPs on hot spot areas of a watershed to minimize sediment output and soil erosion. Uniyal et al. (2020), demonstrated the effectiveness of structural BMPs (0.66-70%) and agricultural BMPs (2-7%) in reducing sediment yields at the watershed level in the Upper Baitarani River basin in Eastern India. In Ethiopia, Nadew et al. (2019) found that applying filter strips and parallel terrace/stone bunds scenarios reduced existing sediment yields by 48 percent and 53 percent, respectively, when compared to the existing condition scenario at the sub-basins and basin outlet in the Guder watershed, Blue Nile Basin. Furthermore, Tesema and Leta (2020) used three management methods to remediate high sediment yield regions: vegetative filter strips, grass waterways, and terracing in high sediment yield areas.

3. MATERIALS AND METHODS

3.1 Description of Study Area

3.1.1. Location

Awash River rises on the high plateau near Ginchi town west of Addis Ababa and flows along the rift valley into the Afar triangle, and terminates in salty Lake Abbe on the border with Djibouti (Tessema, 2011). The geographical location of upper Awash Sub-basin is in between longitude 8° 46′ 24.6″ to 9° 3′ 18.8″ N and latitude 37° 57′ 8.45″ to 39°17.24′ 92″ E. The basin covers about 11,607 km^2. The average altitude ranges from 1688 to 3576 meters above mean sea level.

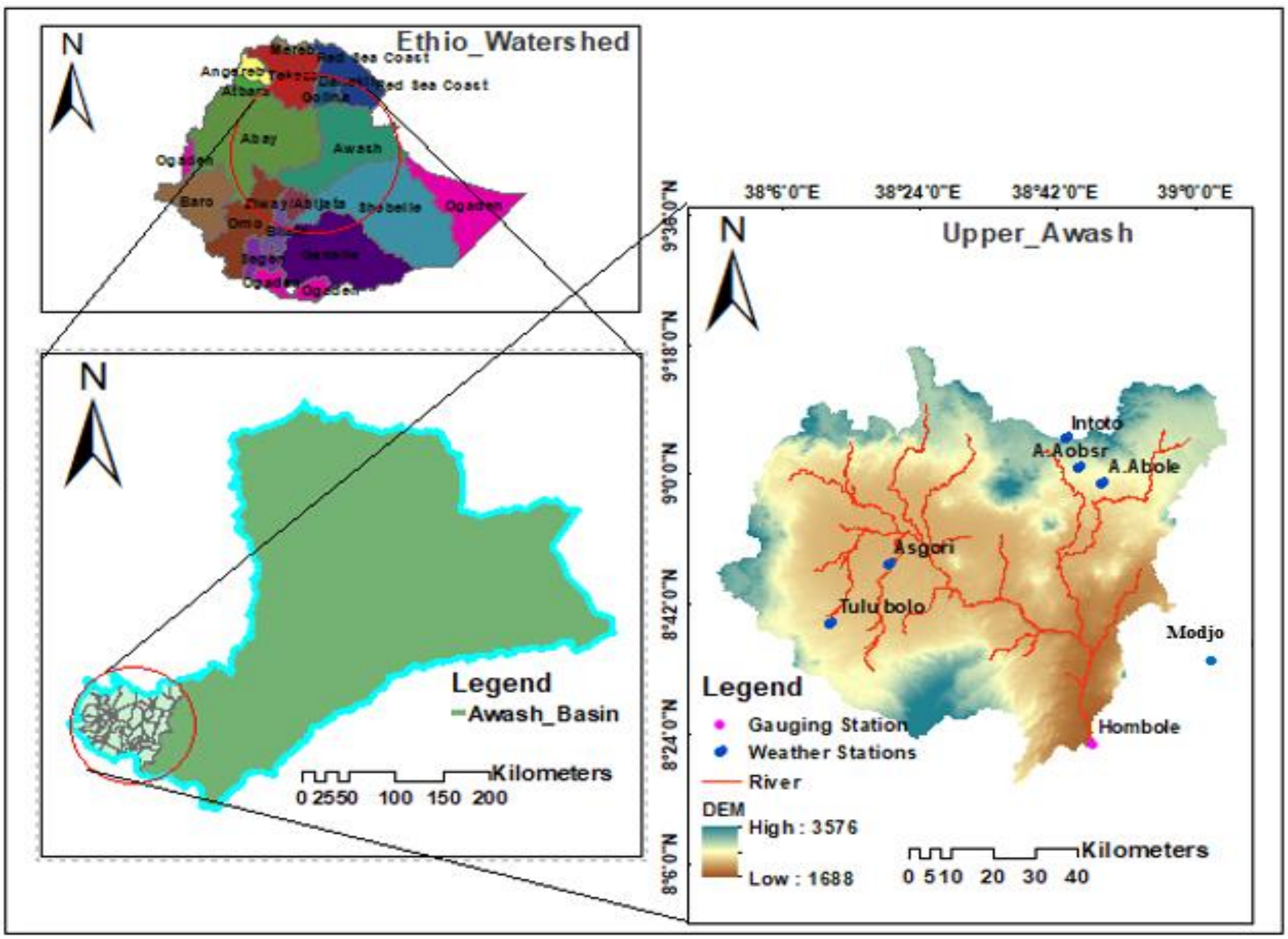

Figure 3.1: Location of Study Area

3.1.2 Climate characteristics of the study area

The climate of the Awash basin is humid to sub-humid in the highlands and semi-arid to arid in the rift valley. The climate of the Awash Basin comes under the influence of the Inter-Tropical Convergence Zone (ITCZ). This zone of low pressure marks the convergence of dry tropical easterlies and the moist equatorial westerlies. The seasonal rainfall distribution within the basin results from the annual migration of the ITCZ. The ITCZ starts its advance across the basin from south in March, bringing the small or spring rains. In June and July reaches its most northerly location beyond the basin, which then experiences the heavy or summer rains throughout. The ITCZ returns southwards during August, September and October, restoring a drier, easterly air stream that prevails until the ITCZ resumes its northward migration in March. The distribution of rainfall over the highland areas tends to be modified by orographic effects. Annual rainfall ranges from 850mm to 1000mm in the plain area and amounts in the mountains of Upper Awash River basin respectively. Mean annual temperature is about 15°C in the highlands and around 21°C in the lowlands. The rainfall shows strong altitudinal variations. The Sub-basin receives approximately 70% -75% of its annual rainfall during the wet season which covers the months June–September (Dilnesaw et al., 2006).

The rainfall pattern in the upper awash sub basin is mostly unimodal, with the majority of rain falling from late June to early September (Kiremt) and the rest of the year mostly dry, with a little amount of rain occurring from March to May (locally known as the rainy season) (Belg) (Tadese et al., 2019). The averages and monthly rainfall, maximum and minimum temperatures of the six stations in the upper awash basin are shown in the (figure 3.2, 3.3 and 3.4) respectively.

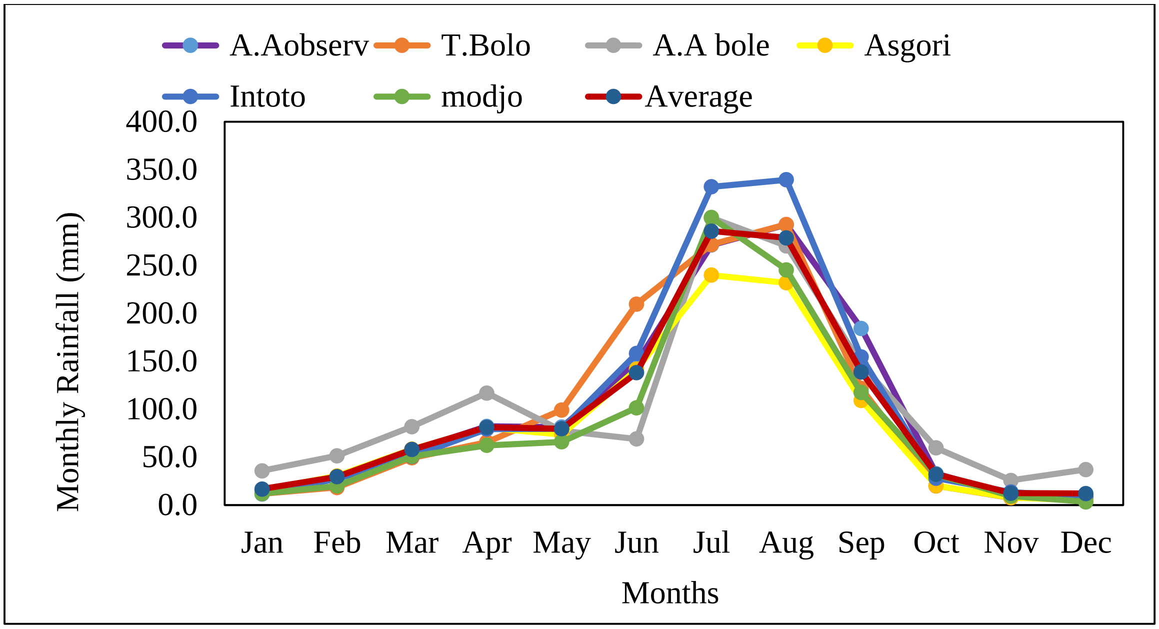

Figure 3.2: Spatiotemporal variation of rainfall over the study area

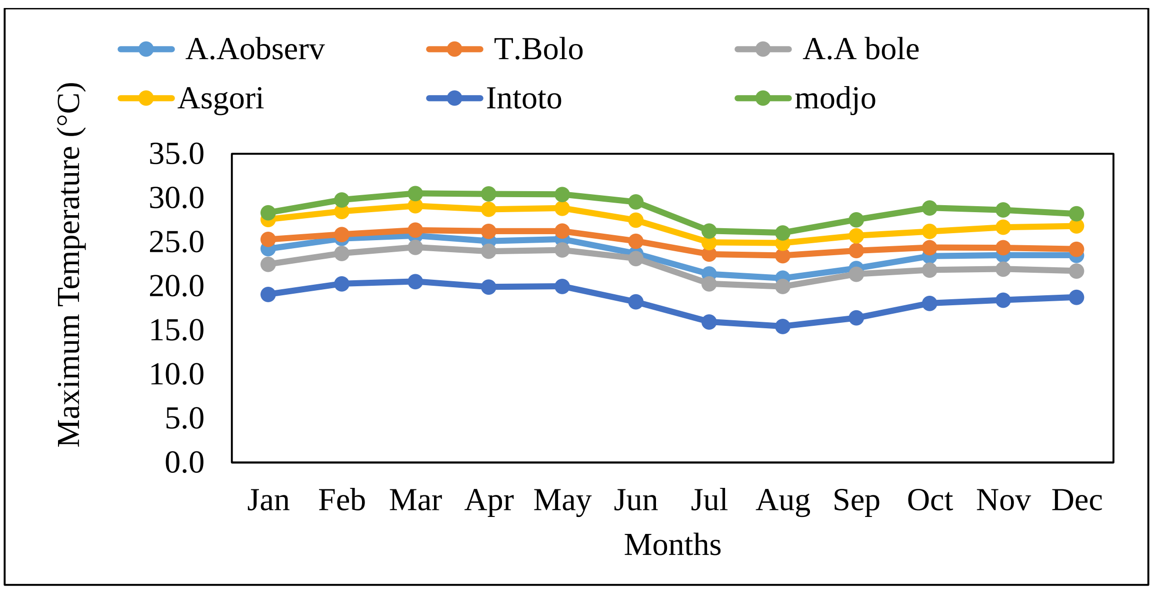

Figure 3.3: Spatiotemporal variations of maximum temperature over the study area

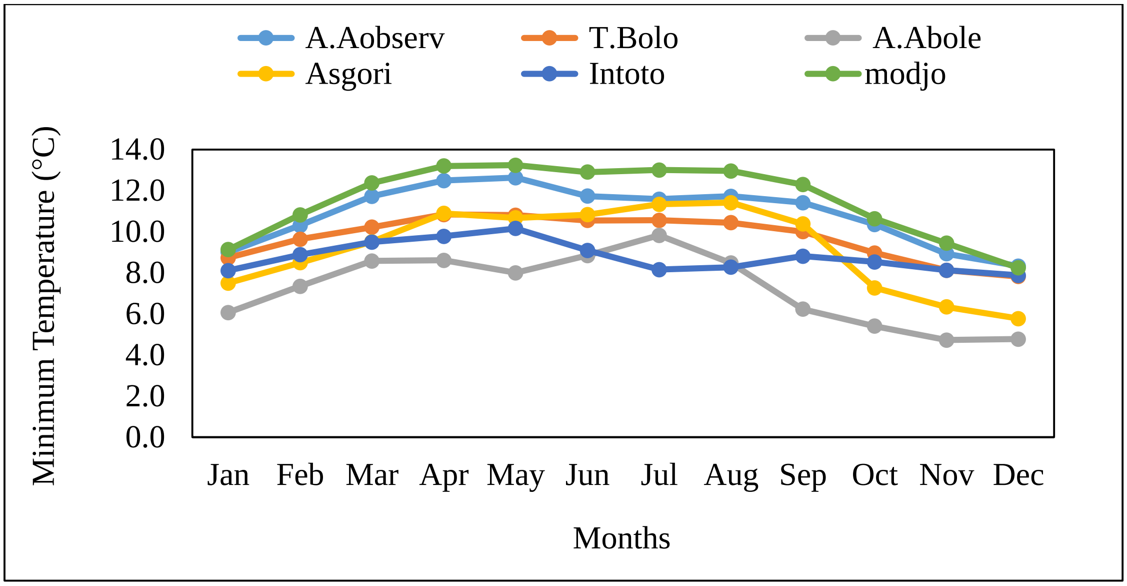

Figure 3.4: Spatiotemporal variations of minimum temperature over the study area

3.1.3. Topography

The research area's physical settings are defined by the heterogeneity of massive natural systems such orographic groups, high plains, mountains, and plateaus. The Upper Awash Sub-Basin is the topographic level of all lands above 1500 m, based on physical and socioeconomic considerations (Yitea, 2015). The region is located to the northeast of the Rift Valley Lakes Basin, and the topographical height drops in general as one move northeast. Relatively, the most utilized river basin and the only river entirely in the country.

3.2 Materials and Software

In order to achieve the goal of the objectives, the following software were used. These software's includes ArcGIS interfaced ArcSWAT-2012 which was used for the SWAT model setup and data preparation, ArcGIS, Googleearth-win-pro-7.3 and ERDAS Imagine 2015 are used for the preparation of spatial data including LULC image classifications, Sequential Uncertainty Fitting version 2 (SUFI-2) algorithm in SWAT calibration and uncertainty program, (SWAT-CUP) software package for model sensitivity, calibration, and validation, Google Colab for Plotting of Graphs and RAINBOW software are used for the homogeneity test of rainfall data.

3.3 Model Input and Data Sources

3.3.1 Weather data

The climatic data (i.e. daily rainfall, maximum and minimum temperature, relative humidity, wind speed and solar radiation) were collected from the National Meteorological Institute of Ethiopia (NMSA) for stations located within the study basin. The weather data used were represented from six stations (A.A Observatory, A.A Bole, Tullu Bollo, Asgori, and Intoto) located in the watershed and one station (Mojo) located around the watershed for the 30 years (1989 to 2019). Hombole Climate Station is not considered due to the short time of recorded data, which was less than 30 years.

Table 3.1: Meteorological station names, locations, and variables

No	Station Name	Lat	Long	Elev(m)	Variables (1989-2019)					
					PCP	Tmax	Tmin	RH	SR	WS
1	A.A Observatory	9.02	38.75	2386	yes	yes	yes	yes	yes	yes
2	Tulu Bollo	8.66	38.21	2190	yes	yes	yes	no	no	no
3	A.A Bole	8.98	38.79	2354	yes	yes	yes	no	no	no
4	Asgori	8.79	38.33	2072	yes	yes	yes	no	no	no
5	Intoto	9.08	38.72	2903	yes	yes	yes	no	no	no
6	Modjo	8.61	39.11	1771	yes	yes	yes	no	no	no

Note PCP is Precipitation, Tmin is minimum temperature, Tmax is maximum temperature, RH is relative humidity, SR is solar radiation, and WS is wind speed.

3.3.2 Hydrological data

3.3.2.1 Streamflow data

The time series of hydrological data (streamflow) which was used for SWAT model calibration and validation was obtained from Ministry of Water and Energy (MoWE) of Ethiopia at hombole hydrometric station for the years 1989- 2016.

Table 3.2: Gauged Hydrological Data

Station	Recorded time	Latitude(°)	Longitude(°)
Hombole	1989-2016	8.38	38.78

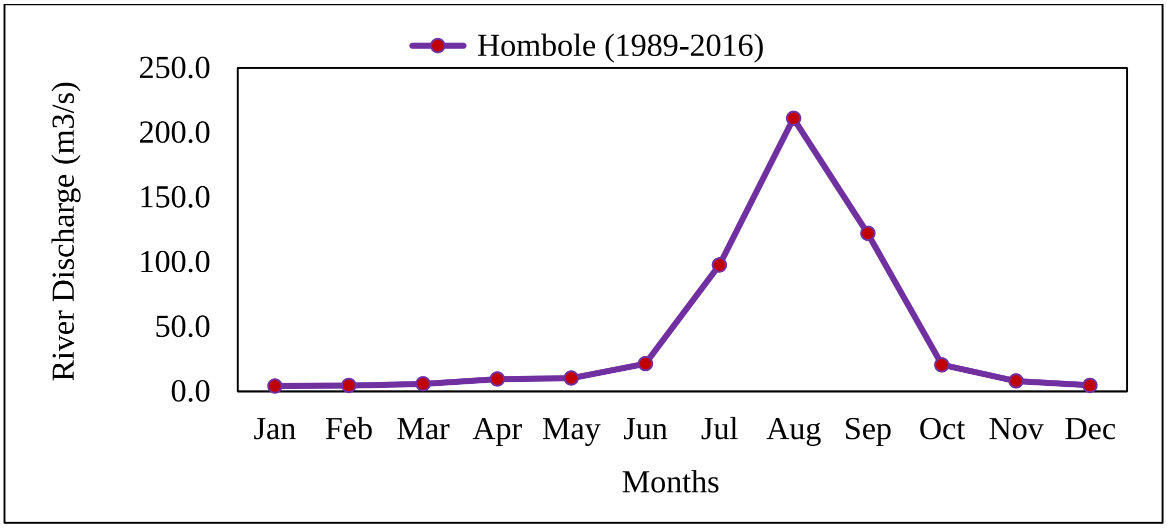

Figure 3.5: Long-term mean monthly river discharge at Hombole hydrometric station

3.3.2.2 Sediment data

There are some sites in the upper Awash Sub-Basin that have measured suspended sediment data with extremely short data. The suspended sediment data in Hombole station at different time was collected from MoWE of Ethiopia. The remaining parameters for sensitivity and calibration analysis were obtained from the sediment rating curve based on the observed suspended sediment data.

According to the constructed rating curve equation, streamflow and suspended sediment yield correlation has a R^2 value of 0.984 (Figure 3.6). In this study, the following equation was used:

$$S_y = 0.086C * Q \tag{3.1}$$

$$S_y = 21.025Q^{1.3355} \tag{3.2}$$

Where S_y is suspended sediment yield (ton/day), C is sediment concentration in mg/l, Q is streamflow (m^3 /s), and 0.086 is a conversion factor.

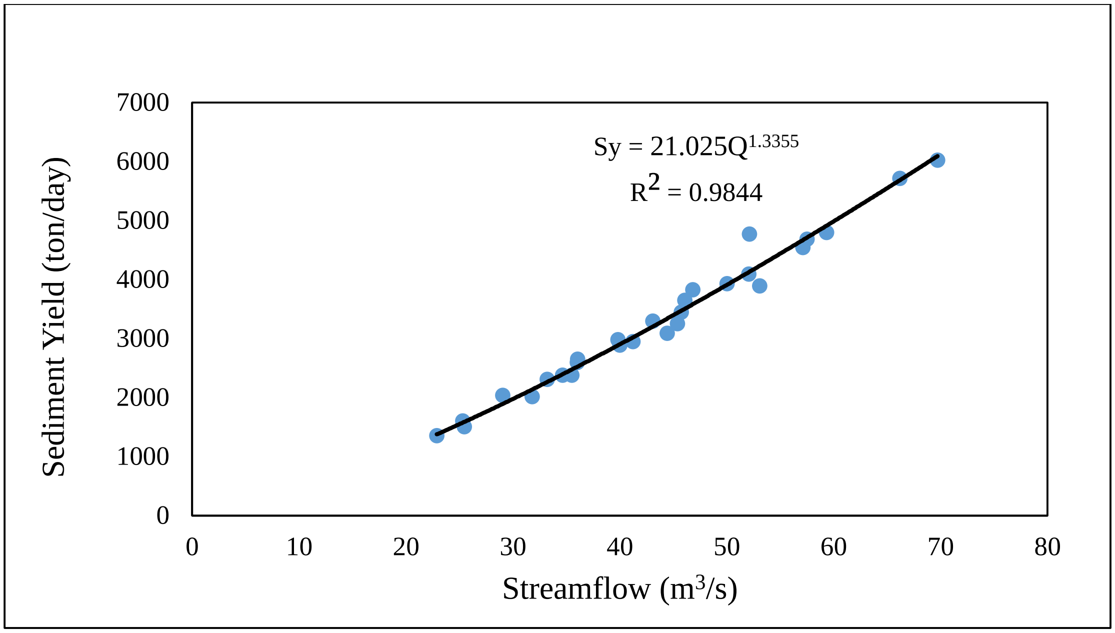

Figure 3.6: Sediment rating curve for Hombole station

3.3.3 Digital elevation model data

SWAT watershed delineator techniques require Digital Elevation Model (DEM) data to calculate flow accumulation, stream networks, and watershed delineation. The ASTER Global Digital Elevation Model with a resolution of 30 m x 30 m was obtained from the MoWE.

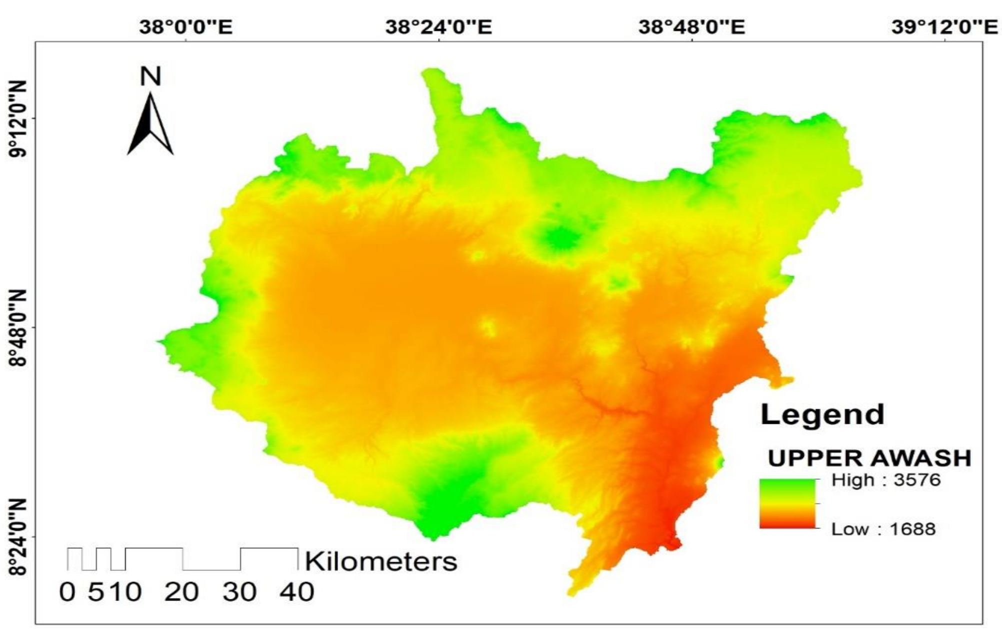

Figure 3.7: Digital Elevation Model (DEM)

3.3.4 Soil data

The soil data was one of the important data used in the SWAT model for considering the physiographic condition of the study area. This was done because the watershed has different landforms that have strong relations with that of soil characteristics. As per the variety of landforms within the watershed, the soil characteristics are different for most of the mapping units. According to the FAO/UNESCO soil classification system the study area comprises eleven major soil types, the soil raster data set was taken from Ethiopian MoWE.

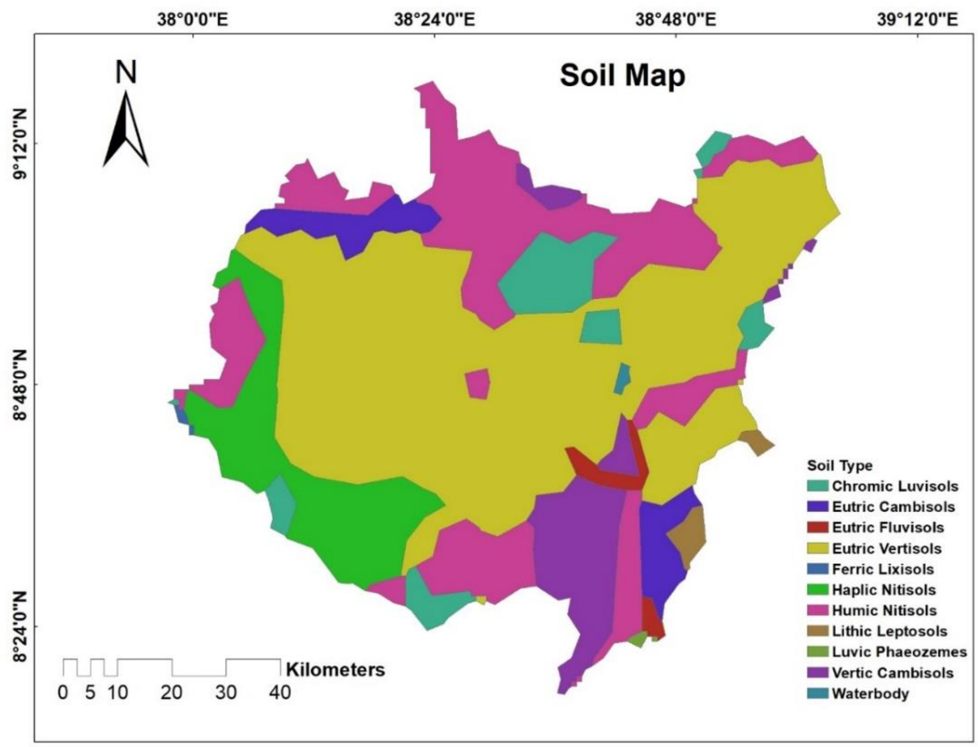

Figure 3.8: Soil map of Upper Awash Sub-Basin

Table 3.3: Soil types of Upper Awash Sub-Basin with their symbols and areal coverage

S/No	Soil Name	Symbol in SWAT Model	Area (Square Kilometers)	% of Watershed Area
1	Chromic Luvisols	LVx	421	5.63
2	Eutric Cambisols	Cme	316	4.22

3	Eutric Fluvisols	FLe	85	1.14
4	Eutric Vertisols	Vre	3624	48.43
5	Ferric Lixisols	LXf	7	0.09
6	Haplic Nitisols	NTh	755	10.09
7	Humic Nitisols	Nyu	1691	22.60
8	Lithic Leptosols	Lpq	62	0.83
9	Luvic Phaeozemes	PHI	7	0.09
10	Vertic Cambisols	CMv	504	6.74
11	Waterbody	WR	11	0.15

3.3.5 Land use land cover data

Land use and land cover is one of the main factors influencing the hydrological properties of a watershed. In hydrological models like Arc SWSAT, it is also one of the main input data to describe and define the Hydrological Response Units (HRUs) of the watershed.

3.3.5.1 Data acquisition and preprocessing

The land use land cover (LULC) data sets for the three historical periods were derived from multi-temporal series Landsat images. Landsat 5 Thematic Mapper (L5-TM) images of 1990, Landsat 7 Enhanced Thematic Mapper Plus (L7-ETM+) of 2005, and Landsat-8 Operational Land Imager and Thermal Infrared Sensor (L8-OLI/TRS) of 2020 at 30 m resolution were obtained from the United States Geological Survey (USGS) earth explorer website (http://earthexplorer.usgs.gov/) in GeoTIFF file format. The Selection of the Land sat satellite images data was influenced by the quality of the image especially for those with limited or low cloud cover and also to prevent seasonal variation of vegetation coverage. Therefore, the images were almost cloud-free and almost in the same annual season (Figure 3.9).

Table 3.4: The acquisition dates, sensor, path/row, resolution, cloud cover and the producers of the images

No	Year	Satellite Data	Path/Row	Acquisition Date	Cloud Cover (%)	Spatial Resolution	Producer
1	1990	L5-TM	168/54 169/54	18-12-1990 22-10-1990	0 0	30m 30m	USGS USGS
2	2005	L7-ETM+	168/54 169/54	19-12-2005 08-11-2005	0 0	30m 30m	USGS USGS
3	2020	L8-OLI	168/54 169/54	16-01-2020 07-01-2020	0 0	30m 30m	USGS USGS

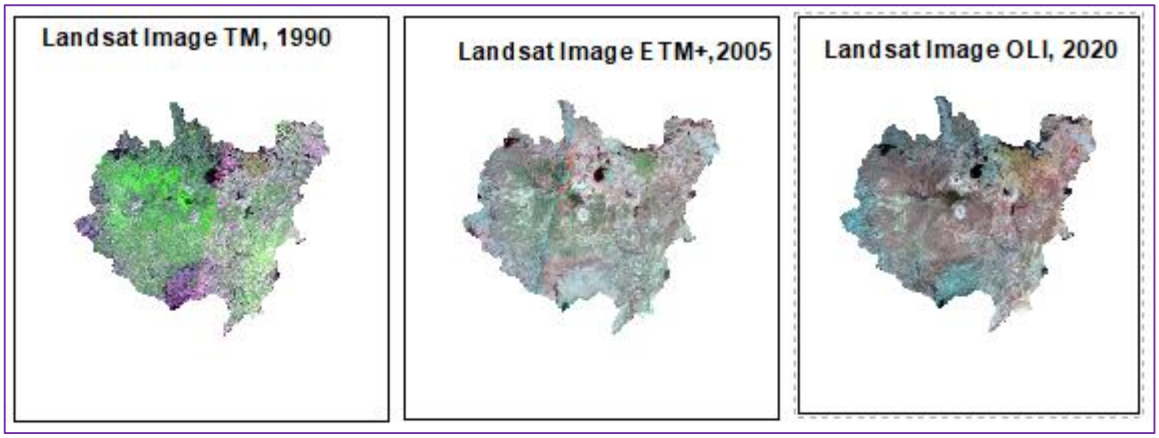

Figure 3.9: False color composite image of Upper Awash Sub-basin.

Preprocessing satellite imagery before conducting image classification and change detection is very vital to minimize instrumental errors and to build a more thorough association between the obtained data and surface features on the ground (Alawamy et al., 2020). Before classification, Layer stacking, mosaicking different layers of satellite image into one layer, Radiometric correction like noise reduction, histogram matching, periodic noise removal, and distrip, TM data and Masking the area of interest with the help of shape file were done using ERDAS IMAGINE 2015. The pre-processed satellite images were then classified by ERDAS IMAGINE 2015 and Google earth pro using supervised classification under the algorithm of Maximum Likelihood. Accordingly, seven categories were identified based on the nature and similarity of the use and cover types (Table 3.5).

Table 3.5: Description of the different LULC classification systems of the Upper Awash Sub-Basin

Land use land changes types	General description	SWAT code
Agriculture	Areas covered with annual crops followed by harvest and bare soil period	AGRL
Forest land	Areas composed of forest land and transplanted	FRSE
Shrubs land	This category includes low woody plants, generally less than three meters in height, usually with multiple stems, and grow vertically.	RNGB
Grassland	Landscapes that have a ground story in which grasses are the dominant vegetation forms	RNGE

Bare land	Areas with little or no vegetation cover consisting of exposed soil and/or bedrock	BARR
Urban	Where the dominant area covered by building and houses	URBN
Water body	Permanent open water, lakes, reservoirs and streams	WATR

3.3.5.2 LULC classification and accuracy assessment

The process of analyzing remote sensing data includes an important step called accuracy assessment. It establishes the information value of the resulting data for a particular user. The accuracy evaluation is used to determine the degree of a map's or categorized image's 'correctness.'

The development of a classification error matrix (also known as a confusion matrix or a contingency table) is one of the most frequent ways of displaying classification accuracy. Error matrices compare the relationship between known reference data (ground truth) and the related results of automated categorization on a category-by-category basis. This was done based on the ground truth in ERDAS Imagine 2015 and Google Earth Pro 7.3.3 software for the LULC maps of 1990, 2005, and 2020. The accuracy of classification was measured using measures generated from the error matrices, such as user, producer, and overall accuracy, as well as the kappa coefficient. If $K \leq 0.5$ shows rare agreement, $0.5 \leq K \leq 0.75$ shows a medium level of agreement, $0.75 \leq K \leq 1$ shows a high level of agreement, and $K = 1$ for perfect agreement (Dibaba et al., 2020).

$$K = \frac{P_O - P_C}{1 - P_C} \quad (3.3)$$

Where K is the Kappa coefficient, P_O is the proportion of correctly predicted cells and P_c is the expected proportion correction by chance between the observed and predicted map.

3.3.5.3 LULC change detection analysis

Land use and land cover change detection at various geographical and temporal scales rely heavily on remotely sensed satellite pictures. LULC change detection was used to identify, characterize, and quantify differences between imageries of the same study area and different periods. Three time periods for change detection were used in this study: 1990, 2005, and 2020. Using Arc GIS software and Microsoft excels, the LULC change detection was done utilizing a post classification cross-tabulation approach. The rate of change of each land use and land cover was calculated using the following formula.

$$\text{Percent change} = \frac{x-y}{y} * 100 \quad (3.4)$$

Where, X is the final area of LC and Y initial area of LC.

3.3.6 GCM/RCM data used

A climate scenario depicts future climate conditions (temperature, precipitation, and other climatological factors). In comparison to general circulation models (GCMs), regional climate models (RCMs) provide a new possibility for climate change effects study since they have a better spatial resolution and more accurate results on a regional scale (Turco et al., 2017). CORDEX-Africa, a project of the World Climate Research Program (WCRP), allows for the creation of high-resolution regional climate forecasts over Africa, which may be used to analyze future climate change consequences at regional and local scales. Climate change scenarios data from the newly released CMIP5 (Kim et al., 2014). CORDEX-Africa RCM ensemble output for African domain forecasts under RCPs 4.5 was utilized in this study. CORDEX Africa datasets are available for free at https://esgf-data.dkrz.de/search/esgf-dkrz/.

The CORDEX-Africa program provided climate data that were simulated GCMs (ICHEC-EC) and dynamically downscaled by RCMs, which is KNMI Regional Atmospheric Climate Model, version 22 (RAMO22 T).

Table 3.6: Description of GCMs and RCMs Considered in this Study

GCMs			RCMs		
Model	Full Name	Resolution (km)	Model	Full Name	Climate center
ICHEC-EC	Irish Center for High-End Computing Earth Consortium	50 × 50	RAMO22T	KNMI Regional Atmospheric Climate Model, version 22	EC-EARTH Consortium

3.4 Data Management and Analysis

3.4.1 Filling missing data

Having investigated the quality of all recorded climatic data, the first step was filling the missing time series data using different techniques. Some precipitation stations may have short breaks in the records because of absence of the observer or because of instrumental failures. It is often necessary to estimate or fill in this missing record. The missing precipitation of a station is estimated from the observations of precipitation at some other stations as close to and as evenly spaced around the station with the missing record as possible. According to Richard (1998), there are several methods for estimating missing rainfall data. These are; station average method, normal ratio methods, inverse distance weighting methods, and regression method. The missed data filling is based on a percent of missing monthly data during the study time series. In this, simple mathematical equation was applied to quantify the total percentage of missed values from the total data series as follows.

$$\text{\% of missed data } = \frac{X1}{X2} * 100 \tag{3.5}$$

Where, X_1 is count of missed data, X_2 is whole data set.

In rainfall data analysis, the big problem is missing of the observed daily data. The gap in the data should be filled before the data are subjected to the analysis. In this study, the percent of calculated missed data for four stations are greater than 10% and the remaining two stations are less than 10%. Therefore, the normal ratio method has been applied using the following equations.

$$P_x = \frac{1}{N}\left(\frac{N_x}{N_A}P_A + \frac{N_x}{N_B}P_B + \frac{N_X}{N_C}P_C \ldots + \frac{N_X}{N_N}P_N\right) \tag{3.6}$$

Where P_x is the precipitation for the station with missed record, $P_{A,}$ $P_{B,}$ P_C….P_N are the corresponding precipitation at the index stations and $N_{A.}$ $N_{B,\ NC}$ and N_X are the long term mean monthly precipitation at the index stations and at station x under consideration respectively.

3.4.2 Consistency test

To detect the possible errors checking the station for data quality using appropriate methods is crucial. Therefore, checking consistency of individual stations, the data qualities with regard to possible temporal variations or errors have been investigated by Double Mass Curve. The double mass analysis is used to detect if data at a site have been subjected to a significant change in magnitude due to external factors such as problems with instrumentation, observation practices, or recording conditions. If significant change in the system of the curve is observed, it should be corrected by:

$$P_x' = P_x * \frac{M'}{M} \tag{3.7}$$

Where P_x' is Corrected precipitation at station x

P_x is Original recorded precipitation at station x

M' is Corrected slope of the double mass curve

M is Original slope of the double mass curve

In these study, a group of six gauging stations was chosen to see if there was any variance in the catchment's gauging stations. Using a Microsoft Excel spreadsheet, the cumulative values of the target stations were displayed against the cumulative average of the surrounding stations. Since the graph was found to follow a nearly straight line, the records of these stations did not show any inconsistency, indicating that they were not subjected to any external factors during the study period. Therefore, Double mass curve for six representative's meteorological stations were illustrated in the appendix (B1).

3.4.3 Homogeneity test

Homogeneity is an important issue to detect the variability of the data. RAINBOW software is designed to study meteorological or hydrologic records by means of a frequency analysis and to test the homogeneity of the record. Frequency analysis of rainfall data requires that the data be homogeneous and independent. The restriction of homogeneity assures that the observations are from the same population. One of the tests of homogeneity is based on the cumulative deviations from the mean.

$$\mathrm{Sk} = \sum_{i=1}^{k} (\mathrm{Xi} - \mathrm{Xmean})\mathrm{k}\ \mathrm{i} = 1\ \mathrm{k} = 1 \tag{3.8}$$

Where Xi are the records from the series X1, X2… Xn and the mean. The initial value of S (k=0) and last value S (k=n) are equal to zero. When plotting the Sk's (sometimes called a residual mass curve) changes in the mean are easily detected. For a record Xi above normal the Sk increases, while for a record below normal Sk decreases. For a homogenous record one may expect that the Sk's fluctuate around zero since there is no systematic pattern in the deviations of the Xi's from their average value. If the cumulative deviation crosses one of the horizontal lines the homogeneity of the data set is rejected with respectively 90, 95 and 99 % probability.

For this study, the probabilities of rejecting the homogeneity of the datasets were evaluated in the homogeneity statistics menu as shown in the appendix (B2).

3.5 Trend analysis and Future Climate Projection

3.5.1 Trend analysis of observed precipitation and temperature

To detect and estimate trends, a variety of tests are available. The most widely used mathematical method for finding patterns in time series is the Mann–Kendall (MK) test. It was widely used to discover important patterns in hydro-meteorological time series, and the World Meteorological Organization strongly recommends it (WMO).

The first step is to determine the difference in sign between successive sample findings. The Sign $X_j - X_i$ is a function which implies that results in the value -1, 0, or +1 based on the sign $X_j - X_i$ where j>i. Positive and negative values of S presents upward and downward trend (Drapela et al., 2011) respectively. Therefore, the Mann–Kendall S Statistic trend test for a time series is computed as follows:

$$S = \sum_{i=1}^{n-1} \sum_{j=i+1}^{n} Sign(X_j - X_i) \tag{3.9}$$

$$Sign(X_j - X_i) = \begin{cases} +1, if\left(X_j - X_i\right) > 0 \\ 0, if\left(X_j - X_i\right) = 0 \\ -1, if\left(X_j - X_i\right) < 0 \end{cases} \tag{3.10}$$

Where 'S'is the rating score (Mann-Kendall sum); 'X' is the observation value; 'n'is the number of observation values in the time series; X_j and X_i are the sequential hydro-meteorological values in month and i (j>i) respectively. The value of S "+, -, and 0" implies increasing, decreasing and no trend, respectively.

If ties (equal values) in the X values happen, the variance of S is computed by

$$Var(S) = \frac{n(n-1) - \sum_{i=1}^{m} t_i(i)(i-1)(2i+5)}{18} \quad (3.11)$$

Whereas if ties are not occurred, the variance of S can compute by:

$$Var)S) = \frac{n(n-1)(2n+5)}{18} \quad (3.12)$$

In the time series data, m is the number of tied groups, and t_i is the number of data points in the i^{th} tied group. When n is more than 10, the Mann-Kendall statistic is used to generate the standard normal Z test statistics.

$$Z = \begin{cases} \frac{1-S}{\sqrt{Var(S)}}, if\ S > 0 \\ 0, if\ S = 0 \\ \frac{1+S}{\sqrt{Var(S)}}, if\ S < 0 \end{cases} \quad (3.13)$$

The test statistic Z is used as measure of significance of trend. In fact, this test statistic is used to test the null hypothesis, H_0. If |Z| is greater than Za/2, where a represents the chosen significance level (e.g.: 5% with Z 0.025 = 1.96) then the null hypothesis is invalid implying that the trend is significant. Software used for performing the statistical Mann–Kendall test is Addinsoft's XLSTAT 2022.

3.5.2 Future climate change impact on rainfall and temperatures

The future impacts of rainfall and temperature were analyzed under RCP4.5 scenarios for the upper Awash Sub-basin. The evaluation was made over 30 years of data ranges: For analysis, the years 2041-2070 are represented as the midterm. The projected change under RCP4.5 scenario was calculated against baseline (1976-2005) period. It is expressed as the difference between projected and historical value as expressed in the below equation.

$$Var_{change(\%)} = \frac{Var_{proj} - Var_{base}ref}{Var_{base}ref} * 100 \quad (3.14)$$

Where;

$Var_{change(\%)}$ is Variable percentage change

Var_{proj} is projected value

$Var_{base}ref$ is base reference value

3.5.3 Bias correction of future climate data

A statistical strategy for correcting the climate model's outputs departure from observable data is known as bias correction. This method is often used in hydrological modeling to adapt simulated climatic data at an appropriate regional and temporal scale. According to Christensen et al. (2007) the RCM's failure to adequately reproduce the current climate conditions is one fundamental source of uncertainty. Before calibrating the hydrological model with the RCM data, it is crucial to validate the output of the RCM using historical measurements. To account for any propensity to overestimate or underestimate the mean of downscaled data, bias correction was used. There are several bias correction techniques, but the Delta approach is one of the most popular and frequently used for RCMs scenarios of future conditions for climate change studies. It was chosen because it is straightforward and simple to apply (Sahilu and Niguse, 2015). The formulas used for rainfall and temperature bias correction are indicated in Equations 3.15 and 3.16, respectively.

$$P_{bc} = P_P \frac{P_O}{P_r} \tag{3.15}$$

$$T_{bc} = T_p + T_O - T_r \tag{3.16}$$

Where, P_{bc} is Bias corrected future rainfall amount in mm: P_P is predicted future rainfall amount in mm; P_O is mean of observed rainfall amount in mm: P_r is mean of computed historical rainfall during the observation period in mm. T_{bc} is Bias corrected future temperature in ^0C; T_p is predicted future temperature in ^0C; T_O is mean of observed temperature in ^0C; T_r is mean of computed historical temperature during the observed period in ^0C.

3.6 Hydrologic Model Setup and Simulation

3.6.1 SWAT model setup

The Soil and Water Assessment Tool (SWAT) model was developed by the US Department of Agriculture Research Service (USDA-ARS). It is a physical-based, semi-distributed, continuous time, and river basin or watershed scale model that operates on a daily time step and employs a command structure to route runoff and chemicals across the watershed. SWAT uses hydrological response units (HRUs) to express spatial variability in terms of land use, soil types, and slope within a watershed as a physical-based model. This model determines surface runoff using two methods; the Soil Conservation Service (SCS) curve number method or Green and Ampt (Green and Ampt, 1911), which gives the Green and Ampt infiltration method. On a daily time, step for watershed hydrological modeling with SWAT necessitates the use of spatially explicit datasets such as land use/land cover, soil data, climate, and hydrological data. The SWAT system is built on top of ArcGIS and incorporates a wide range of spatial environmental data, such as soil, land cover, slope, climate, and topographical features(Arnold and Fohrer, 2005).

3.6.1.1 Watershed delineation

The first step in creating SWAT model input is delineation of the watershed from a DEM. Inputs entered into the SWAT model are organized to have spatial characteristics. Before going in hand with spatial input data i.e. the soil map, LULC map and the DEM are projected into the same projection called UTM Zone 37N, which is a projection parameter for Ethiopia. A watershed is partitioned into a number of sub-basins, for modelling purposes. The watershed delineation process includes five major steps, DEM setup, stream definition, outlet and inlet definition, watershed outlets selection and definition and calculation of sub-basin parameters. For the stream definition the threshold based stream definition option was used to define the minimum size of the sub-basins.

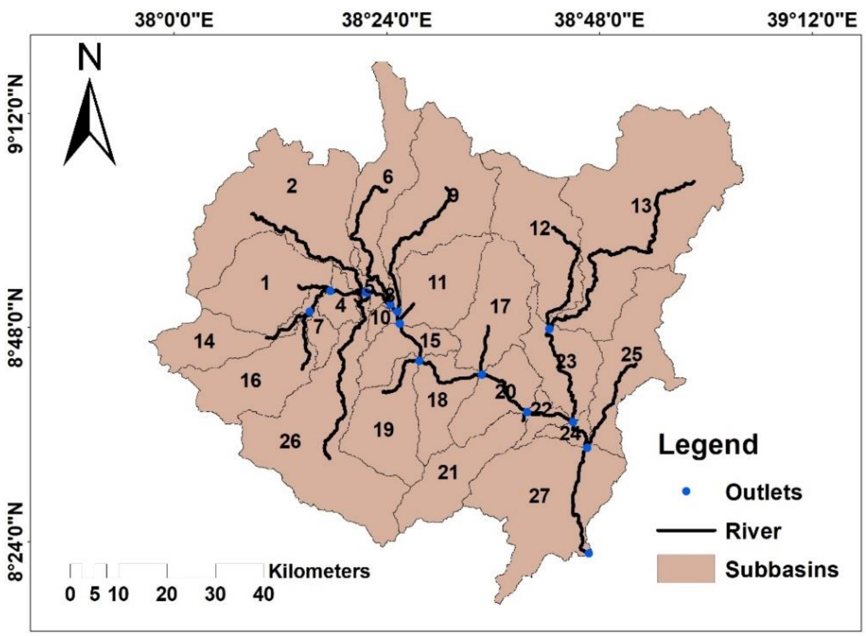

Figure 3.10: Sub-basins of the study area

3.6.1.2 Hydrologic response unit's determination

In SWAT, HRUs are defined as being unique occurrences of soil type, land cover, and slope class. Any parcels of land within one sub basin that share the same combination of these three features will be considered one HRU. All processes modeled by SWAT are done for each unique HRU in the watershed, independent of position within each sub basin. Multiple HRU slope discretization was selected for simplicity & saving time during parameterization of the HRU. In multiple HRU definition, a threshold level was used to eliminate minor land uses, soils or slope classes. The land use, soil, and slope class thresholds were set to 5%, 20%, and 20%, respectively, for the multiple HRU option that was chosen for my study. These numbers represent the proportions of the land use, soil, or slope class that the sub basin falls into. Since this region is deemed minor, it is not included in the analysis. After obtaining an HRU definition report, it was discovered that there were 183 HRUs in the area, which was separated into 27 sub basins.

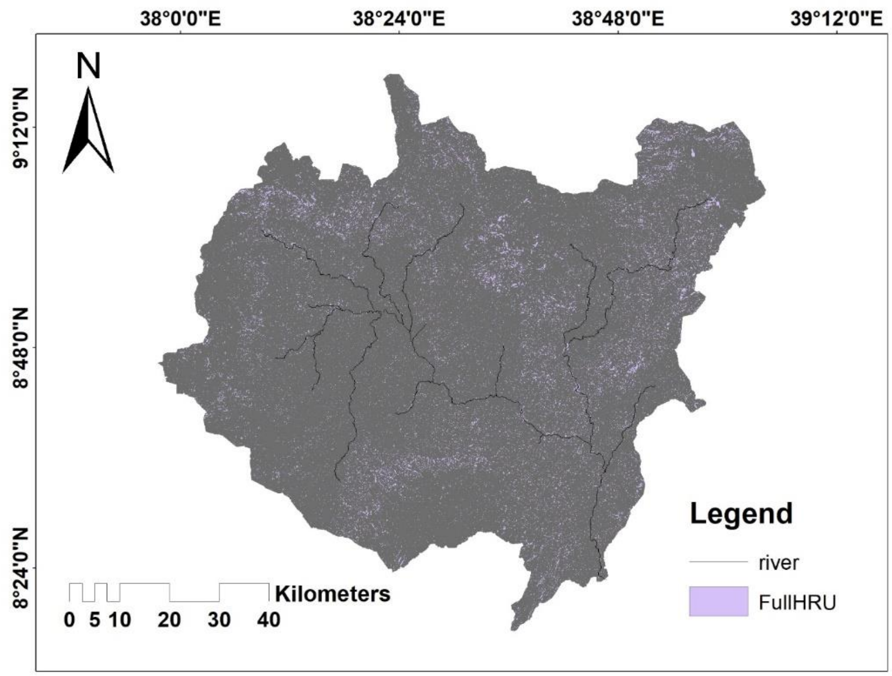

Figure 3.11: HRU map

3.6.1.3 Weather data

The WXGEN (SWAT software specification file coding scheme for weathering Generator file) weather Generator model included in SWAT was used to fill in gaps in measured records. The WGEN weather generator was provided with all the necessary statistical information from the meteorological records of the watershed. The meteorological information that was available in the watershed of the study region was used to construct these statistical values. Depending on the availability of the data in the stations, the number of years used to calculate the statistical values. Other meteorological data, such as daily precipitation, daily maximum and minimum air temperatures, daily relative humidity, daily solar radiation, and daily wind speed, were prepared using the SWAT format and then integrated into the model using the weather data input wizard. They also included the corresponding location table.

3.6.2 Hydrological component of SWAT

SWAT divides a watershed's hydrological simulations into two parts: the land phase and the routing phase. The amount of water, sediment, nutrient, and pesticide loadings to the main channel in each sub basin is controlled by the land phase of the hydrological cycle. During the routing phase, water, sediment, and agricultural chemicals are transported via the channel network to the watershed outlet.

3.6.2.1 Land phase of the hydrologic cycle

SWAT simulates the hydrological cycle based on the water balance in the land phase of the hydrological cycle.

$$SW_t = SW_0 + \sum_{i=1}^{t} \left(R_{day} - Q_{surf} - E_a - \omega_{seep} - Q_{gw}\right) \quad (3.17)$$

Where;

SW_t final soil water content (mm)

SW_0 initial soil water content on the day i (mm)

t time (days)

R_{day} amount of precipitation on the day i (mm)

Q_{surf} amount of surface runoff on the day i (mm)

E_a amount of water evapotranspiration on the day i (mm)

W_{seep} amount of water entering the vadose zone from the soil profile on the day i(mm)

Q_{gw} amount of water return flow on the day i (mm)

A. Surface runoff

The percentage of rainwater that is not lost to interception, infiltration, or evapotranspiration is referred to as surface runoff. surface runoff occurs whenever the rate of precipitation exceeds the rate of infiltration. SWAT offers two methods for estimating the surface runoff, the Soil Conservation Service (SCS) curve number method or the Green and Ampt infiltration method(Green and Ampt 1911) . In the Soil Conservation Service (SCS) curve number method often called the Curve-Number (CN) method, land use and soil characteristics are lumped into a single parameter. Because sub-daily rainfall data for the Green and Ampt infiltration methods was not available in the research area, the modified Soil Conservation Service curve number equation (USDA, 1972) was utilized to estimate the catchment's surface runoff. The SCS curve number method is a simple, commonly used, and effective method for estimating the quantity of runoff following a rainfall event in a variety of land uses and soil types.

The SCS curve number equation is (SCS, 1972):

$$Q_{surf} = \frac{(\mathrm{Rday} - \mathrm{Ia})^2}{(\mathrm{Rday} - \mathrm{Ia} + \mathrm{S})} \tag{3.18}$$

Where;

Q_{surf} accumulated runoff (mm water)

R_{day} Daily rainfall (mm water)

Ia Initial abstraction (mm)

S Retention parameter (mm water),

Where CN is the moisture condition curve number, the retention parameter (S) is defined by the following equation

$$S = 25.4(\frac{1000}{CN} - 10) \tag{3.19}$$

Where, CN = daily curve number. The CN is a function of hydrologic soil group, land use, land management, and antecedent soil moisture conditions.

B. Peak runoff rate

The maximum runoff flow rate that occurs with a specific rainfall event is known as the peak runoff rate. The peak runoff rate is a measure of a storm's erosive intensity and is used to forecast sediment loss. SWAT uses a modified rational method to compute the peak runoff rate.

$$\mathrm{qpeak} = \frac{\mathrm{C} * \mathrm{I} * \mathrm{A}}{3.6} \tag{3.20}$$

where qpeak is the peak runoff rate (m^3 /s), C is the runoff coefficient, i is the rainfall intensity (mm/hr), Area is the sub basin area ((km^2) and 3.6 is a unit conversion factor.

C. Potential Evapotranspiration

Potential evapotranspiration (PET) was a concept originally introduced by Thornthwaite (1948) as part of a climate classification scheme. He defined PET is the rate of evapotranspiration that would occur if a wide area was uniformly covered with growing plants, had an infinite supply of soil water, and was not subjected to advection or heat storage effects.

Numerous methods have been developed to estimate PET. Three of these methods have been incorporated into SWAT: the Penman-Monteith method (Monteith 1965; Allen 1986; Allen et al. 1989), the Priestley-Taylor method (Priestley and Taylor 1972) and the Hargreaves method (Hargreaves et al., 1985). The model will also read in daily PET values if the user prefers to apply a different potential evapotranspiration method

The three PET methods included in SWAT vary in the amount of required inputs. The Penman-Monteith method requires solar radiation, air temperature, relative humidity and wind speed. The Priestley-Taylor method requires solar radiation, air temperature and relative humidity. The Hargreaves method requires air temperature only. Depending upon the availability of input data, I have selected the penman monteith method.

i. Penman-monteith method

The Penman-Monteith equation includes terms for the energy required to maintain evaporation, the strength of the mechanism required to remove the water vapor, and aerodynamic and surface resistance. The following Penman-Monteith formula is used to calculate the evapotranspiration. Because Penman-Monteith considers varies input data, to prove high quality results.

$$\lambda E = \frac{\Delta.(H_{net} - G) + \rho_{air}.[e_z^0 - e_z]/ra}{\Delta + \gamma(1 + \frac{rc}{ra})} \tag{3.21}$$

Where;

λE is the latent heat flux density (MJ m-2 d-1), E is the depth evaporation rate [mm/day], $Hnet$ is net radiation at the crop surface [MJm/day], G is soil heat flux density to the ground [MJ/m2 day], Δ is the slope of the saturated vapor pressure curve, de/d[kpa/°C], γ is Psychrometric constant [kpa/°C], ρair is the air density (kg/m3), Cρ is the specific heat at constant pressure (MJ/kg °C), ezo is the saturated vapor pressure of air at height z [kpa], ez is the water vapor pressure of air at heigh z [kpa], rc is the plant canopy resistance (s/m), ra is the diffusion resistance of the air layer (aerodynamic resistance) (s/m).

3.6.2.2 Routing phase

The routing phase is the second division of hydrological cycle which can be defined as the movement of water, sediments, etc through the channel network of the watershed to the outlet.

Water is routed through the channel network using the variable storage routing method or the Muskingum river routing method. The variable storage routing method was developed by (Williams, 1969) based on the principle continuity equation in routing the storage volume and used in the HYMO (Williams and Hann, 1973) and ROTO (Arnold et al, 1995) models. For a given segment, storage routing is based on the continuity equation. Therefore, this routing method was adopted in this study and it is expressed as:

$$\Delta V_{stored} = V_{in} - V_{out} \quad (3.22)$$

Where: V_{in} is the volume of inflow during the time step (m3 water),V_{out} is the volume of outflow during the time step (m3 water), and $\Delta V_{storage}$ is the change in volume of storage during the time step (m3 water).

3.6.2.3 Soil erosion and simulation

Algorithms to simulate watershed erosion are also included in the SWAT watershed model. Each Hydrologic Response Unit (HRU) has an estimated amount of erosion brought on by rainfall and runoff. use the MUSLE, or Modified Universal Soil Loss Equation (Williams and JR, 1990). The surface runoff volume, peak runoff rate, HRU area, USLE soil erodibility factor, USLE cover and management factor, USLE support practice factor, USLE topographic factor, and a coarse fragment factor are used by MUSLE to estimate sediment yield. The modified universal soil loss equation (MUSLE) (Williams, 1995) is:

$$\mathrm{Sed} = 11.8 * \left(Q_{surf} * Q_{peak} * A_{hru}\right)0.56 * K_{USLE} * C_{USLE} * P_{USLE} * LS_{USLE} * CFRG \quad (3.23)$$

Where: Sed is the sediment yield on a given day in metric tons, Qsurf is the surface runoff from the watershed in (mm), Q_{peak} is the peak runoff rate in cubic meter per second, A_{hru} is the area of HRU, K_{USLE} is the USLE soil erodability factor, C_{USLE} is the USLE land cover and management factor, P_{USLE} is the USLE support practice factor, LS_{USLE} is the USLE topographic factor, and CFRG is the coarse fragment factor.

3.7 Sensitivity Analysis, Calibration, and Validation

The model was then run after it had been set up, however the results of the simulation cannot immediately be applied to further investigation. Instead, sensitivity analysis, model calibration, and model validation should be used to assess the model's capacity to adequately predict the constituent stream flow and sediment yield (White and Chaubey, 2005).

3.7.1 Sensitivity analysis

Sensitivity analysis is a technique of identifying the responsiveness of different parameter involving in the simulation of a hydrological process. Model sensitivity is defined as the change in model output per change in parameter input. Sensitivity analysis describes how model output varies over a range of a given input variable (Arnold et al., 2012).

In general, an important aim of the parameter sensitivity analysis is to allow the possible reduction in the number of parameters that must be estimated, thereby reducing the computational time required for model calibration.

3.7.2 Model calibration and validation

3.7.2.1 Model calibration

Model calibration is the processes of estimating model parameters by comparing model prediction (output) for a given set of assumed conditions with observed data for the same conditions. The calibration of the model has been done based on the assumption of there is a linear relation between the observed and the simulated one. That mean all of the error variance is contained in the simulated values and the measured data are free of error. But in reality the measured data are not free of error (Moriasi et al, 2007). The goal of calibration is to find those set of parameter values for the model that gives a simulated hydrological series adequately matches with the observed series. Therefore, for this study, the calibration was carried out at monthly time steps using flow and sediment data series.

3.7.2.2 Model validation

Validation is comparison of the model outputs with an independent dataset without further adjustments of the values of the parameters (Neitsch, 2002). In order to utilize any predictive watershed model for estimating the effectiveness of future potential management practices the model must be first calibrated to measured data and should then be tested (without further parameter adjustment) against an independent set of measured data. This testing of a model on an independent data set is commonly referred to as model validation.

Generally, Calibration and validation of the SWAT hydrological model were undertaken using the sequential uncertainty fitting ver-2 (SUFI-2) algorithm in SWAT CUP (Abbaspour et al., 2012). In SUFI-2, all sources of uncertainties, such as uncertainty in driving variables, conceptual model, parameters, and measured data, are mapped to a set of parameter ranges. The uncertainty is quantified at the 2.5% and 97.5% levels of the cumulative distribution of an output variable obtained through Latin hypercube sampling, and it is referred to as the 95% prediction uncertainty (95PPU) (Abbaspour et al., 2015).

3.7.3 Model performance evaluation

There are different types of statistical method of model performance evaluation techniques. Among this the, most commonly used for this study are: - coefficient of determination (R^2) and Nash-sutcliffe efficiency (NSE), percent bias (PBIAS) and root mean square error standard deviation ratio (RSR) are the most widely used to evaluate the performance of the hydrological model using the following equations.

i. **Coefficient of determination (R^2):** the values show the strength of the association between the observed and simulated value. The R^2 varies from 0 to 1, the higher the values, the less error variance (Moriasi et al., 2007). The R^2 > 0.5 is acceptable (Santhi et al., 2001).

$$R^2 = \frac{\left(\sum_{i=1}^{n}(Oi - Oav)(Pi - Pav)\right)^2}{\sum_{i=1}^{n}(Oi - Oav)^2 \sum_{i=1}^{n}(Pi - Pav)^2} \quad (3.24)$$

ii. **Nash-Sutcliffe Efficiency (NSE):** it shows how well the plot of measured data versus simulated data closes the 1:1 line. NSE ranges between −∞ and 1.0 (1 inclusive), with NSE = 1 being the optimal value. Values between 0.0 and 1.0 are generally viewed as acceptable levels of performance(Moriasi et al., 2007)

$$NSE = \frac{\sum_{i=1}^{n}(Oi - Oav)^2 - \sum_{i=1}^{n}(Pi - Pav)^2}{\sum_{i=1}^{n}(Oi - Oav)^2} \quad (3.25)$$

iii. **Percent bias (PBIAS):** The average tendency of the simulated data to be larger or smaller than their observed counterparts is measured by percent bias (PBIAS). optimal value of PBIAS is 0.0, with low-magnitude values indicating accurate model simulation. Positive values indicate model underestimation bias, and negative values indicate model overestimation bias.

$$PBIAS = \frac{\sum_{i=1}^{n}(Oi - Pi) * (100)}{\sum_{i=1}^{n}(Oi)} \quad (3.26)$$

iv. **RMSE-observations standard deviation ratio (RSR):** RMSE is one of the commonly used error index statistics. it is commonly accepted that the lower the RMSE the better the model performance. RSR is calculated as the ratio of the RMSE and standard deviation of measured data.

$$RSR = \frac{RMSE}{STDEV_{Obs}} = \frac{[\sqrt{\sum_{i}^{n}(Oi - Pi)^2}]}{[\sqrt{\sum_{i}^{n}(Oi - Oav)^2}]} \quad (3.27)$$

Where; Oi is observed discharge, Pi is predicted discharge, Oav is average observed discharge, Pav is average predicted discharge.

Table 3.7: General performance ratings for recommended statistics for a monthly time step *(Moriasi et al., 2007)*

Performance Rating	R^2	RSR	NSE	PBIAS (%)	
				Streamflow	Sediment
Very good	$0.7< R^2 \leq 1$	$0 \leq$ RSP ≤ 0.5	0.75<NSE≤1	PBIAS<±10	PBIAS<±15
Good	$0.6<R^2\leq 0.7$	0.5≤ RSP ≤0.6	0.65<NSE≤0.75	±10≤ PBIAS<±15	±15≤ PBIAS<±30
Satisfactory	$0.5<R^2\leq 0.6$	0.6 ≤ RSP ≤ 0.7	0. 5<NSE≤0.65	±15≤ PBIAS<±25	±30≤ PBIAS<±55
Unsatisfactory	$R^2<0.5$	RSP > 0.7	NSE ≤ 0.5	PBIAS≥±25	PBIAS≥±55

3.8 Analysis of Streamflow and Sediment Yield Responses under Changing Climate and LULC

To analyses the outcome of change in LULC and climate upon the streamflow and sediments, Climatic datasets for the period of 1989–2019 were broken into three periods, i.e., 1989-1999, 2000-2010 and 2011-2019 and LULC maps for the year of 1990, 2005 and 2020 were used in this study. Four scenarios were created using these datasets and are displayed in Table 3.8. The first period with 1990LULC and climate of (1989–1999) was regarded as the baseline period and the other periods were regarded as altered periods (Kidane et al., 2019).

Table 3.8: Different scenario for assessing hydrological impacts of land use and climatic during 1989–2019

Scenario Considered	Land Use	Timeline of considered climatic conditions (Temp., Rainfall.)
S1 Baseline scenario	1990	1989–1999
S2 Climate change scenario	1990	2011–2019
S3 LUCC scenario	2020	1989–1999
S4 Combined scenario	2020	2011–2019

3.8.1 Analysis of streamflow responses under changing climate and LULC

A fixing-changing method was used to assess the effect of LULC and climate change on the hydrological process (Woldesenbet et al., 2017; Yang et al., 2017; Yin et al., 2017). The difference between hydrological variables (streamflow) for baseline and Altered scenarios would give the isolated and combined impact of climate and LULC change. The difference between streamflow obtained from scenario S2 and S1 would give the isolated impact of climate during 1989-2019. The 2020 LULC and 1989-1999 climate were utilized in scenario S3, and the difference between the streamflow derived under S3 and S1 would indicate the impact of climate change. Climate data from 2011 to 2019 and the LULC of 2020 were used in scenario S4. The combined impact of LULC and climate change between 1989 and 2019 would be represented by the difference between streamflow calculated from S4 and S1.

The percentage change in streamflow is given by the following equations.

$$\Delta SR_{Climate=} \frac{S2 - S1}{S1} * 100 \qquad (3.28)$$

$$\Delta SR_{LULC=} \frac{S3 - S1}{S1} * 100 \qquad (3.29)$$

$$\Delta SR_{Combined=} \frac{S4 - S1}{S1} * 100 \qquad (3.30)$$

Where ΔSR is change in streamflow and S is Scenario.

3.8.2 Analysis of sediment yield responses under changing climate and LULC

Similarly, a fixing-changing method was applied for analysis of sediment yield Responses under changing climate and LULC. The percentage change in Sediment Load is given by the following equations.

$$\Delta SED_{Climate=}\frac{S2-S1}{S1}*100 \quad (3.31)$$

$$\Delta SED_{LULC=}\frac{S3-S1}{S1}*100 \quad (3.32)$$

$$\Delta SED_{Combined=}\frac{S4-S1}{S1}*100 \quad (3.33)$$

Where ΔSED is change in Sediment load (Tons) and S is Scenario.

3.9 Identification of Critical Sub-Watersheds

Once SWAT model was calibrated and validated, it was run for a period 30 years (1989 to 2019), then the overall simulated output can be used for further and sediment source areas were identified. Based on the spatial variability of sedimentation rate the potential area of intervention can be identified. SWAT calculates the soil erosion and sediment yield within each hydrological response units (HRU's) within each sub basins. The average annual yield of sedimentation for each sub-basin was used to generate sediment source map. From the model simulation output, sediment source areas were identified in the Upper Awash Sub-Basin. This helps to prioterize and formulate development and conservation plans in order to use available economic resource optimally. Since the erosion process occurred in the watershed is believed to be the major source of sediment load, it is important to give due attention for appropriate watershed management practices at least for those places which are major cause for higher sediment yield.

In this study, high sediment source sub basins to reduce sediment yield were identified and prioritized based on annual sediment yield simulated using current 2020 LULC in the SWAT model from the sub-watershed.

3.10 Developing Best Management Practices

To reduce soil erosion and sediment transport, the implementation of best management practices (BMPs) in watersheds has been recognized as an effective method (Betrie et al., 2010). According to spatial variability of sediment yield, the source-level identified by SWAT model was applied to simulate the effectiveness of BMPs to reduce sediment yield. The best management practices are represented in the SWAT model by modifying SWAT parameters to reflect the effects of practices on the process simulated within the SWAT model (Waidler et al., 2011). However, the selection of these best management practices and the values of their parameters are site-specific and should reflect the reality of the study area (Nadew et al., 2019).

In this study, there will be three different management scenarios (filter strips, terracing, and reforestation) can be selected and implemented in the SWAT model based on the Ministry of Agriculture and Rural Development guideline (Desta et al., 2005). The effectiveness of these BMPs scenarios was quantified by comparing each one with the baseline scenario to obtain a percent of the reduction. This effectiveness will be computed using Equation below.

$$\text{Effectiveness } (\%) = \frac{Y_{\text{baseline}-Y_{\text{BMP}}}}{Y_{\text{baseline}}} * 100 \tag{3.35}$$

Where Y_{baseline} and Y_{BMP} are the average annual sediment yields in the baseline scenario and BMP scenario respectively.

Three distinct scenarios were created for this study and compared based on how well they would conserve soil or reduce silt. The three situations were Parallel Terracing, Filter Strip (5m), and Reforestation. Comparisons of the efficacy of the suggested sediment reduction scenarios were made using the baseline scenario as a point of comparison.

3.10.1 Baseline scenario

In the baseline scenario, the existing watershed condition was considered. The baseline scenario corresponds to the current land management practice without conservation measures. The baseline scenario was obtained by running the SWAT model using the 2020 LULC.

3.10.2 Filter strip

Between cropland, grazing land, forest land, or other disturbed land and surface water bodies are vegetated areas called "filter strips." Filter strips are also known as buffer filters or vegetative filters. To get rid of bigger soil particles, they are typically installed where runoff water exits a field. Larger particles, such as soil erosion, may settle out when runoff water leaves a field later than expected. In this case, agricultural fields in each key sub-basin were given 5 m wide filter strips. Through the FILTREW parameter specified in MGT (.mgt) of the SWAT input table, which indicates the width of the strip, SWAT offers a specific technique to incorporate filter strips. The model can simulate the width of filter strips from 1 m to 30 m based on local research experiences in Ethiopian watersheds (Gashaw et al., 2021). Equation 3.36 is used by the SWAT model to determine sediment trapping effectiveness (Neitsch et al., 2012).

$$trap_{eff} = 0.367*FILTREW^{0.2967} \quad (3.36)$$

Where $trap_{eff}$ is trapping efficiency and FILTERW is the width of the vegetation strips.

3.10.3 Parallel terrace

In order to lessen erosion by shortening the slope and retaining runoff for moisture conservation, terraces are an earthen embankment or combination of ridge and channel built across the field slope. Terracing a field reduces peak flow rate by reducing the slope, reduces sheet and gully erosion by increasing the quantity of sediment settling in the runoff, and reduces surface runoff by trapping water in shallow depressions. Terracing was simulated in this study by turning on the terracing option in the SWAT's planned management operations tool (.mgt). The USLE support practice factor (USLE P) and average slope length are the model parameters that are suitable for representing the effect of parallel terraces (SLSUBBSN). The values of SLSUBBSN for the average slope of the HRU were set based on Equation 3.23 (Arabi et al., 2006) whereas USLE_P were assigned from the SWAT user's manual version 2012 for terraced conditions (Neitsch et al., 2012).

$$\mathrm{SLSUBBSN} = (0.21 * \mathrm{S} + 0.9)\frac{100}{S} \quad 3.37$$

Where SLSUBBSN is the average slope length of the sub-basin and S is the average slope of the HRU.

3.10.4 Reforestation

Reforestation calls for returning the area to its previous state of natural vegetation. Reforestation of agricultural land that is prone to large sediment yields, bare land was all taken into consideration in this study and compared to the aforementioned two possibilities. These were carried out by turning on the SWAT model's Land Use Update (. LUP) tool, which enables the addition of new land use updates and the deletion of current ones.

3.11. Conceptual Framework on General Methodology of the Study

In this work, BMPs were created and hydrological model SWAT was utilized to investigate hydrological impacts of Climate and LULC change. Figure 3.12 outlines the techniques' sequential processes together with the data the SWAT model needs in order to accomplish the study's goals. The general process of the study is shown in the following framework.

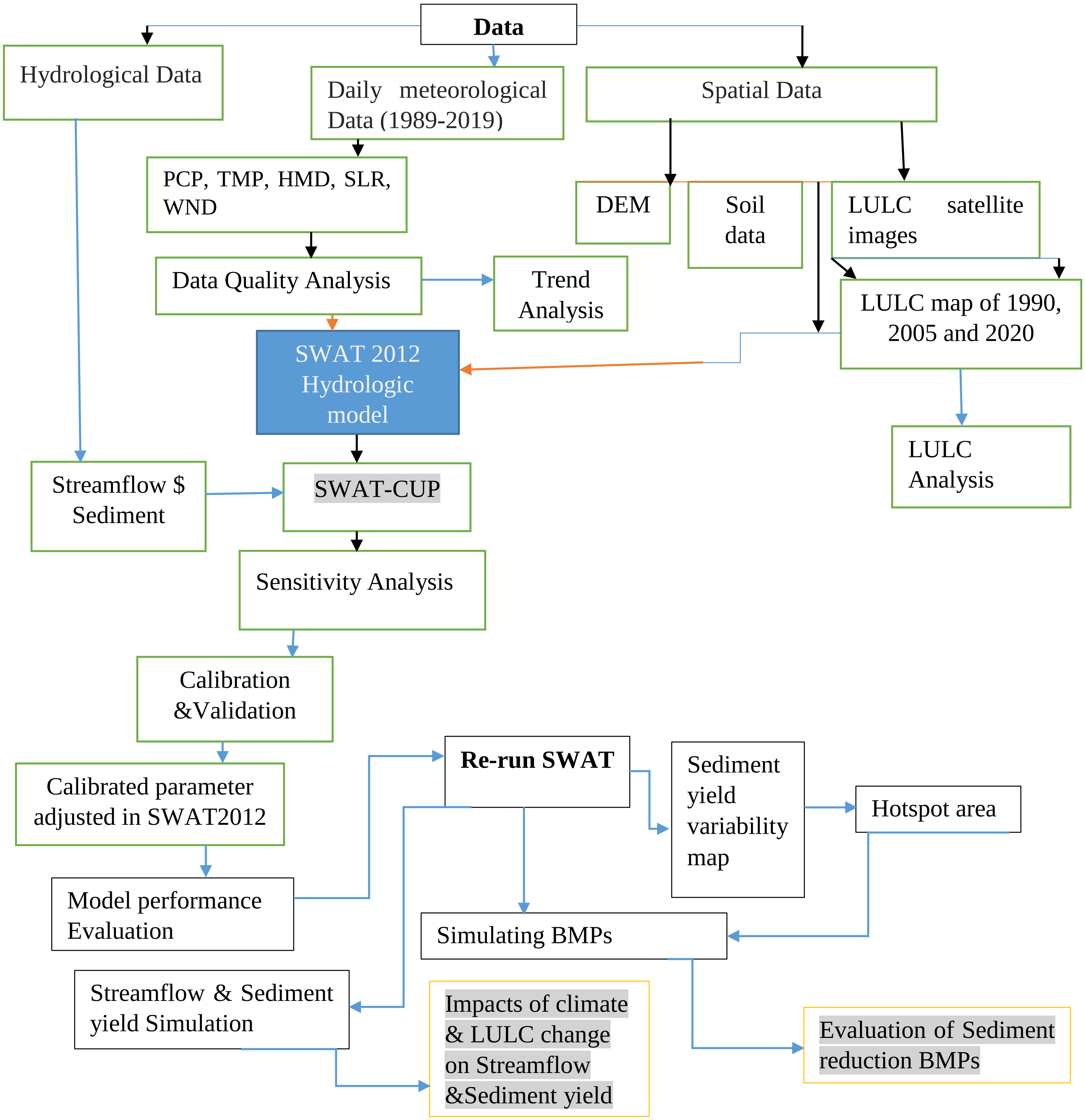

Figure 3.12: Conceptual Framework

4. RESULTS AND DISCUSSIONS

4.1 Trend Analysis and Future Climate Projections

4.1.1 Trend analysis of observed precipitation and temperature

The upper Awash basin's long-term trend of observed rainfall was analyzed in terms of annual time series using a non-parametric Kendall trend test with a significance level of 5%. The significance test in this study used normalized P-values. When the P-value is smaller than the significance level at alpha 0.05, the null hypothesis is rejected, and the alternative hypothesis should be accepted, and vice versa. The figure below and in the appendix shows upward trend for Mojo, Intoto, and Tulu Bolo rainfall station while downward trend for A.A.Bole and Asgori stations. The annual rate of change in rainfall is more at Mojo station (+11.791) while decreasing at A.A Bole station (-15.945) as shown in Figure 4.1. The study conducted by Tadese et al. (2019) on Hydro-Climatic Variability (Characterization and Trend Study) of the Awash River Basin, conclude that the MK test showed that most of the significant trends in annual rainfall were decreasing. The annual rainfall trend for remaining stations were illustrated in the appendix B3.

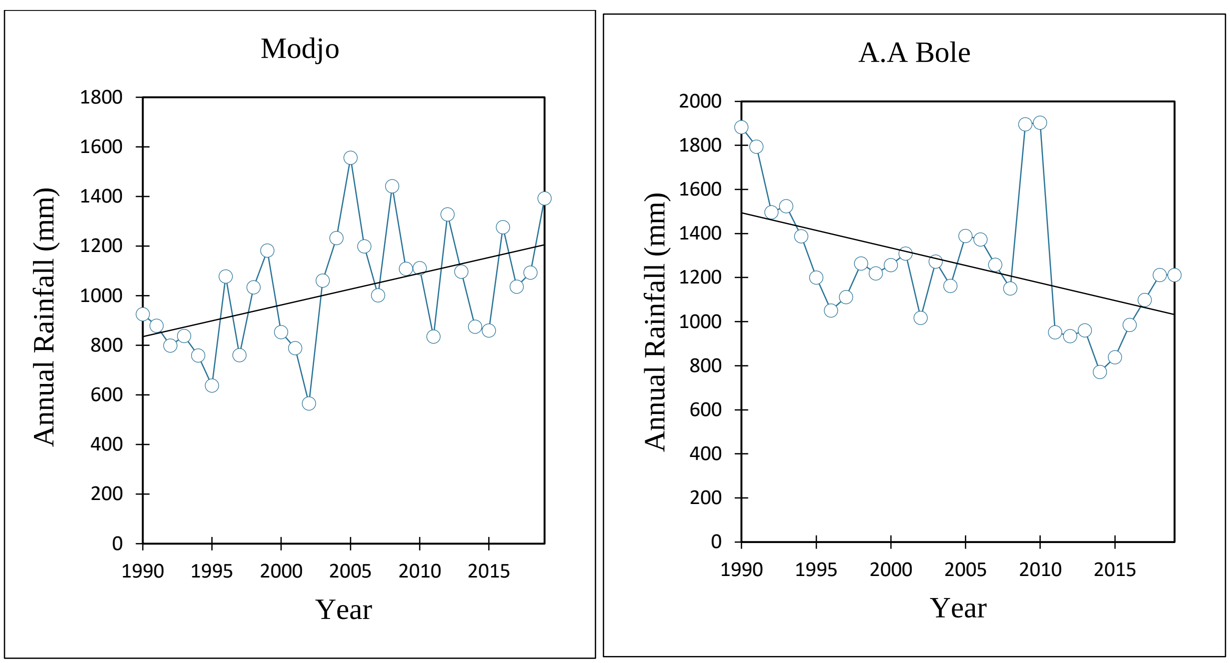

Figure 4.1: Observed long-term annual of rainfall trend distribution from 1989-2019

Table 4.1: Mann-Kendal trend test and statistical summary of Rainfall of all stations in upper Awash Sub-basin (1989-2019)

Stations Name	**S**	Kendall's tau	p value	Sen's slope
A.A Obsrv	-16	-0.039	0.778	-2.323
T.Bolo	23	0.053	0.695	2.681
A.A Bole	-154	-0.354	0.006	-15.945
Asgori	-119	-0.274	0.035	-8.175
Intoto	37	0.085	0.521	2.773
Modjo	135	0.310	0.017	11.791

Most studies showed that temperature is expected to rise worldwide and the result was also found relatively similar for this study as shown in Appendix. As summarized in Table 4.2 (A) and (B) for each station both maximum and minimum temperature respectively indicates warming trend. On average, maximum and minimum temperature in the study area increased by 0.06°C and 0.02°C per annual, respectively. Similarly, increasing trends for maximum temperature was observed at Intoto station. For minimum temperature, A.A Bole and Asgori station indicates increasing trend while Mojo presents insignificant decreasing trend.

Table 4.2: Mann-Kendal trend test and statistical summary of annual maximum (A) and minimum (B) temperature at six stations in Upper Awash Sub-basin (1989-2019)

(A). Maximum temperature (°C)

Station	S	Kendall‟s tau	P-value	Sen‟s
A.A Obsrv	189	0.434	0.001	0.033
T.Bolo	91	0.209	0.108	0.056
A.A Bole	187	0.430	0.001	0.137
Asgori	157	0.361	0.005	0.063
Intoto	19	0.044	0.748	0.008
Modjo	199	0.457	0.0001	0.062

(B). Minimum temperature (°C)

Station	S	Kendall"s tau	P-value	Sen"s
A.A Obsrv	149	0.343	0.008	0.031
T.Bolo	31	0.071	0.592	0.008
A.A Bole	145	0.333	0.01	0.066
Asgori	157	0.361	0.005	0.058
Intoto	157	0.361	0.005	0.024
Modjo	-117	-0.269	0.038	-0.033

4.1.2 Future climate projection (2041-2070)

The future climate data was projected using the selected climate model under RCP4.5 scenarios. This future climate data includes precipitation and, maximum and minimum temperature The downscaled values of precipitation for the base period were averaged into a monthly time step to compare with the observed values, which are shown in figure. 4.2.

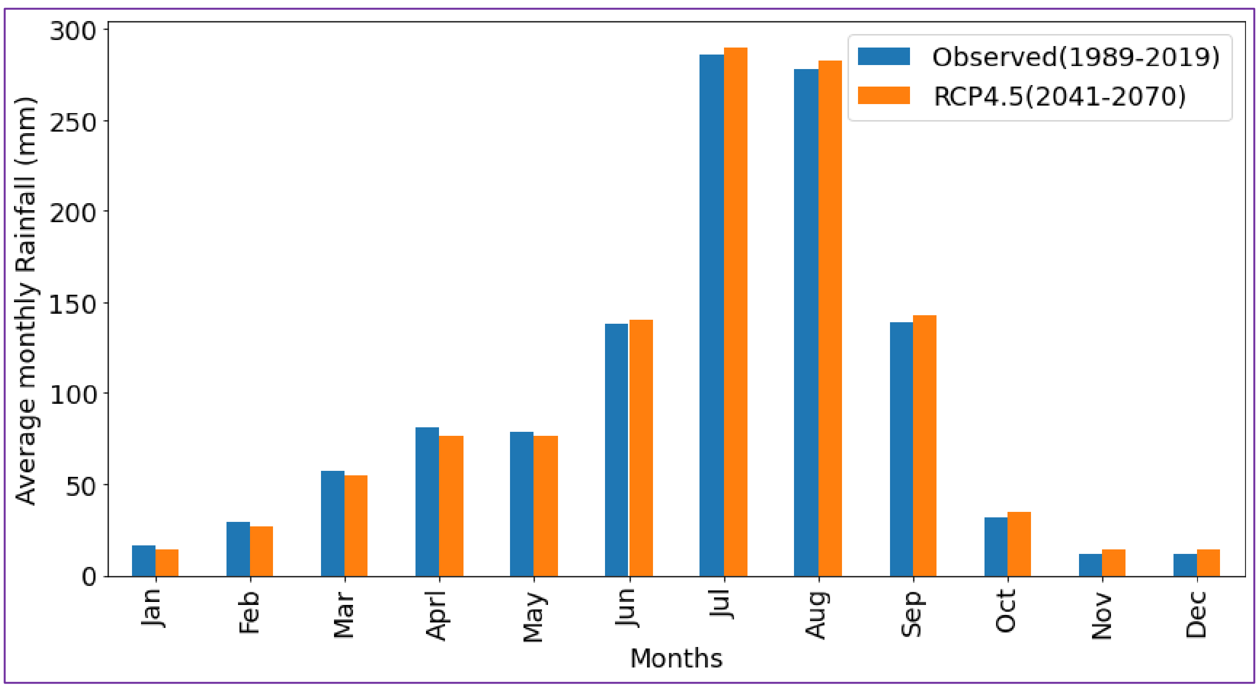

Figure 4.2: Future bias corrected and observed Rainfall

(A). Projected change of rainfall.

The properties of precipitation at the basin can be assessed using projected changes in precipitation data. The average mean monthly rainfall result shows that in the future monthly rainfall decreases in all months during (2041-2070) compared to the observed rain fall. Except, July, August, September, October, November and December in which increasing mean monthly rainfall is observed under RCP 4.5 scenario.

Figure 4.3 shows the percentage change in precipitation between the reference period (1989–2019) and projected periods of (2041–2070). The projected change shows an increasing pattern principally from August-December. December will be the highest 11% increasing change. and Decreasing pattern from January-July. Similarly, Kiya (2018) reported that the mean areal annual rainfall over upper Awash sub-basin decrease by 1.11 % and 8.15 % in 2030's and 2050's respectively under RCP 4.5 scenarios. Also decreasing future annual rainfall is observed in 2030's and 2050's in RCP 8.5 scenarios by 16.93 % and 22.59 % respectively.

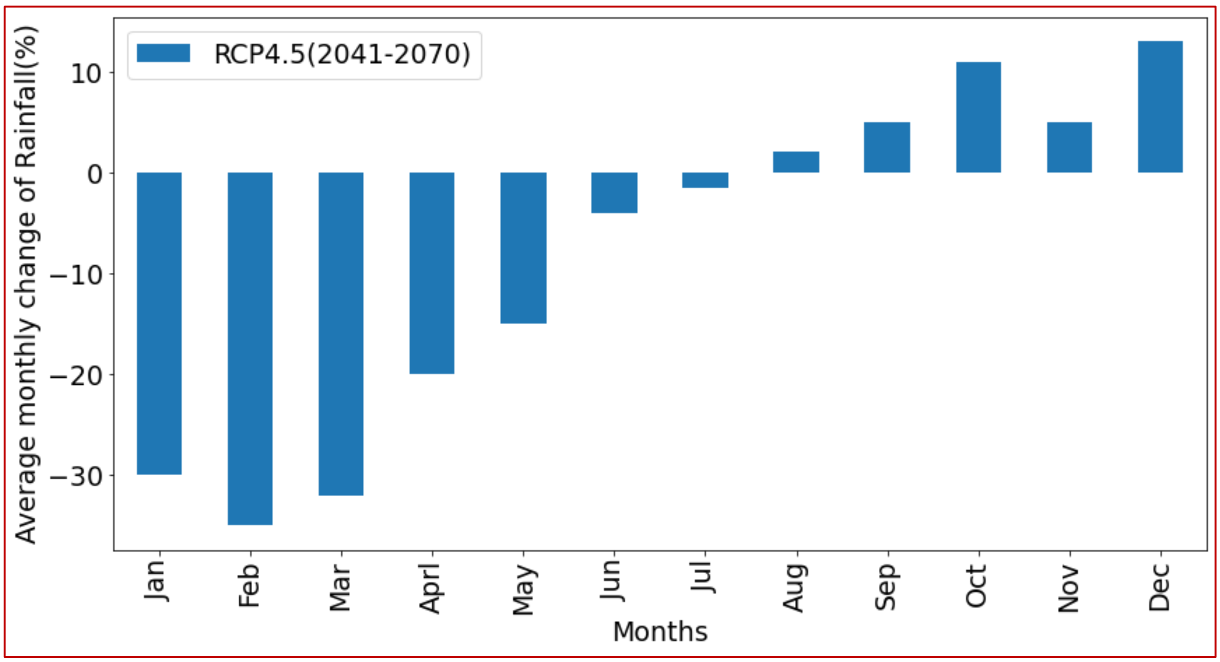

Figure 4.3: Change in monthly rain fall over the period (2041-2070)

(B). Projected Maximum Temperature

The majority of research indicate that global temperatures are expected to rise, and this study's findings were pretty similar. Figure 4.4 presents the average monthly maximum temperature change for RCP4.5 over the period of 2041-2070. The maximum temperature scenario generation showed an increase in mean maximum temperature in all the months. RCP4.5 scenario suggests increase of temperature by 8.7.%. Also the change in mean monthly maximum temperature ranges between 0.4°C in June and 2.3 °C in April for RCP4.5 scenarios in 2041-2070. The result is consistent with the study found by Abdulahi et al. (2021) on the response of climate change impacts on streamflow in the Upper Awash Basin and reported that the maximum temperature change could be +6.3% under RCP4.5 and +7.6% under RCP8.5 for the period of 2041-2060. Generally, IPCC (Pacheri et al.,2014) indicated that, "under high emission scenario, average temperature will rise more than 2°C, the threshold set in current international agreement, over most of the continent by the mid-21st century". Average temperature will rise more than 4°C across most areas by the late 21st century". The projected temperature in this study for mid-term under both RCP4.5 scenario lies within the range of temperature projected in the AR5 for Africa‟s future climate trends (Pacheri et al., 2014).

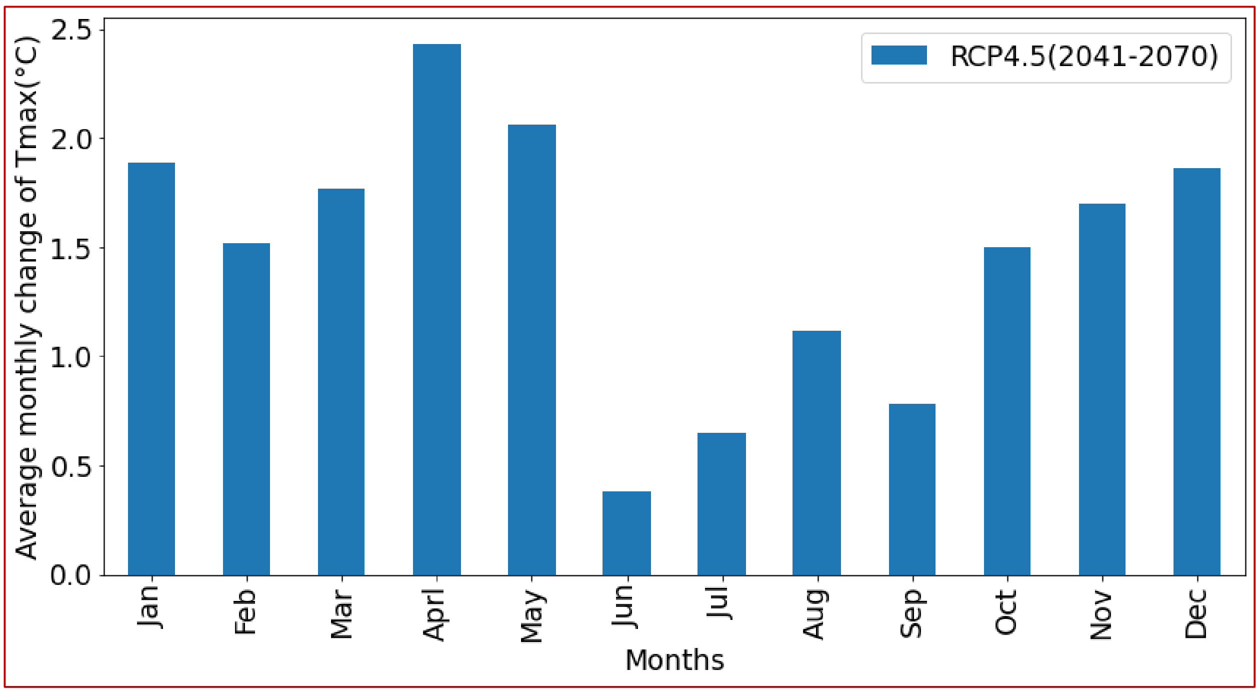

Figure 4.4: Monthly maximum temperature changes over the period (2041-2070)

(C). Projected Minimum Temperature

Figure 4.5, Average monthly percentage change of minimum temperature under RCP 4.5 scenarios. As can be seen the minimum temperature under RCP 4.5 is expected to increase. As shown below the change in mean monthly minimum temperature increases in range between 0.95 °C in April and 1.98 °C in September for RCP4.5 scenarios in 2041-2070. On average the projected minimum temperature is expected to increase by 12.5% under RCP 4.5. Moreover, the increment of minimum temperature is relatively high compared to the maximum. The predicted temperature is within the predicted range of average temperature increases from 1.4% to 20% at the end of the 21st century IPCC (2007).

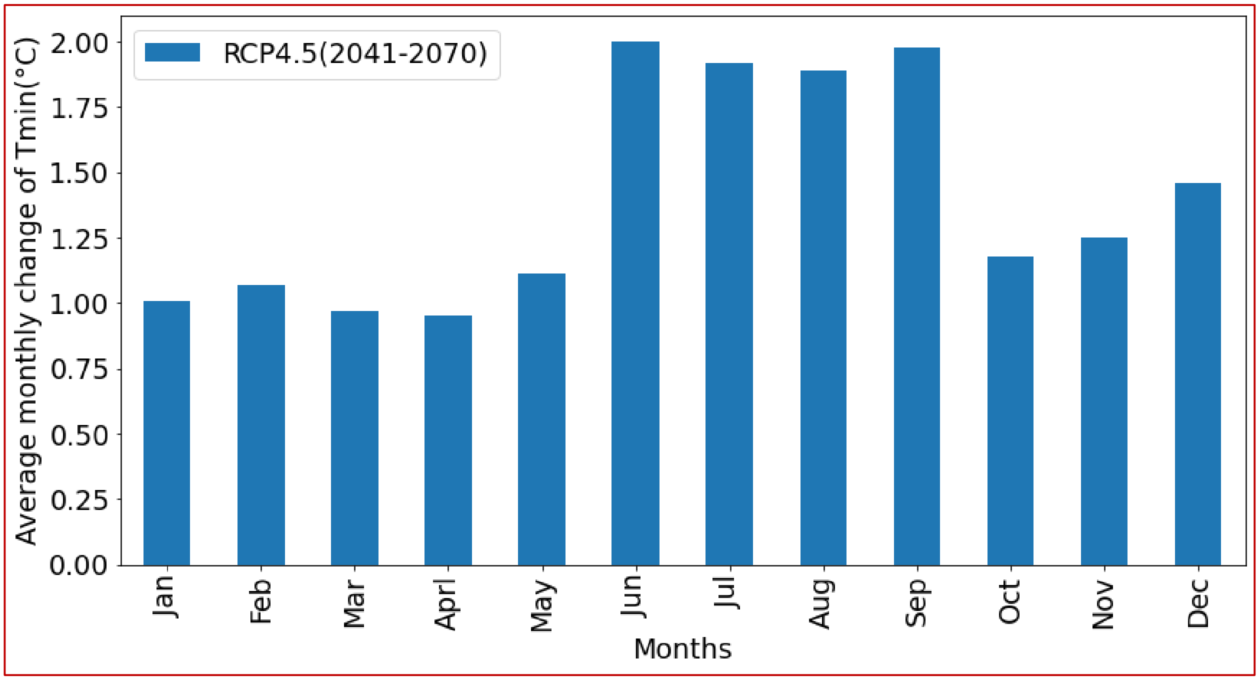

Figure 4.5: Monthly minimum temperature changes over the period (2041-2070)

4.2 Land Use Land Cover Change

4.2.1 Land use land cover classification accuracy assessment

An important step in the analysis of remote sensing data is accuracy assessment. It establishes the information value, or the worth of the resulting data to a specific user. A map's or categorized image's level of "correctness" is assessed using the accuracy criteria. Numbers are used in the confusion matrix/error matrix as the sample size. Accordingly, the overall accuracy of classified maps of 1990, 2005, and 2020 were 93.2%, 90.1%, and 89.5%. Additionally, the calculated kappa coefficient for the maps 1990, 2005, and 2020 were 0.92, 0.88, and 0.87 respectively which indicated a high level of agreement because the values were greater than 0.75. The user, producer, overall accuracy assessment, and kappa coefficient for the 2020 LULC classification are presented in Table 4.3. The rest of the accuracy assessments for 1990 and 2005 LULC classifications are illustrated in Appendix A.2.

Table 4.3: 2020 Land use land cover classification accuracy assessment

Classification	AGRL	FRSE	RNGE	RNGB	URBN	BARR	WATR	Total	User Accuracy %
AGRL	43	0	2	3	2	1	0	51	84.3
FRSE	0	27	2	3	0	1	0	33	81.8
RNGE	1	0	25	2	1	0	0	29	86.2
RNGB	0	1	0	32	0	0	0	33	96.9
URBN	0	0	2	0	30	0	0	32	93.7
BARR	0	0	0	1	1	22	0	24	91.6
WATR	0	0	0	0	0	0	18	18	100
Total	44	28	31	41	34	24	18	220	
Producer Accuracy (%)	97.7	96.4	80.6	78.1	88.2	91.6	100		
Overall Classification Accuracy = 89.5%									
Overall Kappa Statistics =0.87									

4.2.2 Land use land cover classification

Using supervised image classification techniques in the Upper Awash Basin seven main land use types have been identified such as Agriculture Bareland, Forest, Grassland, Shrubland, Urban and Water bodies. The 1990, 2005 and 2020 land use map generated from Landsat-5-TM, Landsat-7-ETM+ and Landsat-8- OLI image classification respectively was shown in Figure 4.6 below.

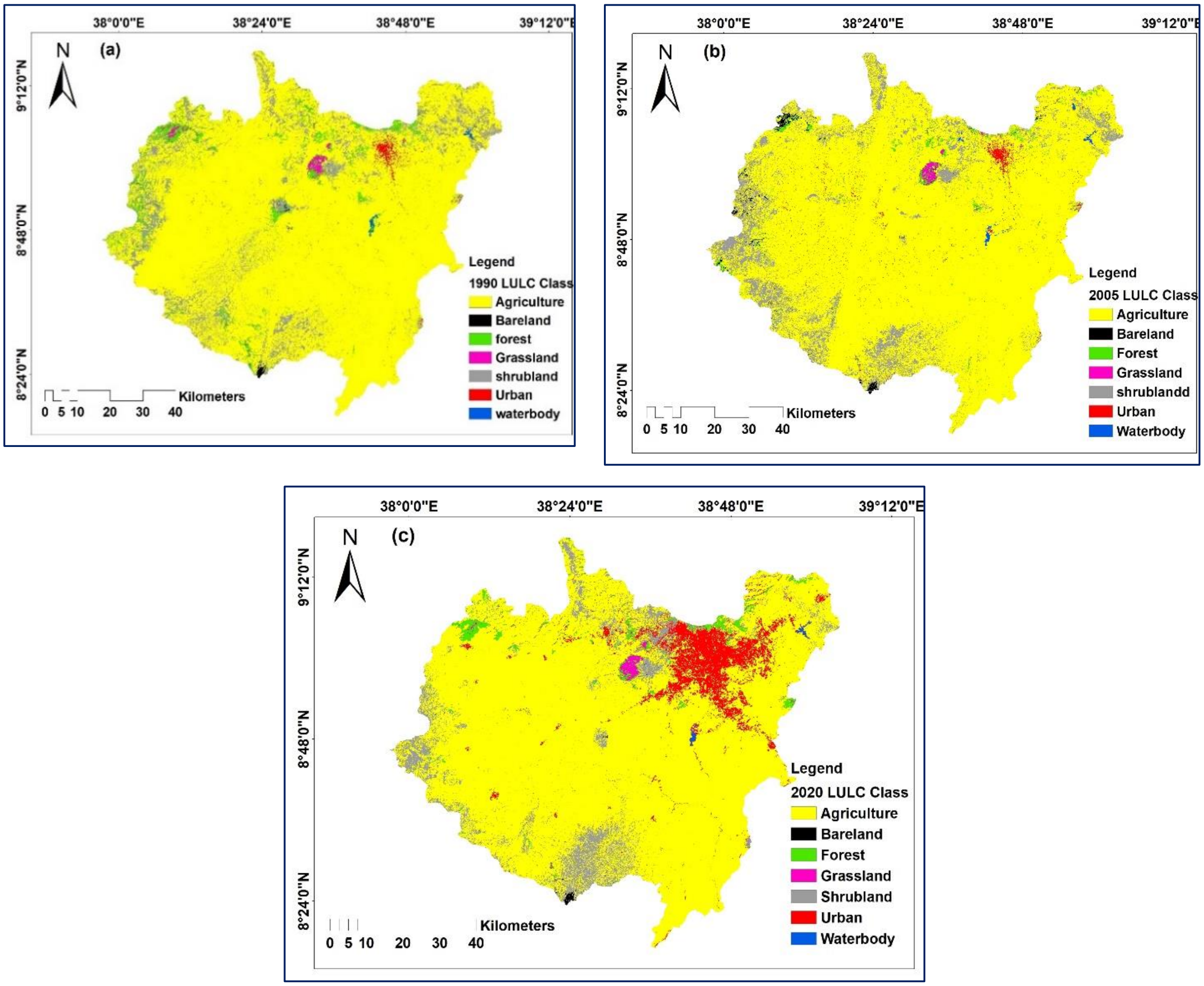

Figure 4.6: Land cover map of Upper Awash basin in the year a) 1990, b) 2005 and c) 2020

4.2.3 Land use land cover change detection

Table 4.4: Land use land cover change detection

LULC	1990		2005		2020		LULC change					
							1990 -2005		2005 - 2020		1990 -1990	
	Area Km^2	Area %	Area Km^2	Area %	Area Km^2	Area %	Area Km^2	Area %	Area Km^2	Area %	Area Km^2	Area %
Agriculture	4812	64.2	5771	76.9	6150	82	959	12.7	379	5.06	1338	17.84
Bareland	30	0.4	43	0.57	50	0.66	13	0.17	7	0.09	20	0.26
Forest	438	5.84	279	3.72	205	2.74	-158	-2.12	-73.6	-0.9	-232	-3.1
Grassland	812.5	10.8	319	4.23	80	1.06	-493	-6.6	-239	-3.2	-732	-9.77

Shrubland	1312	17.5	919	12.2	664.4	8.86	-393	-5.24	-255	-3.4	-648	-8.64
Urban	70	0.93	148	1.97	339	4.52	78	1.04	191	2.55	269	3.59
Waterbody	25	0.33	18	0.24	11	0.14	-7	-0.09	-7	-0.1	-14	-0.19
Total	7500	100	7500	100	7500	100						

Note: Negative and positive signs indicate the decrease and increase of LULC class, respectively.

Therefore, from the result shown in the table 4.4, Agricultural land was the most common LC type, followed by shrubland and forest regions, according to the LC change analysis from 1990 to 2020. From 64.16 % in 1990 to 82 % in 2020, the total area of agricultural land has increased. in contrary, shrubland was shrunk from 17.5% in 1990 to 8.86% in 2020. As a result, the urban area in the entire basin grew from 0.93 % in 1990 to 4.52 % in 2020, and it is predicted to continue to rise due to the region's higher population growth rate and socioeconomic development.

According to the study by Shawul et al. (2019) reported that the land use change from 1974 to 2014 revealed that the major LULC classes were cropland, shrub land and forest areas. There were a continuous increment of cropland and urban area in the Upper Awash Basin. The cropland expanded from 49.0% to 72.1% from 1974 to 2014 and the urban area escalation was expected particularly in Akaki sub basin due to the expansion of Addis Ababa and surrounding towns because of the higher population growth and the rapid socio economic development. Shawul et al. (2019) found that the urban area was increased by 6.06.2%. The forest and shrub land were decreased from 7.1% in 1974 to 5.35% in 2014 and from 19.6% in 1974 to 2.5% in 2014, respectively. Similarly, Kassa (2009) discovered that a huge tract of forest, shrubland, and grassland was converted to agricultural and urban sites at Hare watershed. Moreover, bare land increased by 0.26 % which indicates the degradation of the watershed.

In this study (1990 to 2020) the forest and grass land have decreased by 3.1 % and 9.77 % respectively. The increments of agriculture and settlement have a negative impact on the forest, shrubland, and grassland. Generally, significantly increasing rates were observed in urban/settlement, and agriculture and a decreasing rate were observed in forest, grassland, and shrubland figure 4.7 and 4.8.

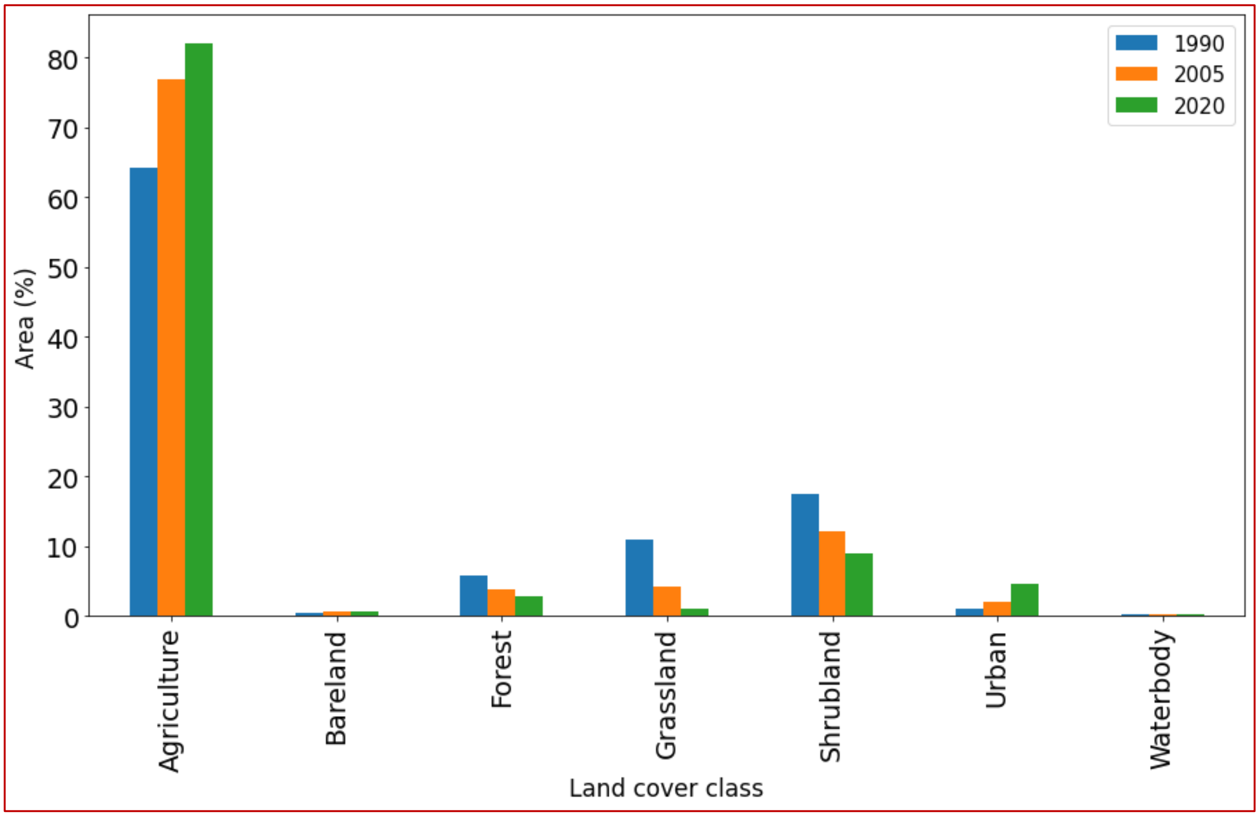

Figure 4.7: LULC changes for the years 1990, 2005, and 2020

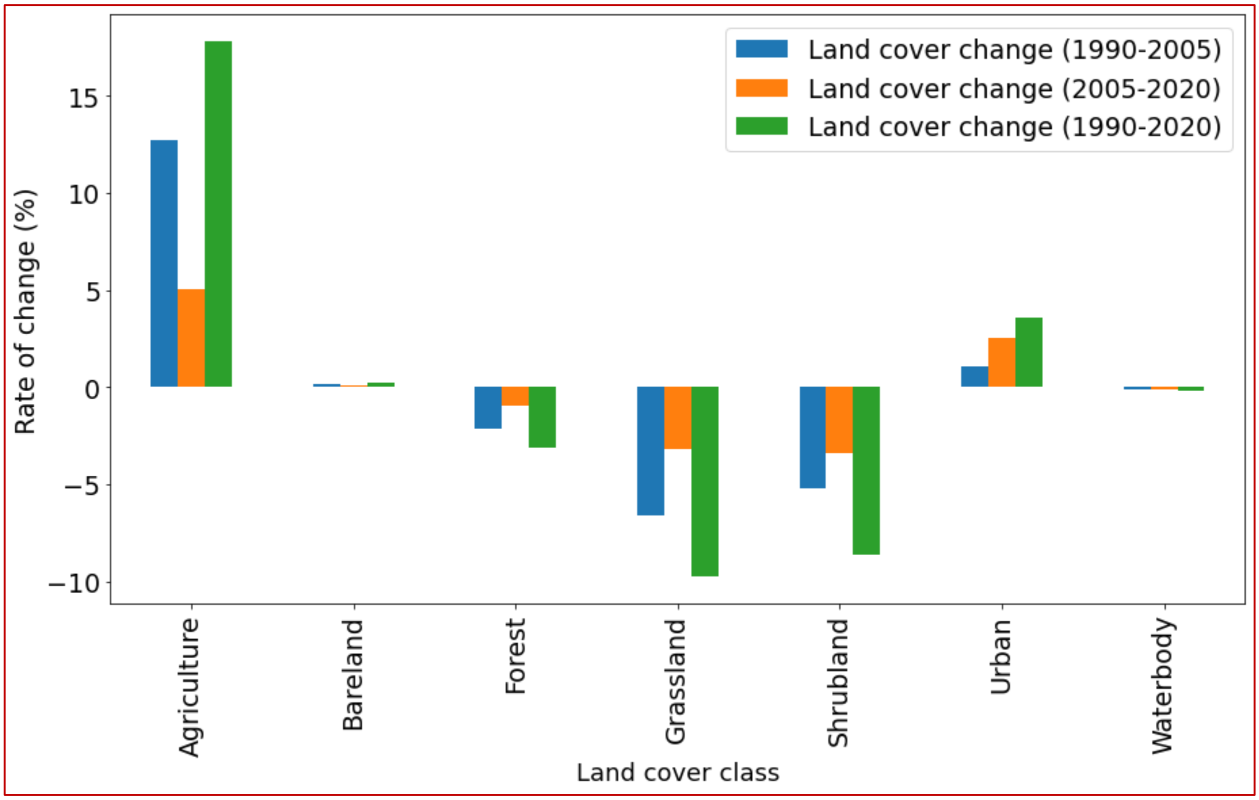

Figure 4.8: Comparison of Rate of Land Cover change

4.3 Streamflow Modelling

4.3.1 Streamflow sensitivity analysis

SWAT's sensitivity study for flow calibration involved about 500 iterations, and 11 parameters were identified as sensitive to varying degrees for flow. The Eleven most sensitive hydrologic flow parameters during calibration and validation in the watershed are given below in Figure 4.9.

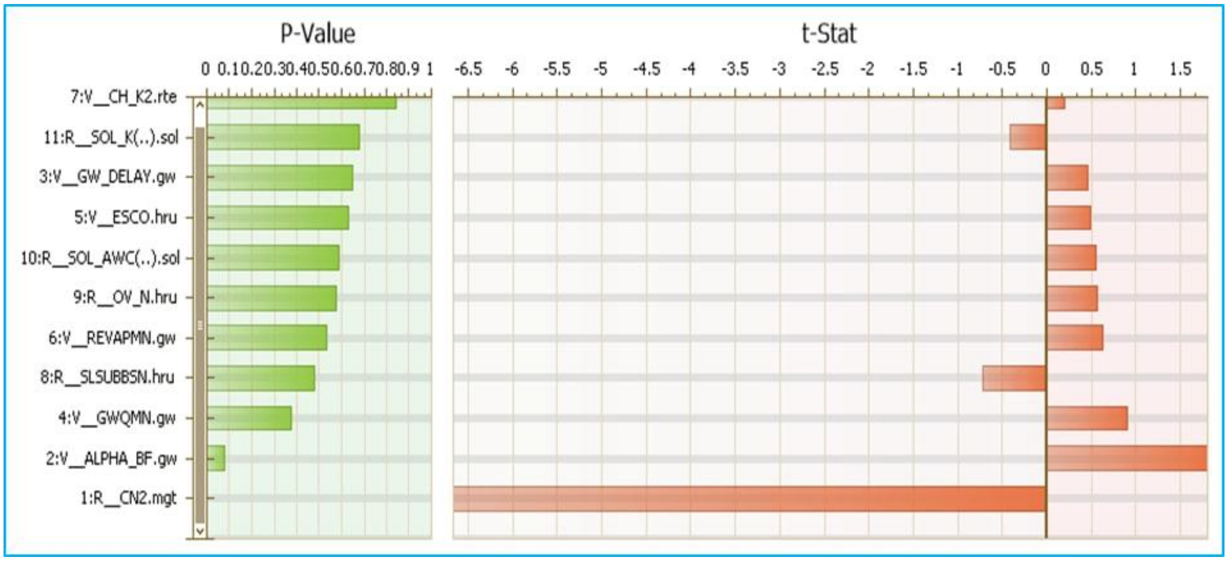

Figure 4.9: Streamflow sensitive parameters

Table 4.5: Streamflow parameters sensitivity rank

Parameter Name	Parameter Range	Fitted Value	Rank
R__CN2.mgt	-0.25-0.25	11.84%	1
V__ALPHA_BF.gw	0-1	0.2	2
V__GWQMN.gw	0-5000	226.23	3
R__SLSUBBSN.hru	10-150	76.3	4
V__REVAPMN.gw	0-1000	282.3	5
R__OV_N.hru	0.01-1	-0.082	6
R__SOL_AWC(..).sol	0-1	0.73	7
V__ESCO.hru	0-1	0.52	8
V__GW_DELAY.gw	0-500	268.45	9
R__SOL_K(..).sol	0-2000	-0.183	10
V__CH_K2.rte	-0.01-500	136.1	11

4.3.2 Streamflow calibration and Validation

4.3.2.1 Flow Calibration

Following the sensitivity analysis, the Upper Awash Basin flow calibration for the model was carried out. In the SWAT model, the simulated streamflow at the watershed outflow was calibrated using the SWAT-CUP (SUFI2-algorithm) Land use 2005. R^2, ENS, and PBAIS were used to assess the model's performance based on the execution of the SUFI-2 optimization function for the given observed data. During the calibration period from 2002- 2006, the simulated average monthly flow matched well with the average monthly measured flow (with R^2 = 0.83, ENS = 0.78 and PBIA= 11.35). The values indicate that there is good agreement between observed and simulated stream flow.

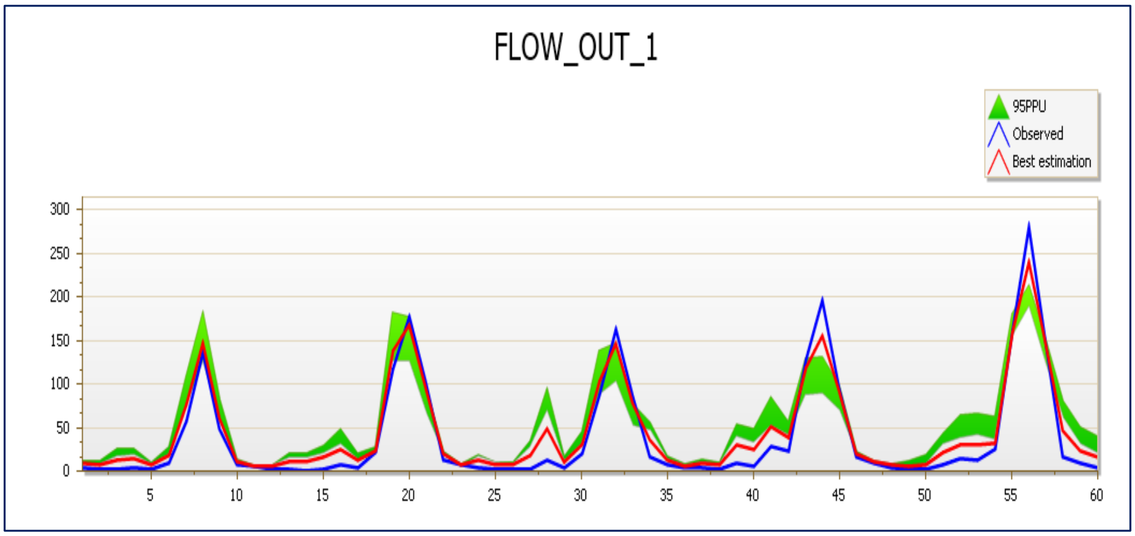

Figure 4.10: Streamflow calibration 95PPU plot

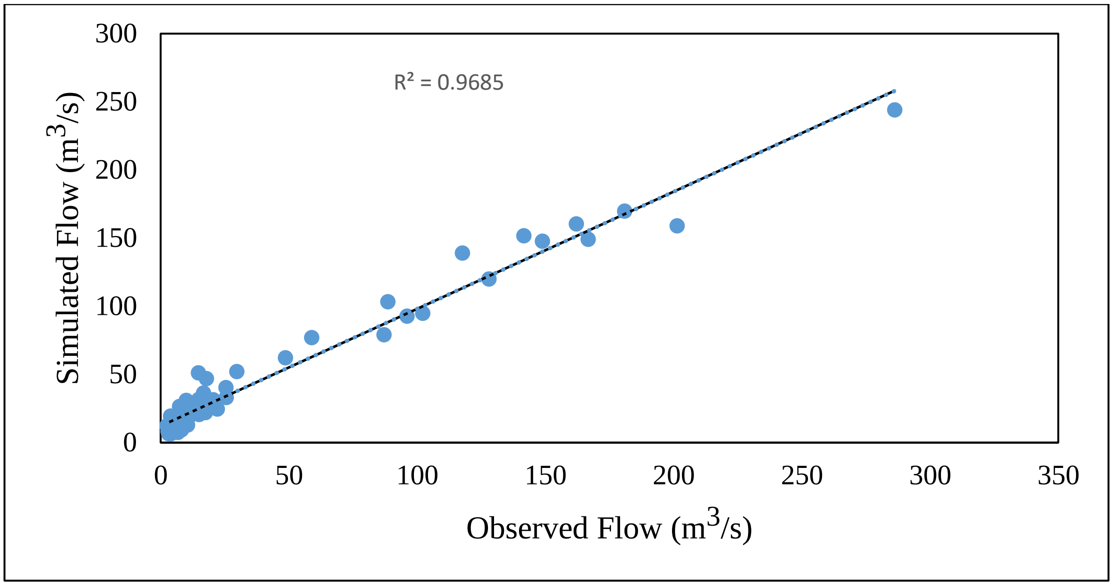

Figure 4.11: Scatter plot of the simulated vs observed average monthly flow during calibration

4.3.2.2 Flow validation

An independent set of observed flow data that had not been used for model calibration was used to validate the model. Validation demonstrates that the model and its parameters are taken into account as the representative of the system of the research watershed once the simulated variable is successful with the corresponding observation. The validation period of this study was from Jan/1/2007to Dec/31/2010 and it is a total of four years.

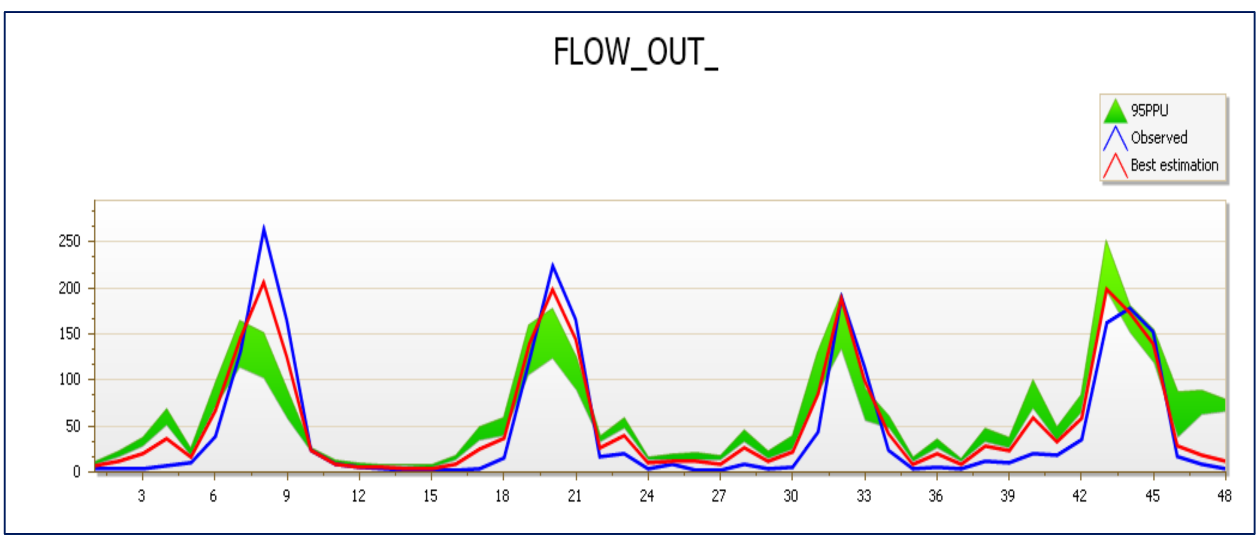

Figure 4.12: Streamflow validation 95PPU plot

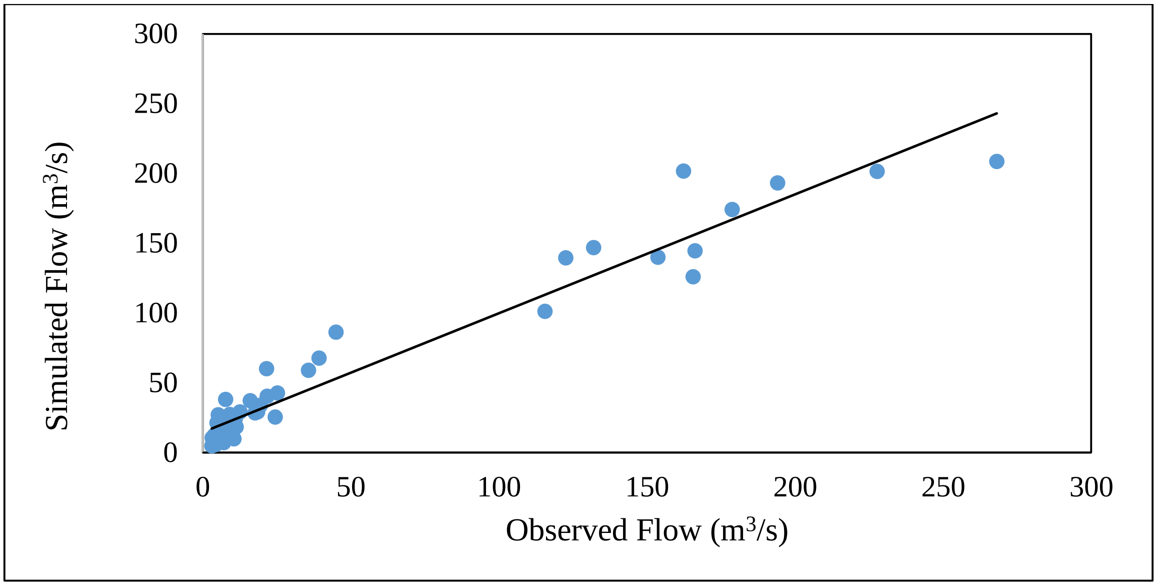

Figure 4.13: Scatter plot of the simulated vs. observed average monthly flow during Validation

Table 4.6: Summary of calibration and validation period of flow parameter model performance indicators

Period	Simulation	R^2	ENS	RSR (%)	PBIAS (%)
2002-2006	Calibration	0.83	0.78	0.49	11.35
2007-2010	Validation	0.77	0.73	0.58	8.9

Similarly, Mitiku et al. (2023) examining the impacts of climate variabilities and land use change on hydrological responses of Awash River basin and calibrated and validated the hydrological model in awash Hombole and reported that R^2=0.92, NSE=0.77 for calibration and R^2=0.87.NSE=0.52.

4.4 Sediment Yield Modelling

4.4.1 Sediment yield sensitivity analysis

The monthly observed sediment yield was used in a sensitivity analysis of the simulated sediment yield for the Upper Awash Basin to determine the most sensitive parameter and to further calibrate and validate the simulation of sediment yield. Therefore, the USLE support practice factor (USLE P), the linear factor for channel sediment routing (SPCON), and the exponential factor for channel sediment routing (SPEXP) were shown to be highly sensitive factors for sediment yield in the basin.

Table 4.7: Sediment yield parameters sensitivity rank

Parameter Name	Parameter Range	Fitted Value	Rank
R__USLE_P.mgt	0-1	0.470	1
R__SPCON.bsn	0.0001-0.01	0.0017	2
R__SPEXP.bsn	1-1.5	1.493	3
R__CH_COV1.rte	-0.05-0.6	0.254	4
R__LAT_SED.hru	0-5000	1752.39	5
R__CH_EQN.rte	0-1	0.61	6
R__ADJ_PKR.bsn	0.5-2	1.84	7

4.4.2 Sediment yield calibration and validation

4.4.2.1 Sediment yield Calibration

Following the identification of the parameters that were susceptible to silt during the sensitivity study, calibration took place. Similar to flow, the model was calibrated for sediment yield from 2002 to 2006. Model calibration was performed by comparing simulated sediment yield versus observed sediment yield of gauging station at the Hombole based on sediment rating curve developed. Up until the simulated and observed sediment yield fitted and adequate model performance indicators were obtained, sediment yield calibration and sediment parameter adjustments were made iteratively.

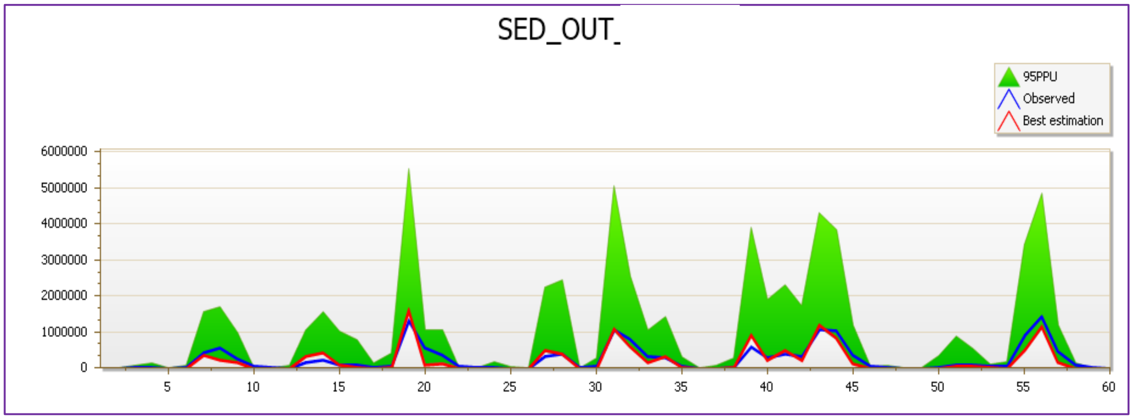

Figure 4.14: Sediment yield calibration 95PPU plot

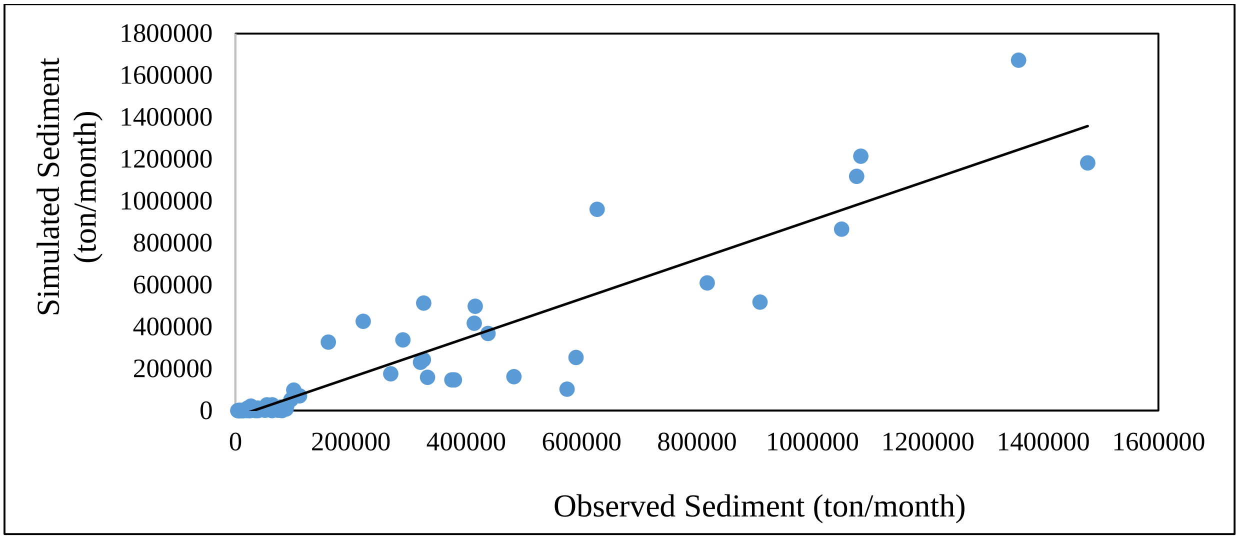

Figure 4.15: Scatter plot of the simulated vs. observed average monthly Sediments during calibration

4.4.2.2 Sediment yield validation

The validation period for sediment yield run from January 1, 2007, to December 31, 2010. It was carried out using independently measured sediment data that had not been used throughout the calibration period. A very good agreement between the predicted and actual sediment output was seen during this validation stage, as evidenced by the R^2 of 0.8, NSE of 0.78, and PBIAS of 12.5 percent.

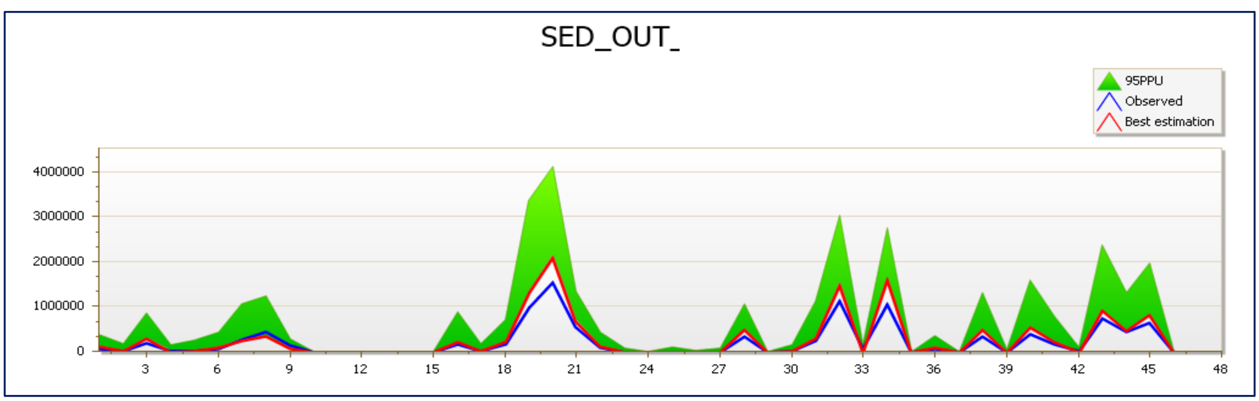

Figure 4.16: Sediment yield validation 95PPU plot

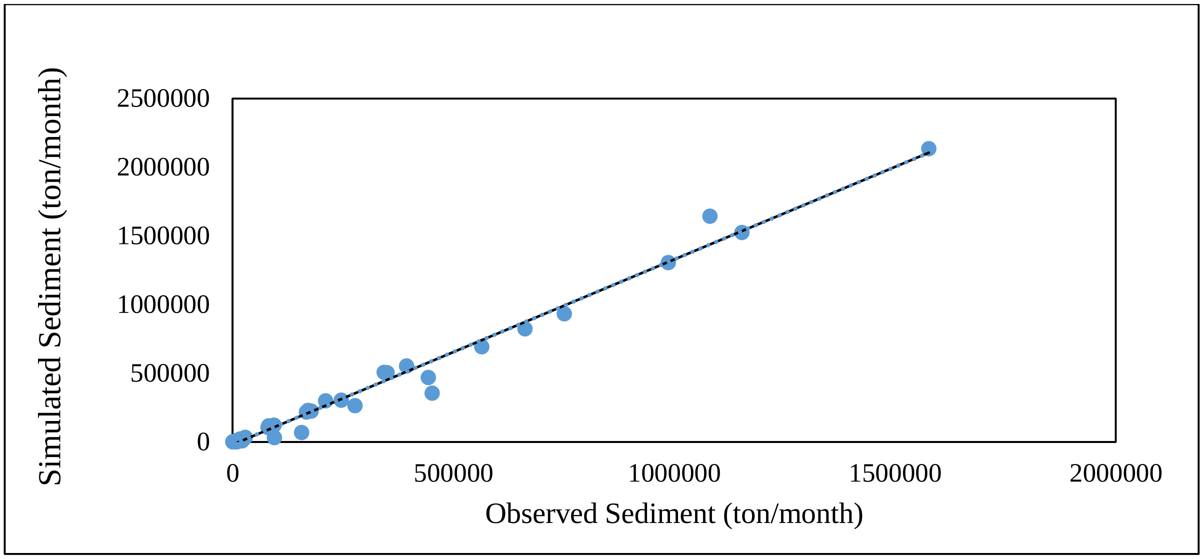

Figure 4.16: Scatter plot of the simulated vs. observed average monthly Sediments during validation

Table 4.8: Model performance test for calibration and validation period of sediment parameter

Period	Simulation	R^2	ENS	RSR (%)	PBIAS (%)
2002-2006	Calibration	0.85	0.81	0.41	14.1
2007-2010	Validation	0.8	0.78	0.42	12.5

4.5 Streamflow and Sediment Yield Responses to Climate and LULC Change

Based on historical LULC of 1990, 2005, and 2020, the calibrated and validated SWAT model was used to assess the impact of land use and land cover (LULC) and climate change on streamflow and Sediment yield. The impact of LULC change and Climate Change on streamflow and Sediment at a specific watershed and sub-basins was examined using the long-term Climate simulation from the years 1989 to 2019. This analysis was done on a monthly basis.

4.5.1 Streamflow Responses to Climate and LULC change

Understanding the past effects of LU/LC and the climate system on river flow is necessary to comprehend the effects they will have in the future on the hydrological regimes at various levels of a watershed. LULC contributes to increase in the streamflow during 1989-1999 periods analyzed. During this period the streamflow increased by 4.8%. The growth of agriculture and degradation of forest area, which results in an increase in surface runoff, is the main cause of the increase in streamflow. Agricultural land expanded by 17.8% between 1989 and 2019. We can explain this in terms of the crop soil moisture demands. Crops need less soil moisture than forests; therefore, the rainfall satisfies the soil moisture deficit in cultivation lands more quickly than in forests there by generating more surface runoff where the area under cultivation land is extensive. Wilk and Hughes (2002) also found that converting forest and Grassland to agriculture increases runoff whereas conversion of other LC to forest largely decreases runoff amount. Similarly, Beyene et al. (2016) found that Upper Awash watershed experienced an increase of streamflow due to drastic LULC change.

Climate change contributes to the decrease in the streamflow during 2011-2019. In this period the streamflow decreased by 1.26%. The average precipitation decreased from 1163.4 mm during 1989–1999 period to 1022.9 in 2011-2019 period, which resulted in decrease of streamflow.

Table 4.9: The variations in monthly streamflow under the different scenarios

Scenarios	Average monthly Streamflow ($m^3/_s$)	Streamflow Change ($m^3/_s$)	Streamflow Change (%)
S1 (baseline)	119.3	-	-
S2 (climate)	117.8	-0.0126	-1.26
S3 (LULC)	125.1	0.048	4.81

4.5.2 Sediment yield Responses to Climate and LULC change

The results showed that climate change and LUCC had a consistent positive effect on sediment yield. Compared to the baseline scenario (S1), the change in sediment were 12.64% under LULC change and 3.28% under climate change effect. The LULC change had a greater contribution to changes in sediment yield than climate change. The result is consistent with Shawul et al. (2019) reported that the increment of cropland at the expense of grassland increased the water yield which might lead to more sediment yield in the watershed of Upper Awash Sub-Basin. From this we can conclude that change in the land use/ land cover does haves an impact on the runoff and sediment yield behaviour of the watershed.

Table 4.10: The average monthly sediment simulated by the calibrated SWAT model under different scenarios

Scenarios	Simulated Sediment Load (Tons)	Sediment Load Change (Tons)	Sediment Load Change (%)
S1 (baseline)	12528	-	-
S2 (climate)	12940	0.0328	3.28
S3 (LULC)	14112	0.126	12.64

4.5.3 Combined impact of climate and LULC change on streamflow and sediment yield

According to the simulations of the four SWAT model runs, streamflow and sediment have changed over the past 30 years as a result of the combined effects of LULC and climate change. Combined effect of LULC and climate change showed an increase in the streamflow and the sediment yield from 1989-2019. Both discharge and sediment load increased relative to the baseline scenario (S1), with 4.6% for discharge and 15.54% for sediment yield. Zhang et al. (2022) found that the simulation results indicated a decreasing trend in both annual discharge and sediment load under the combined impact of LUCC and climate change with −22.65% for discharge and −31.51% for sediment load in the Hunhe River Basin, Northeast China.

Table 4.11: The average monthly simulated streamflow and Sediment used to detect the combine effects of climate and LULC change on streamflow and sediment

Scenarios	Simulated Streamflow (m^3/s)	Streamflow Change (m^3/s)	Streamflow Change (%)	Simulated Sediment Load (Tons)	Sediment Load Change (Tons)	Sediment Load Change (%)
S1 (baseline)	119.3	-	-	12528	-	-
S2 (climate)	117.8	-0.0126	-1.26	12940	0.0328	3.28
S3 (LULC)	125.1	0.048	4.8	14112	0.126	12.64
S4 (Combined)	124.8	0.046	4.6	14476	0.1554	15.54

4.6 Spatial Distribution of Sediment Yield and Prioritization of Critical Sub-Basins

There is never a spatially uniform process involved in the delivery of sediment to a basin's outlet during erosion. Any scale at which a landscape unit is examined will typically reveal significant variations in the specific sediment yields (Morris and Fan, 2009). To concentrate yield reduction efforts on the landscape units that deliver the most sediment to the reservoir, knowledge of the spatial variation in yield is necessary. The sediment outflow from every tributary and the main river section has been modeled after the flow and sediment yield at Hombole gauging station were successfully calibrated. Based on this finding, potential intervention areas were prioritized, and three management/conservation measure scenarios were developed and simulated by SWAT model to determine the most suitable management/conservation measures within the Upper Awash Sub-basin.

The Upper Awash watershed's annual sediment outputs, as predicted by SWAT, ranged from 0.2 to 77.3 tons/ha/yr from 1991 to 2019, with a 29-year average of 19.31 tons/ha/yr. A mean annual sediment output of 21.5 ton/ha/yr was reported in the study by Dilnesaw et al. (2006) at the Hambole sub-basin. Additionally, Setegn et al. (2010) estimated a mean annual sediment yield of 24.6 tons/ha/yr for Ethiopia's Anjeni watershed, which is situated in the country's Blue Nile Basin. Sediment source maps were created using the model's average yearly sediment yield from each sub basin. In order to determine the rates of soil formation for Ethiopia, Hurni (1985) carried out research. For the various agro-ecological zones of Ethiopia, the acceptable soil loss level ranged from 2 to 18 tons per hectare per year. The model's output revealed that, under the current conditions, the Upper Awash River Basin produces an average yearly yield of 19.31 tons/ha/yr of sediment (Figure 4.19). Some sub watersheds in the research region have real annual soil loss rates that are higher than the acceptable upper limit of 18ton/ha/yr. This fact demonstrates how seriously soil erosion threatens the study region.

Surface runoff and sediment yield had a direct relationship since surface runoff influences detaching and moving soil particles. Most of the sub-watersheds that generate a high amount of surface runoff produce a high amount of sediment yield. Spatial distribution of surface runoff and annual sediment yield were illustrated in Figure 4.18 and 4.19 respectively.

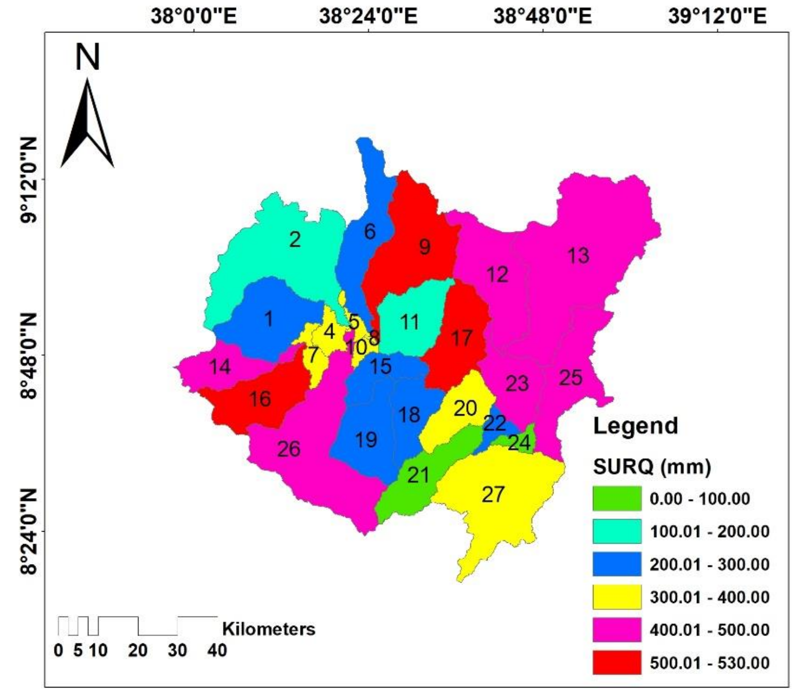

Figure 4.18: A spatial distribution of surface runoff in upper Awash Sub-Basin

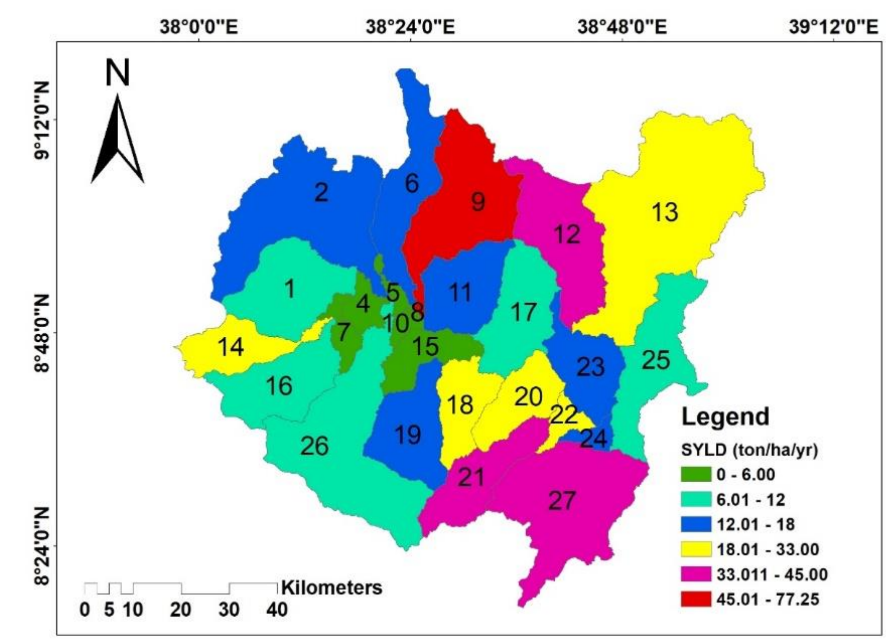

Figure 4.19: A spatial distribution of annual sediment yield in upper Awash Sub-Basin

According to the model's spatial distribution, sediment yield in the watershed varies from HRU to HRU based on the type of soil, slope, and land use in each HRU. The study's Sub basin 9, 12, 13, 14, 18, 20, 21, 22, and 27 create the most sediment and are hence most susceptible to erosion (Figure above). Sub-basin 9 and 12 are urban section, it is well known that the increase in urban area will result in the increase in surface runoff. Because, earthworks are required to establish roads and building sites and exposed soils are prone to erosion and can cause large quantities of sediment to be washed into nearby waterways through surface runoff, especially after heavy rain. The aforementioned sub basin was therefore chosen for the management intervention scenario that would follow.

4.7 Effectiveness of Best Management Practices

This research assisted in locating sub-watersheds with the potential to yield more sediment. A number of BMP scenarios were developed to observe how the catchment would react in terms of sediment output. Both the overall catchment's impact and the effects of the particular sub basins that were determined to provide substantial sediment yields were evaluated. Additionally, because agriculture was the primary land use in the research area, these best management techniques were exclusively applied to agricultural land. Three distinct scenarios were created for this study and compared based on how well they would conserve soil or reduce silt. The three situations were Terracing, Filter Strip, and Reforestation. Each scenario was simulated for the 1989–2019 period.

Table 4.12: Scenario description and SWAT parameter used to represent BMPs

Scenarios	Description	Parameter Name	Input file	Calibrated Value	Modified Value
Scenario 0	Baseline	-	-	-	-
Scenario 1	Filter strip	FILTERW (.hru)	5m	0	5m
Scenario 2	Parallel terrace	SLSUBBSN (.hru) USLE_P (.mgt)	Slope 0-5% Slope 5-10% Slope 10-20% Slope >20%	91.46 60.97 18.29 9.14 1	18m 12m 10m 9.14 0.5
Scenario 3	Reforestation	BARR (.LUP)		BARR	FRST

Baseline scenario (S0): The baseline scenario took into account the watershed's current status. For the modeling of three chosen scenarios for sediment reduction, nine important sediment source sub basins were identified in this scenario. The baseline scenario illustrated in Figure 4.20 named on map as (a) Baseline.

Table 4.13: Average annual sediment yield of selected critical sub-basin

Selected Sub-basin	Sediment yield (ton/ha/yr.)
9	73.84
12	21.03
13	18.9
14	27.30
18	27.24
20	31.94
21	36.6
22	33.37
27	44.93

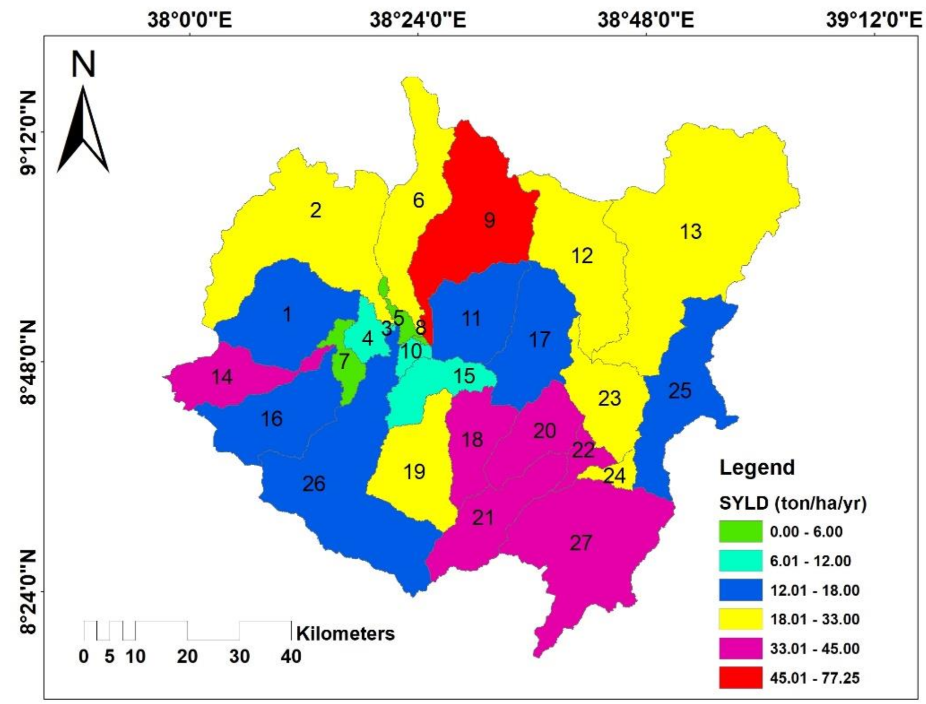

Figure 4.20: Sediment yield of Baseline scenario

Filter strip (S1): This management strategy was used on all agricultural Croplands, soils, and all slope classes combined into HRUs. The excursions have the effect of reducing runoff and trapping silt in a certain plot (Bracmort et al., 2006). According to Table 4.14, the installation of 5m filter strips decreased the crucial sub basins' average annual sediment yield from 35 ton/ha/year to 16.6 ton/ha/year, with an average reduction capacity of 52.5%. These results are consistent and similar with the previous research work in Ethiopian. Nadew et al. (2019) reported 48% of annual average sediment yield reduction by applying a 5 m wide filter strip in Guder watershed. Zeberie, (2020) reported 50% of annual average sediment yield reduction by applying a 1m wide filter strip in Akaki watershed, Upper Awash Basin. Boru et al. (2022) concluded that the implementation of 5 and 10 m filter strips reduced the mean annual sediment yield by 31.68% and 46.6%, respectively in the middle and Upper awash basin, Ethiopia.

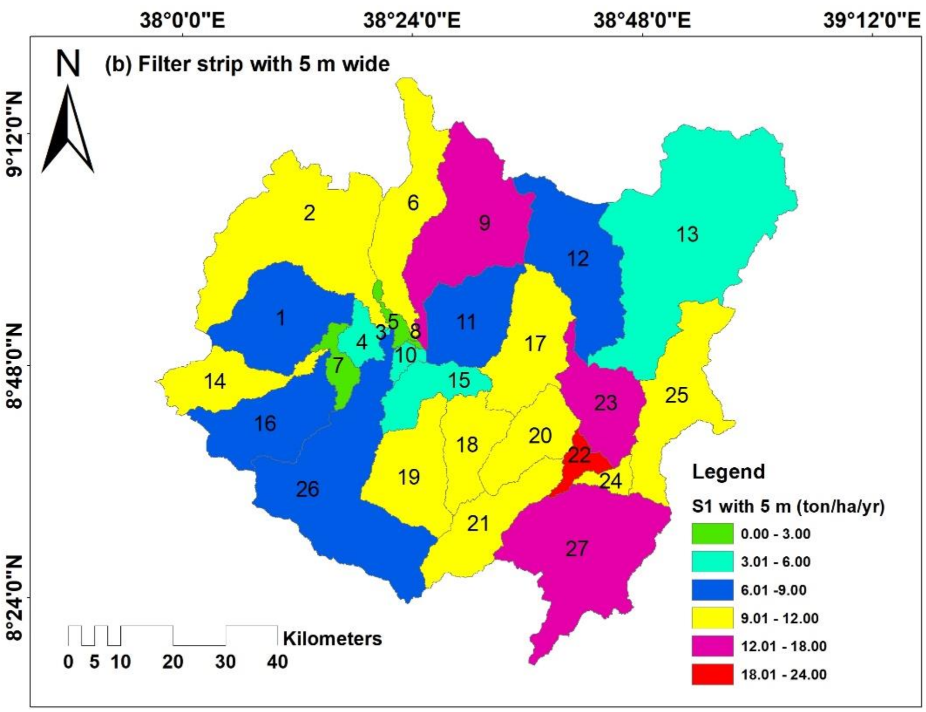

Figure 4.21: Mean annual sediment yield reduction due to application of filter strip

Terracing (S2): Terracing is used to minimize the slope of the HRU and the length of the sub basin in a watershed. Adjusting the parameters for erosion and runoff simulates terracing in SWAT. The USLE support practice factor (USLE_P), SCS curve number (CN2), and slope length of the hillside (SLSUBBSN) are the parameters to be modified based on the land slope in the modeling of the influence of terracing on sediment reduction. By installing terraces, the chosen critical sub basins' mean annual sediment output rate was decreased by 44%. The average sediment yield rate of the sub basins was drastically decreased from 35 ton/ha/year to 19.6 ton/ha/year. Similarly, (Kefay et al., 2022) reported that implementing terraces in the selected critical sub basins reduced the mean annual sediment yield rate by 47.05% in the Awata river, southern Ethiopia. And also Tesema and Leta (2020) found that applying terracing to the critically affected sub basins reduced sediment yield by 73.11% on Sediment Yield Estimation and Effect of Management Options on Sediment Yield of the kesem dam watershed, Awash basin, Ethiopia.

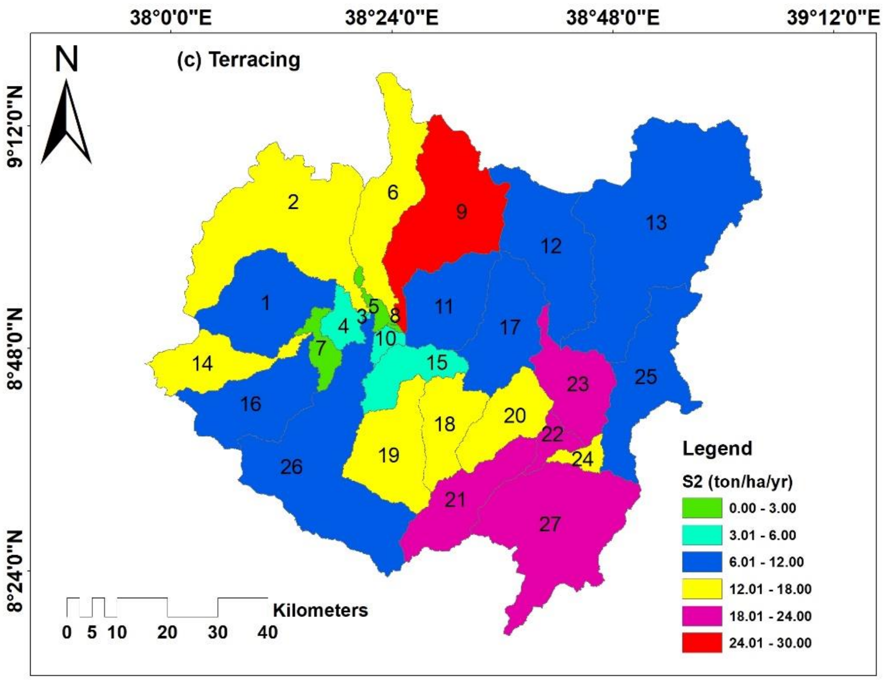

Figure 4.22: Mean annual sediment yield reduction due to application of Terracing

Reforestation (S3): Reforestation serves to lessen the erosivity of rainfall and overland flow. Simulated results show how reforestation affects the decline in sediment yield. By shielding the soil from the direct impact of raindrops and promoting infiltration, a good vegetative cover offers the best, most affordable, and long-lasting protection against erosion (Morris and Fan, 1998). Thus, the effect of reforestation on soil erosion was modelled in this scenario. In order to determine the amount of sediment yield reduction in the Upper Awash Basin, completely replanting of bare land on sediment-prone locations were taken into consideration. By applying reforestation for the selected critical source sub basins, 37.1% of the average sediment yield has been reduced from 35 ton/ha/yr. to 22 ton/ha/yr. The study conducted by Tesfaye et al. (2022) reported that applying reforestation management reduces watershed sediment output by 21.05% on average annually in the Gojeb catchment Ethiopia. And also Demissie et al. (2013) found that the simulation of reforestation scenario showed the average reduction of sediment yield by 9.1% for the critical sub basins from the current condition in Gilgel Gibe Basin Watershed, Ethiopia.

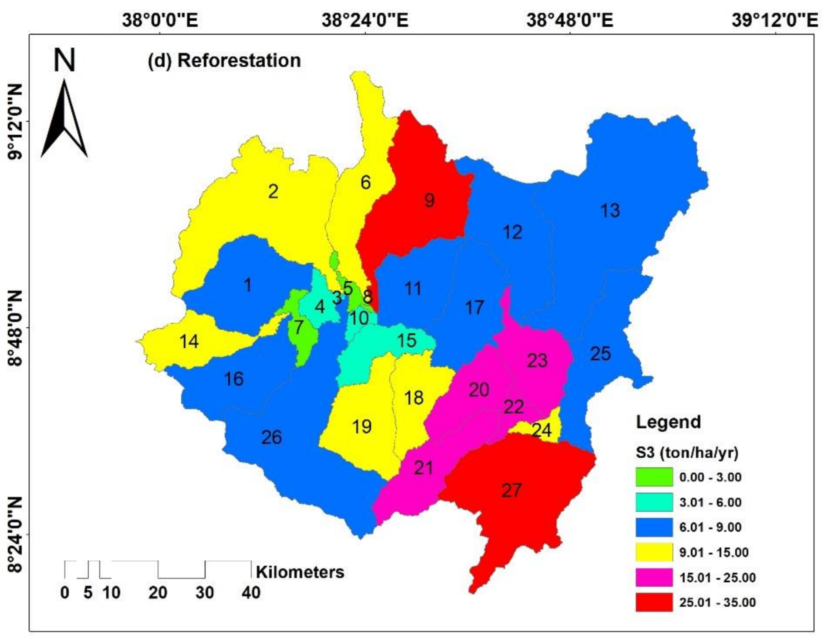

Figure 4.23: Mean annual sediment yield reduction due to application of Reforestation

4.7.1 Comparison of the above BMPs Scenario

Management techniques were crucial tools for preserving soil and lowering the sediment production in watershed-prone locations. Based on this idea, an intriguing result was produced by running the model with various watershed management scenarios implemented in the watershed. The table below illustrates how the influence of watershed management options on the crucial sub basin level that was chosen revealed a wider regional diversity on sediment reduction from baseline conditions.

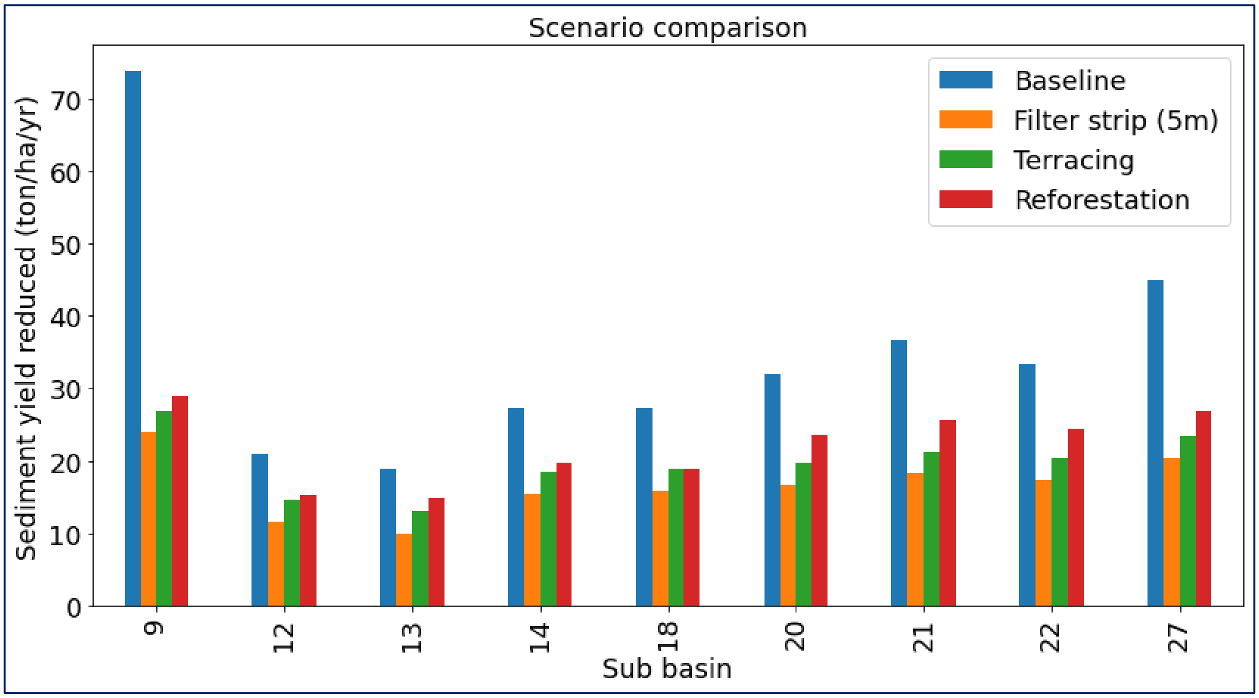

Figure 4.24: Scenarios comparison with their sediment yield reduction

Table 4.14: Sediment yield reduction effectiveness and rank of BMPs

BMPs	SED before BMPs (ton/ha/yr)	SED after BMPs (ton/ha/yr)	Reduction (%)
Filter strip (5m)	35.0	16.6	52.5
Terracing	35.0	19.6	44
Reforestation	35.0	22	37.1

5. CONCLUSIONS AND RECOMMENDATIONS

5.1 Conclusions

Ethiopia is a country which is highly dependent on agricultural products for development. The availability of water resources could be highly influenced by climate and Land use land cover change. The influence of various land use and climate change scenarios on stream flow and sediment and developing of BMPs in the basin was investigated using the Soil and Water Assessment Tool (SWAT) model. SWAT proved to be a practical technique for determining how land use and climatic changes would affect sediment and stream flow. For monthly flow, the respective NSE, R^2, and PBIAS values were 0.78, 0.83, and 11.35% for the calibration period, and 0.73, 0.77, and 8.9% for the validation period. Similar assessments were made for the monthly sediment load, which was estimated to be 0.81, 0.85, and 14.1% for the calibration period and 0.78, 0.8, and 12.5% for the validation period, respectively. This suggests that despite the lack of information on observed suspended sediment load, the SWAT model's performance in the Upper Awash Sub-Basin was very good at predicting flow and sediment load.

The remotely sensed data of 1990, 2005, and 2020 were classified using ERDAS Imagine 2015 integrated with GIS data to analyze spatiotemporal LULC dynamics in the study area. The analysis of 1990, 2005, and 2020 LULC indicates, Upper Awash Sub-basin had experienced significant changes in the land use land cover over the past 30 years. The agricultural land was the dominant LC type in the Upper Awash Sub-basin. There were increasing in agricultural land, built-up area/Urban, and bare land whereas decreasing forest land, shrubland, and Grassland for the period of (1990-2020). Agricultural land was increased by 12.7% but forest land and shrubland were decreased by 2.12% and52.2% for the period 1990-2005. For the period 2005-2020 a slight increase in agricultural and a decrease in forest land with the high increment of Urban were obtained as compared with the first period. The result revealed that agricultural land was increased by 5.1% and forest land were decreased 0.9% and Urban land were increased by 2.5%. Rapid population growth in the area is the reason for the expansion of agricultural land which later causes a reduction in forest land and shrubland.

The Mann-Kendal trend test result of observed annual rainfall for the past 30 years shows both upward and downward trends. This implies that the trends of rainfall over the study area are not uniform and consistent in both time and space. Therefore, the rainfall distribution in the upper

Awash Sub-basin has not shown a systematic trend in the past 30 years. But the measured temperature in the study area showed a significant rising trend. During 2041-2070, the prediction of precipitation and temperature compared with observed data shows that rainfall will decrease from January to June and will increase from July to December. But maximum and minimum temperatures will increase for all months.

The changes in Climate and land use land cover resulted in streamflow and sediment yield changes. During 1989-2019, LULC rather than climate change dominated the hydrological changes in the basins, and combined impacts of climate and LULC played more important role in alterations of streamflow and sediment than individual impacts. Generally, the expansion of agricultural land, bare land, and built-up area/Urban over forest land and shrubland which leads to increasing surface runoff and decreasing of lateral flow was highly responsible for increasing streamflow and sediment yield.

Using GIS, the geographical heterogeneity of sediment source locations was located and mapped. Sub basins 9, 12, 13, 14, 18, 20, 21, 22, and 27 were consequently recognized as additional potential sediment source sites (highly erodible). As a result, best management practices in those sub basins were implemented. Following the installation of filter strips (5m), terracing, and reforestation, the average annual sediment yield reduction at the level of the entire basin was shown to be 52.5%, 44%, and 37.1%, respectively, according to the proposed sediment yield reduction scenarios. A 5 m-wide filter strip was found to be the most effective BMP for reducing the sediment yield during the implementation of management scenarios to evaluate their effects on sediment reductions.

5.2 Recommendations

The following points recommended as emanated from the study result.

- In this study, Climate change scenarios data from CMIP5 for rainfall and temperatures projection was used. Newly developed climate change scenarios such as SSPs under CMIP6 is recommended for further study.
- The land use as shown has been changed to urbanization; this change will be increased, and there should be a regulation policy on the watershed area by the administration.
- This research was taking in to account the dominant land use/cover feature of the watershed, but better result could be obtained if the detailed land use/cover data of watershed was considered. three land use/cover maps were used for comparison, if more map were used it is easy to identify the change.
- The SWAT model was used to simulate the hydrological impacts of climate and LULC. However, different hydrological models and programming language like python should be considered for further research activities.
- One of the difficulties encountered during model calibration and validation is the lack of continuously observed suspended sediment data. Due consideration should be given to the timing, procedure, and frequency of sediment sampling for further studies of this nature when providing the results to the appropriate parties.

REFERENCES

Abbaspour E. Rouholahnejad S. Vaghefi, R. S. H. Y. B. K. (2015). A continental-scale hydrology and water quality model for Europe: Calibration and uncertainty of a high-resolution large-scale SWAT model. Journal of Hydrology, 524.

Abbaspour, K.(2012). Federal Institute of Aquatic Science and Technology Switzerland: Calibration and Uncertainty Programs. p. 106.

Abdulahi, S. D., Abate, B., Harka, A. E., & Husen, S. B. (2021). Response of climate change impact on streamflow: The case of the Upper Awash sub-basin, Ethiopia. *Journal of Water and Climate Change*, *13*(2), 607.

Alawamy, J. S., Balasundram, S. K., Hanif, A. H. M., and Sung, C. T. B. (2020). Detecting and analyzing land use and land cover changes in the Region of Al-Jabal Al-Akhdar, Libya using time-series Landsat data from 1985 to 2017. Sustainability (Switzerland), 12(11) https://doi.org/10.3390/su12114490.

Alerts J. and P. Droogers P. (2004). Adaptation for Regional Water management. Institute for Environmental studies, Vrije University Amsterdam, Amsterdam, The Netherlands; Future Water, Arnhem, the Netherlands.

Allen, R. G. (1986). A Penman for All Seasons. Journal of Irrigation and Drainage Engineering, 112(4), 348–368. https://doi.org/10.1061/(ASCE)0733-9437(1986)112:4(348).

Allen, R. G., Jensen, M. E., Wright, J. L., & Burman, R. D. (1989). Operational Estimates of Reference Evapotranspiration. Agronomy Journal, 81(4), 650–662. https://doi.org/10.2134/agronj1989.00021962008100040019.

Amsalu, A., Stroosnijder, L., & de Graaff, J. (2007). Long-term dynamics in land resource use and the driving forces in the Beressa watershed, highlands of Ethiopia. Journal of environmental management, 83, 448 – 459.

Arabi, M., Govindaraju, R. S., Hantush, M. M., and Engel, B. A. (2006). Role of watershed sub-divisions on modeling the effectiveness of best management practices using SWAT. JAWRA Journal of the American Water Resources Association, 42(2), 513-528. https://doi.org/https://doi.org/10.1111/j.1752-1688.2006.tb03854.x

Arnold, J.G., Srinivasan, R., Muttiah, R.S., Williams, J.R. (1998). Large area hydrologic modeling and assessment part I: model development. J. Am. Water Resource. Assoc. 34 (1), 7389.

Arnold, J. G., & Fohrer, N. (2005). SWAT2000: Current capabilities and research opportunities in applied watershed modelling. Hydrological Processes, 19(3), 563–572. https://doi.org/10.1002/hyp.5611.

Badege, B. (2001). "Deforestation and land degradation in the Ethiopian Highlands: A strategy for physical recovery." Northeast African Studies, 8(1): 7-25.

Bedassa, R. and Erik, S. (2015). WRF Preliminary Results Simulation of JJASPrecipitation over Ethiopia under different land surface Models. Journal of Ethiopian Meteorological Society, Volume 2.

Betrie, G. D., Mohamed, Y. A., Griensven, A. Van, and Srinivasan, R. (2010). Sediment management modeling in Blue Nile Basin using SWAT model. Hydrology and Earth System Sciences Discussions, 7(4), 5497-5524. https://doi.org/10.5194/hessd-7-5497-2010.

Beyene, S. K., Kemal, A., & Pingale, S. M. (2016). The Impact of Land Use Land Cover Change On Watershed Hydrology (A Case Study of Upper Awash Basin).

Boru, N., Gurara, M., Tolche, A. D., & Edo, A. (2022). Impacts of Management Scenarios on Sediment Yield Simulation in Upper and Middle Awash River Basin, Ethiopia. Ecohydrology and Hydrobiology. https://doi.org/10.1016/j.ecohyd.2021.11.003

Bracmort, K. S., Arabi, M., Frankenberger, J. R., Engel, B. a, & Arnold, J. G. (2006). Modeling Long-Term Water Quality Impact of Structural BMPs. Transactions of the American Society of Agricultural and Biological Engineers, 49(2), 367–374. https://doi.org/10.13031/2013.20411.

Bronstert, A., Niehoff, D., & Burger, G. (2002). Effects of climate and land use change on storm runoff generation: Present knowledge and modelling capabilities. Hydrologic Process, 16, 509–529.

Canadian Centre for Remote Sensing. (1999): Fundamentals of remote sensing tutorial. Natural resource, Canada: Government of Canada.

Cestti, R., Srivastava, J., & Jung, S. (2003). Agriculture Non-Point Source Pollution Control Good Management Practices the Chesapeake Bay Experience, 44.

Chakma, D. S., & Shawul, A. A. B. A. T. E. (2019). Spatiotemporal detection of land use/land cover change in the large basin using integrated approaches of remote sensing and GIS in the Upper Awash basin, Ethiopia. Https://Link.Springer.Com/Article/10.1007%2Fs12665-019-8154-y.

Charron I. (2014). A Guidebook on Climate Scenarios: Using Climate Information to guide Adaptation Research and Decisions, Ouranos.

Chaubey, I., Chiang, L., Gitau, M. W., & Mohamed, S. (2010). Effectiveness of best management practices in improving water quality in a pasture-dominated watershed. Journal of Soil and Water Conservation, 65(6), 424-437.

Choto, M., and Fetene, A. (2019). Impacts of land use/land cover change on streamflow and sediment yield of Gojeb watershed, Omo-Gibe basin, Ethiopia. Remote Sensing Applications: Society and Environment, 14, 84-99. https://doi.org/10.1016/j.rsase.2019.01.003

Christensen, J., Boberg, F., Christensen, O., and Lucas-Picher, P (2007). On the need for bias correction of regional climate change projections of temperature and precipitation.

Clarke, T. (2007). Scenarios of Greenhouse Gas Emissions and Atmospheric Concentrations (Sub-report 2.1A of Synthesis and Assessment Product 2.1, US Climate Change Science Program.

CORDAID (Catholic Organization for Relief and Development Aid) (2012). Community managed disaster risk reduction in an urban river basin, Dire Dawa, Easter Ethiopia.

Cunderlik, J. (2003). Hydrological model selection for CFCAS project, Assessment of water resource risk and vulnerability to change in climate condition, University of Western Ontario.

Daba, Mekonnen H., and Songcai You. (2020). "Assessment of Climate Change Impacts on River Flow Regimes in the Upstream of Awash Basin, Ethiopia: Based on IPCC Fifth Assessment Report (AR5) Climate Change Scenarios." *Hydrology* 7 (4): 98. https://doi.org/10.3390/hydrology7040098.

Demissie, T. A., Saathoff, F., Seleshi, Y., & Gebissa, A. (2013). Evaluating the Effectiveness of Best Management Practices in Gilgel Gibe Basin Watershed—Ethiopia. Journal of Civil Engineering and Architecture, 7(10). https://doi.org/10.17265/1934-7359/2013.10.007.

Desta, L., Volli, C., Asrat, W. A., and Yiteyew, A. (2005). Community-Based Participatory Watershed Development: A Guideline. Federal Democratic Republic of Ethiopia Ministry of Agriculture and Rural Development, Addis Ababa, Ethiopia.

Dibaba, W. T., Demissie, T. A., and Miegel, K. (2020). Watershed hydrological response to combined land use/land cover and climate change in highland Ethiopia: Finchaa catchment. Water (Switzerland), 12(6). https://doi.org/10.3390/w12061801.

Dickinson, Robert E., Ronald M. Errico, Filippo Giorgi, and Gary T. Bates. (1989). "A Regional Climate Model for the Western United States." *Climatic Change* 15 (3): 383–422. https://doi.org/10.1007/BF00240465.

Dilnesaw Alamirew. (2006). Modelling of Hydrology and Soil Erosion of Upper Awash River Basin. PhD Thesis, University of Bonn.

Ding Y., Ahlonsou E., and Schimel D. (2018). An Overview of the Climate System.

Drapela, K., Drapelova, I. (2011). Application of Mann-Kendall test and sen"s slope estimates for trend detection in deposition data from Beskydy Mts; the Czech Republic 1997-2010. Beskdy Mendel University in Brno, 133-146.

Endris, H. (2013). Assessment of the performance of CORDEX regional climate models in simulating east african rainfall. J. Clim 26, 8453–8475. (https://doi.org/10.1175/JCLI-D-12-00708.1)

Fujino, Matsuoka, (2006). Multigas mitigation analysis on stabilization scenarios using AIM global model. Multigas Mitigation and Climate Policy.

Gao, Guangyao, Bojie Fu, Shuai Wang, Wei Liang, and Xiaohui Jiang. (2016). "Determining the Hydrological Responses to Climate Variability and Land Use/Cover Change in the Loess Plateau with the Budyko Framework." *Science of The Total Environment* 557–558 (July): 331–42. https://doi.org/10.1016/j.scitotenv.2016.03.019.

Gashaw, A. W., T., Tulu, T., Argaw, M., &. Worqlul. (2018). Modeling the hydrological impacts of land use/land cover changes in the Andassa watershed, Blue Nile Basin, Ethiopia. Science of the Total Environment, 619, 1394-1408.

Gemeda, D. O., & Sima, A. D. (2015). The impacts of climate change on African continent and the way forward. Journal of Ecology and The Natural Environment, 7(10), 256–262. https://doi.org/10.5897/JENE2015.0533.

Getachew, H. E., and Melesse, A. M. (2012). The Impact of Land Use Change on the Hydrology of the Angereb Watershed, Ethiopia. International Journal of Water Sciences, 1. https://doi.org/10.5772/56266.

Giorgi, Filippo, Colin Jones, and Ghassem R Asrar. (2009). "Addressing Climate Information Needs at the Regional Level: The CORDEX Framework," 9.

Gitau, M. W., Gburek, W. J., & Bishop, P. L. (2008). Use of the SWAT model to quantify water quality effects of agricultural BMPs at the farm-scale level. Transactions of the ASABE, 51(6), 1925-1936.

Green, W. H., & Ampt, G. A. (1911). Studies on Soil Phyics. The Journal of Agricultural Science, 4(1), 1–24. https://doi.org/10.1017/S0021859600001441.

Guo, D. L., and H. J. Wang, (2016). Comparison of a very-fine-resolution GCM with RCM dynamical downscaling in simulating climate in China. Adv. Atmos. Sci., 33, 559–570, https://doi.org/10.1007/s00376-015-5147-y

Hadgu, K. M. (2008). Temporal and spatial changes in land use patterns and biodiversity in relation to farm productivity at multiple scales in Tigray, Ethiopia. PhD thesis Wageningen University, Netherland.

Haile, A.T., and Rietjes, T. H.. M.(2015). Evaluation of regional climate model simulations of rainfall over the upper Blue Nile basin. Atmospheric Research, 161-162, 57-64.

Haile E., Assefa M., (2012). The impact of land use change on the hydrology of Angereb Watershed. International Journal of Water Sciences. 1: 1-7.

Hargreaves, G.H. and Z.A. Samani. (1985). Reference crop evapotranspiration from temperature. Applied Engineering in Agriculture 1:96-99.

Hedlund, L., & Tekle, K. (2000). Land cover changes between 1958 and 1986 in Kalu district, Southern Wello, Ethiopia. Mountain research and development, 20(1), 42–51.

Herweg, K., & Ludi, E. (1999). The performance of selected soil and water conservation measures-case studies from Ethiopia and Eritrea. Catena, 36(1-2), 99-114.

Hijioka, Kainuma (2008). Global GHG emissions scenarios under GHG concentration stabilization targets.J.Glob. Environ. Eng.13,97–108

Hulme M, L. D., Doherty R, Ngara T, New M. (2011). African climate change. 1900-2100. Climate Res, 17, 145-168.

Hurni, H. (1985). Erosion-productivity-conservation systems in Ethiopia. IV International Conference on Soil Conservation November 3-9, 1985 Maracay, Venezuela, January 1985, 654-674.

Hurni, H., & Zeleke, G. (2001). Implications of land use and land cover dynamics for mountain resource degradation in the Northwestern Ethiopian highlands. Mountain research and development, 21(2), 184–191.

IPCC (2001): the scientific basis technical summary of the working group I report. Cambridge university press, New York, 94pp.

IPCC (2007). Climate Change: The Physical Science Basis. Contribution of working group 1 to the fourth assessment report of the intergovernmental panel on climate change. In:Solomon S,Qin D,Manning ,M,Chen Z,Marquis M,Averyt KB,Tignor M,Miller HL(eds) Cambridge University Press, Cambridge and New York.

IPCCII, W. (2007). Climate change impacts, adaptation and vulnerability. Contribution of Working Group II to the Fourth Assessment Report of the IPCC. Cambridge University Press: Cambridge, UK.

IPCC (2013). Climate Change: The Physical Science Basis. Contribution of Working Group I to the Fifth Assessment Report of the Intergovernmental Panel on Climate Change [Stoker, T.F., D. Qin, G. K.Plattner, M. Tigner, S.K.Allen, J. Boschung, A. Nauels, Y. Xia, V. Bex and P.M. Midgley (eds.)]. Cambridge University Press, Cambridge, United Kingdom and New York, NY, USA and C.E. Hanson, Eds., Cambridge University Press, Cambridge, UK.

Jingan, S., Jiupai, N., Chaofu,W., & Deti, X. (2005). Land use change and its corresponding ecological responses. Journal of geographical sciences, 15(3), 305-328.

Jung, B. M., Fernandes, E. H., Möller, O. O., and García-Rodríguez, F. (2020). Estimating suspended sediment concentrations from river discharge data for reconstructing gaps of information of long-term variability studies. Water (Switzerland), 12(9). https://doi.org/10.3390/W12092382.

Jury, C., M. R., &. Funk. (2013). Climatic trends over Ethiopia: regional signals and drivers. International Journal of Climatology. International Journal of Climatology, 33(8), 1924-1935.

Kabite, G., Muleta, M., & Gessesse, B. (2020). Separate and Combined Impacts of Land Cover and Climate Changes on Hydrological Responses of Dhidhessa River Basin, Ethiopia. https://doi.org/10.20944/preprints202012.0595.v1

Kassa, G. (2003). GIS based analysis of land use/ cover, land degradation and population changes: A study of Boru Metero area of south Wello, Amhara region, M.Sc. thesis, Addis Ababa University, Ethiopia.

Kassa, T. (2009). Watershed hydrological responses to changes in land use and land cover, and management practices at Hare watershed, Ethiopia. Ph.D. Thesis, University of Siegen, Germany, 229.

Kassa, T. (2009). Watershed Hydrological responses to changes in land use and land cover, and Management Practices at Hare Watershed, Ethiopia. Dissertation. University of Siegen, Germen.

Kebede Asfaw., Diekkruger B., Moges SA. (2013). An assessment of temperature and precipitation projections using a regional and a global climate model for the Baro-Akobo basin, Nile basin, Ethiopia. J.Earth Sci.Climate Change 4:133.doi:104172/2157-7617.1000133.

Kefay, T., Abdisa, T., & Chelkeba Tumsa, B. (2022). Prioritization of Susceptible Watershed to Sediment Yield and Evaluation of Best Management Practice: A Case Study of Awata River, Southern Ethiopia. Applied and Environmental Soil Science, 2022, 1–16. https://doi.org/10.1155/2022/1460945.

Kidane, M., Tolessa, T., Bezie, A., Kessete, N., & Endrias, M. (2019). Evaluating the impacts of climate and land use/land cover (LU/LC) dynamics on the Hydrological Responses of the Upper Blue Nile in the Central Highlands of Ethiopia. Spatial Information Research, 27(2), 151–167. https://doi.org/10.1007/s41324-018-0222-y.

Kim, J., Waliser, D. E., Mattmann, C. A., Goodale, C. E., Hart, A. F., Zimdars, P. A., Crichton, D. J., Jones, C., Nikulin, G., Hewitson, B. & Jack, C. 2014 Evaluation of the CORDEXAfrica multi-RCM hindcast: systematic model errors. Climate Dynamics 42 (5), 1189–1202.

Kiya, K. (2018). Assessing Climate Change Impacts on Water Availability in Upper Awash Sub-Basin, Ethiopia. MSc Thesis. Adama Science and Technology University, Ethiopia.

Laprise, Tete et al. (2013.). Climate projections over CORDEX Africa domain using the fifth generation Canadian Regional Climate Model (CRCM5). . Climate Dynamics, , 41(11-12),pp.3219-3246

Legesse, D., Abiye, T. A., Vallet-Coulomb, C., & Abate, H. (2010). Streamflow sensitivity to climate and land cover changes: Meki River, Ethiopia. Hydrology and Earth System Sciences, 14(11), 2277–2287. https://doi.org/10.5194/hess-14-2277-2010.

Li, Zhi, Wen-zhao Liu, Xun-chang Zhang, and Fen-li Zheng. (2009). “Impacts of Land Use Change and Climate Variability on Hydrology in an Agricultural Catchment on the Loess Plateau of China.” *Journal of Hydrology* 377 (1): 35–42. https://doi.org/10.1016/j.jhydrol.2009.08.007.

Liang, X. Z., (2019). CWRF performance at downscaling China climate characteristics. Climate Dyn., 52, 2159–2184, https://doi.org/10.1007/s00382-018-4257-5.

Malede, D. A., Alamirew, T., & Andualem, T. G. (2023). Integrated and Individual Impacts of Use Land Cover and Climate Changes on Hydrological Flows over Birr River Watershed, Abbay Basin, Ethiopia. Water, 15(1), Article 1. https://doi.org/10.3390/w15010166

Mango, S. G., L. M., Melesse, A. M., McClain, M. E., Gann, D., &. Setegn. (2015). Land use and climate change impacts on the hydrology of the upper Mara River Basin, Kenya: results of a modeling study to support better resource management. Hydrology and Earth System Sciences, 15(7), 2245-2258.

Mekonnen K, Tadele K (2012) Analyzing the impact of land use and climate changes on soilerosion and stream flow in the upper Gilgel Abbay catchment, Ethiopia. Ohrid, Republic of Macedonia, pp 1–13.

Meyer, L., Brinkman, S., van Kesteren, L., Leprince-Ringuet, N., & van Boxmeer, F. (2014). Technical Support Unit for the Synthesis Report. 169.

Mitiku, A. B., Meresa, G. A., Mulu, T., & Woldemichael, A. T. (2023). Examining the impacts of climate variabilities and land use change on hydrological responses of Awash River basin, Ethiopia. HydroResearch, 6, 16–28. https://doi.org/10.1016/j.hydres.2022.12.002.

Mitiku, H., Herweg, K., & Stillhardt, B. (2006). Sustainable Land Management – A New Approach to Soil and Water Conservation in Ethiopia. Mekelle, Ethiopia: Land Resources Management and Environmental Protection Department, Mekelle University; Bern, Switzerland: Centre for Development and Environment (CDE), University of Bern, and Swiss National Centre of Competence in Research (NCCR) North-South. 269pp.

MoARD and WB (Ministry of Agriculture and Rural Development and World Bank) (2007). Ethiopia: Thematic papers on land degradation in Ethiopia. Ministry of Agriculture and Rural Development and World Bank publication, Addis Ababa.

Monteith, J. L. (1965). Evaporation and environment. Symposia of the Society for Experimental Biology, 19, 205–234.

Moriasi, D.N., Arnold, J.G., Van Liew, M.W., Binger, R.L., Harmel, R.D., Veith, T. (2007). Model evaluation guidelines for systematic quantification of accuracy in watershed simulations. Transactions of the American Society of Agricultural and Biological Engineers 50(3): 885-900.

Morris & Fan, J. (1998). Design and management of dams, reservoirs and watersheds for sustainable use. NEW YORK: Reservoir Sedimentation Handbook.

Mulu T., Mitiku A.B., Woldemichael, T.A., (2022). Flood Hazard Zoning of Upper Awash River Basin Using Analytical Hierarchy Process (AHP) as Compared to Sensitivity Analysis (under revision).

Nadew, B., Chaniyalew, E., and Tsegaye, T. (2019). Runoff sediment yield modeling and development of management intervention scenarios, a case study of Guder watershed, Blue Nile Basin. Hydrol Current Res, 9(4), 1-16. https://doi.org/10.4172/2157- 7587.1000306.

Negese, A. (2021). Impacts of Land Use and Land Cover Change on Soil Erosion and Hydrological Responses in Ethiopia. Applied and Environmental Soil Science, 2021, 1–10. https://doi.org/10.1155/2021/6669438.

Neitsch, S.L., Arnold, J.G. Kiniry, J.R. Srinivasan, R. J. Williams, R. (2002). Soil and Water Assessment Tool (SWAT) User's Manual, Version 2000, Texas Water Resources Institute, College Station.

Neitsch, S. L., Arnold, J. G., Kiniry, J. R., Srinivasan, R., Williams, J. R., and Haney, E. B. (2012). Soil and water assessment tool theoretical documentation version 2012. Texas Water Resource Institute TR-439., 1-650.

NMSA (1996). Climate and agro climatic resource of Ethiopia. Meteorological Research Report Series. Vol. 1, No.1, Addis Ababa.

Novotny, V. (2003). Water Quality: Diffuse Pollution and Watershed Management (2nd ed.). New York: John Wiley & Sons, Inc.

Nyssen, J., Poesen J., Gebremichael, D., Vancampenhout, K., D'aes, M., Yihdego, G., Govers, G., Leirs, H., Moeyersons, J., & Naudts, J. (2007). Interdisciplinary on-site evaluation of stone bunds to control soil erosion on cropland in Northern Ethiopia. Soil & Tillage Research, 94, 151-163.

Nyssen, J., Poesen, J., Moeyersons, J., Haile, M., & Deckers, J. (2008). Dynamics of soil erosion rates and controlling factors in the Northern Ethiopian Highlands–towards a sediment budget. Earth surface processes and landforms, 33, 695-711.

Nyssen, Jan, Clymans, W., Descheemaeker, K., Poesen, J., Vandecasteele, I., Vanmaercke, M., & Walraevens, K. (2010). Impact of soil and water conservation measures on catchment hydrological response - a case in north Ethiopia. Hydrological Processes, 24, 1880–1895.

O'Neill, E. Kriegler, K. Riahi, K. Ebi, S. Hallegatte, T. Carter, R. Mathur, D. van Vuuren A new scenario framework for climate change research: the concept of shared socioeconomic pathways Clim. Change, 122 (2013), pp. 387-400.

Pachauri, R.K., Allen, M., Barros, V., Broome, J., Cramer, W. Christ, Church, J., Clarke, L., Dahe, Q. Dasgupta, P. Climate Change (2014). Synthesis Report. Contribution of Working Group I, II and III to the Fifth Assessment Report of the Intergovernmental Panel on climate change; IPCC: Geneva, Switzerland.

Pan, Sihui, Dedi Liu, Zhaoli Wang, Qin Zhao, Hui Zou, Yukun Hou, Pan Liu, and Lihua Xiong. (2017). "Runoff Responses to Climate and Land Use/Cover Changes under Future Scenarios." *Water* 9 (7): 475. https://doi.org/10.3390/w9070475.

Priestley, C. H. B., & Taylor, R. J. (1972). On the Assessment of Surface Heat Flux and Evaporation Using Large-Scale Parameters. Monthly Weather Review, 100(2), 81–92. https://doi.org/10.1175/1520-0493(1972)100<0081: OTAOSH>2.3.CO;2

Rahman,T. (2019) 'Addressing Climate Change and grass roots level adaptation measures to food security in North western Bangladesh.

Randhir, T. O. and Tsvetkova, O. (2011). "Analysis of the Spatiotemporal Changes in Watershed Landscape Pattern and Its Influencing Factors in Rapidly Urbanizing Areas Using Satellite Data." J. Hydrology 404: 1–12.

Rathjens, J., H.,. Bieger, K. ,. Srinivasan, R. ,. Chaubey, I. ,. Arnold. (2016). CMhyd User Manual.

Riahi, Nakicenovic (2011) Scenarios of long-term socio-economic and environmental development under climate stabilization.Technol. Forecast. Soc. Change74,887–935 (2007). DOI: 10.1016/j.techfore.2006.05.02

Rose, R. M. (2015). The Impact of Climate Change on Human Security in the Sahel Region of Africa.

Rummukainen. (2013). Evaluation of climate models. The Physical Science Basis. Contribution of working group 1 to the fifth assessment report of the intergovernmental panel on climate change. Cambridge University Press, Cambridge, United Kingdom and New York, NY, USA.

Sahilu G and Nigussie A. (2015). Climate Modelling of the Impact of Climate Change on Sugarcane and Cotton for Project on ‗a Climate Resilient Production of Cotton and Sugar in Ethiopia' Climate Change and Modelling. EDRI Research Report 21 .

Schwab, G. O., Fangmeier, D. D., Elliot, W. J., & Frevert, R. K. (1993). Soil and Water Conservation Engineering (4th ed.). John Wiley & Sons, Inc.

Setegn S.G., R. Srinivasan, B. Dargahi and A. M. Melessa. (2009). Spatial delineation of soil Vulnerability in the Lake Tana Basin, Ethiopia. Hydrological Processes 23, 3738 -3750.

Setegn S.G., B Dargahi, R Srinivasan, A M Melesse, Modeling of sediment yield from Anjeni-Gauged watershed, Ethiopia using SWAT model. Journal of the American Water Resource Association. 46 (3) (2010) 514–526, doi:10.1111/j.1752-1688.2010. 00431.x.

Sharpley, A. N., Daniel, T., Gibson, G., Bundy, L., Cabrera, M., Sims, T., … Parry, R. (2006). Best Management Practices To Minimize Agricultural Phosphorus Impacts on Water Quality, ARS-163(July). Retrieved from http://www.ars.usda.gov/is/np/BestMgmtPractices/Best Management Practices.pdf.

Shawul, A. A., Chakma, S., and Melesse, A. M. (2019). The response of water balance components to land cover change based on hydrologic modeling and partial least squares regression (PLSR) analysis in the Upper Awash Basin. Journal of Hydrology: Regional Studies, 26, 100640. https://doi.org/10.1016/j.ejrh.2019.100640.

Shiberu, T. and Kifle, L. (1998). Environmental management in Ethiopia: Have the national conservation plans worked? Environmental Forum Publications Series, No.1. OSSREA, Addis Ababa.

Shiferaw, B., & Holden, S. T. (1998). Resource degradation and adoption of land conservation Resource degradation and adoption of land conservation technologies in the Ethiopian Highlands: A case study in Andit Tid, North Shewa. Agricultural Economics, 18, 233–247.

Shiferaw, B., & Holden, S. (1999). Soil erosion and smallholders' conservation decisions in the highlands of Ethiopia. World Development, 27(4), 739–752.

Shiferaw, A., H. ,. Gebremedhin, A. ,. Gebretsadkan, T. ,. &. Zenebe. (2018). Modelling hydrological response under climate change scenarios using SWAT model: the case of Ilala watershed, Northern Ethiopia. Modeling Earth Systems and Environment, 4(1), 437-449.

Smith, Wigley, (2006). Multi-gas forcing stabilization with the MiniCAM. Multigas Mitigation and Climate Policy. The Energy Journal Special Issue.

Tadese, M. T., Kumar, L., Koech, R., & Zemadim, B. (2019). Hydro-Climatic Variability: A Characterisation and Trend Study of the Awash River Basin, Ethiopia. Hydrology, 6(2), Article 2. https://doi.org/10.3390/hydrology6020035.

Teklay, A., Dile, Y. T., Asfaw, D. H., Bayabil, H. K., & Sisay, K. (2021). Impacts of Climate and Land Use Change on Hydrological Response in Gumara Watershed, Ethiopia. Ecohydrology & Hydro biology, 21(2),315–332. https://doi.org/10.1016/j.ecohyd.2020.12.001.

Tesema, N., Kebede, A., & Yadeta, D. (2020). Modeling land use dynamics in the Kesem sub-basin, Awash River basin, Ethiopia. Cogent Environmental Science, 6(1), 1782006. https://doi.org/10.1080/23311843.2020.1782006.

Tessema, S. M. (2011). Hydrological modeling as a tool for sustainable water resources management: a case study of the Awash River Basin (Doctoral dissertation, KTH Royal Institute of Technology).

Tesema, T. A., and Leta, O. T. (2020). Sediment yield estimation and effect of management options on sediment yield of Kesem Dam watershed, Awash Basin, Ethiopia. Scientific African, 9, e00425. https://doi.org/10.1016/j.sciaf.2020.e00425.

Tesfa Gebrie, G. B., & Guadie, A. (2018). Land Use Change Detection Using Remote Sensing Technology

Tesfahunegn, G.B., Vlek, P.L.G., Tamene, L. (2012). Management strategies for reducing soil Degradation through modeling in a GIS environment in northern Ethiopia catchment. Nutrient Cycling in Agro ecosystems, 92: 255-272.

Tesfaye, Y. A., Alamirew, T., Zeleke, G., & Kassawmar, T. (2022). Modeling runoff-sediment influx responses to alternative BMP interventions in the Gojeb catchment, Ethiopia, using the SWAT hydrological model [Preprint]. In Review. https://doi.org/10.21203/rs.3.rs-1693072/v1.

Tilahun, S., Guzman, C. D., Zegeye, A. D., Engda, T. A., Collick, A. S., Rimmer, A., & Steenhuis, T. S. (2013). An efficient semi-distributed hillslope erosion model for the subhumid Ethiopian Highlands. Hydrology and Earth System Science, 17, 1051– 1063.

Troeh, F. R., Hobbs, J. A., & Donahue, R. L. (2004). Soil and Water Conservation for Productivity and Environmental Proteciton. (S. Helba, Ed.) (4th ed.). New Jersey: Pearson Education.

Turco, M., Llasat, M. C., Herrera, S. & Gutiérrez, J. M. 2017 Bias correction and downscaling of future RCM precipitation projections using a MOS-Analog technique. Journal of Geophysical Research: Atmospheres 122 (5), 2631–2648

Uniyal, B., Jha, M. K., Verma, A. K., and Anebagilu, P. K. (2020). Identification of critical areas and evaluation of best management practices using SWAT for sustainable watershed management. Science of the Total Environment, 744, 140737. https://doi.org/10.1016/j.scitotenv.2020.140737.

Vancampenhout, K., Nyssen, J., Gebremichael, D., Deckers, J., Poesen, J., Haile, M., & Moeyersons, J. (2006). Stone bunds for soil conservation in northern Ethiopian highlands: Impacts on soil fertility and crop yield. Soil & Tillage Research 90(1-3), 1-14.

Van Vuuren, Elzen, (2006). Long-term multi-gas scenarios to stabilise radiative forcing - Exploring costs and benefits within an integrated assessment framework. Multigas Mitigation and Climate Policy. The Energy Journal Special Issue. pp. 201-233. Vol. 27

Van Vuuren, van Houdt, (2007). Stabilizing greenhouse gas concentrations at low levels: an assessment of reduction strategies and costs. Climatic Change, 81:119–159.

Van Vuuren D.P., Edmonds J., Thomson A., Raihi K., Kainuma M., Matsui T., Hurtt G.C., Lamrque J-F., Meinshausen M., Smith S. (2011). Representative Concentration Pathways: an overview. In: Climate change, 5-31.

Vörösmarty, C. J., Green, P., Salisbury, J., & Lammers, R. B. (2000). Global Water Resources: Vulnerability from Climate Change and Population Growth. Science, 289(5477), 284–288. https://doi.org/10.1126/science.289.5477.284.

Waidler, D., White, M., Steglich, E., Wang, S., Williams, J., Jones, C. A., and Srinivasan, R. (2011). Conservation practice modeling guide for SWAT and APEX. Journal of Hydrology, 50(1-2), 30-49. http://linkinghub.elsevier.com/retrieve/pii/S0022169410006554%0.

Walling DE (2009) The impact of global change on erosion and sediment transport by rivers:current progress and future challenges, UNESCO.

Wang, C. G., J. Liang, and K. I. Hodges, 2017: Projections of tropical cyclones affecting Vietnam under climate change: Downscaled HadGEM2-ES using PRECIS 2.1. Quart. J. Roy. Meteor. Soc., 143, 1844–1859, https://doi.org/10.1002/qj.3046.

White, K.L., Chaubey, I., (2005). Sensitivity analysis, calibrations, and validation for a multisite and multivariate SWAT model. Journal of the American Water Resources Association 41 (5), 1077–1089.

Wilby,R. Charles,S and Timbal,B (2004). Guidelines for Use of Climate Scenarios Developed from Statistical Downscaling Methods. USA: National Center of Atomosphere.

Wilk, J., Hughes, D.A., 2002. Simulating the impacts of land-use and climate change on water resource availability for a large south Indian catchment. Hydrol. Sci. J. Des Sci. Hydrol. 47 (1), 19–30.

Williams, J.R. (1990). The erosion productivity impact calculator (EPIC) model: A case history. Phil. Trans. R. Soc. London 329(1255): 421-428.

Woldesenbet, T.A., Elagib, N.A., Ribbe, L., Heinrich, J. (2017). Hydrological Responses to Land Use/Cover Changes in the Source Region of the upper Blue Nile Basin, Ethiopia. Sci. Total Environ. 575.

World Bank (2008). Ethiopia - A country study on the economic impacts of climate change (English). Washington, DC.

Yang, L. Feng, Q. Yin, Z. Wen, X. Si, J. Li, C. Deo, R. (2017). Identifying Separate Impacts of Climate and Land Use/Cover Change on Hydrological Processes in Upper Stream of Heihe River, Northwest China. Hydrol Process 31, 1100–1112.

Yin, J. F., Xiong, Y.J., Qiu, G.Y. (2017). “Effects of Land Use/Land Cover and Climate Changes on Surface Runoff in a Semi-Humid and Semi-Arid Transition Zone in Northwest China.” *Hydrology and Earth System Sciences* 21 (1): 183–96. https://doi.org/10.5194/hess-21-183-2017.

Yitea S, (2015). Impact of climate change on hydrology of upper Awash River Basin: Intercomparison of old SRES and new RCP scenarios.

Zaroug M.A.H., E.A.B.Eltahir, and F.Giorgi, (2014). Droughts and floods over the upper catchment of the Blue Nile and their connections to the timing of ElNino and La Nina events. Hydro. Earth Syst. Sci., 1239-2014.

Zeberie W. (2020). Assessment of sediment yield and conservation practices in Akaki watershed, Upper Awash Basin, Ethiopia.

Zhang, Mingfang, Ning Liu, Richard Harper, Qiang Li, Kuan Liu, Xiaohua Wei, Dingyuan Ning, Yiping Hou, and Shirong Liu. (2017). "A Global Review on Hydrological Responses to Forest Change across Multiple Spatial Scales: Importance of Scale, Climate, Forest Type and Hydrological Regime." *Journal of Hydrology* 546 (March): 44–59. https://doi.org/10.1016/j.jhydrol.2016.12.040.

Zhang, L., Jiang, Y., Yang, M., Wang, H., Dong, N., Wang, H., Liu, X., Chen, L., & Liu, K. (2022). Quantifying the Impacts of Land Use and Cover Change (LUCC) and Climate Change on Discharge and Sediment Load in the Hunhe River Basin, Liaoning Province, Northeast China. Water, 14(5), Article 5. https://doi.org/10.3390/w14050737.

Zhou, F., Xu, Y., Chen, Y., Xu, C.-Y., Gao, Y., & Du, J. (2013). Hydrological response to urbanization at different spatio-temporal scales simulated by coupling of CLUE-S and the SWAT model in the Yangtze River Delta region. Journal of Hydrology, 485, 113–125. https://doi.org/10.1016/j.jhydrol.2012.12.040.

APPINDICES

Appendix A. 1: Average annual rainfall of stations in the study area

year	A.Aobserv	T.Bolo	A.A bole	Asgori	Intoto	modjo
1989	1321	1165	1316	926	1476	1034
1990	1125	851	1583	1139	1454	925
1991	1160	779	1495	1074	1328	879
1992	1101	1362	1497	1025	1232	798
1993	1568	2156	1525	1256	1271	837
1994	1043	1209	1388	1170	1175	759
1995	1146	793	1201	1111	1175	637
1996	1549	1208	1051	1209	1649	1077
1997	952	1224	1112	849	987	760
1998	1338	1369	1264	1198	1436	1034
1999	934	1276	1219	928	974	1182
2000	1191	1050	1257	835	1163	852
2001	1452	821	1310	896	1263	788
2002	1016	1031	1017	933	1099	564
2003	1173	973	1273	1127	1222	1060
2004	1159	1159	1163	917	1195	1133
2005	1394	1131	1390	901	1155	1356
2006	1364	1042	1373	918	1255	1199
2007	1311	1129	1259	1064	1195	1002
2008	1331	1148	1151	940	1369	1441
2009	1241	1161	1896	848	1173	1108
2010	1381	1411	1903	1085	1441	1110
2011	1052	854	952	910	1148	835
2012	1063	920	935	774	1294	1327
2013	1252	1684	961	1292	1547	1096
2014	1081	1032	772	906	1029	875
2015	1053	827	838	787	1106	859
2016	1222	974	986	882	1274	1276
2017	1322	1046	1098	911	1556	1036
2018	972	1373	1212	960	1648	1093
2019	1345	1092	1212	1174	1493	1392

Appendix A. 2: LULC classification accuracy assessment

i. 1990 LULC

Classification	AGRL	FRSE	RNGE	RNGB	URBN	BARR	WATR	Total	User Accuracy (%)
AGRL	45	1	0	0	1	0	0	47	95.7
FRSE	1	29	0	2	2	1	0	35	82.8
RNGE	0	0	28	1	1	0	0	30	93.3
RNGB	0	1	0	32	0	0	0	33	96.9
URBN	0	0	1	0	28	0	0	29	96.5
BARR	0	0	0	1	1	23	0	25	92
WATR	0	0	0	0	0	0	20	20	100
Total	46	31	29	36	33	24	20	220	
Producer Accuracy (%)	97.8	93.5	96.5	88.8	87.9	95.8	100		
Overall Classification Accuracy = 93.2%									
Overall Kappa Statistics =0.92									

ii. 2005 LULC

Classification	AGRL	FRSE	RNGE	RNGB	URBN	BARR	WATR	Total	User Accuracy (%)
AGRL	46	1	1	3	1	1	0	54	85.2
FRSE	1	27	0	1	0	1	0	30	90
RNGE	1	0	26	2	1	0	0	30	86.6
RNGB	1	1	0	33	0	0	0	35	94.2
URBN	0	0	2	0	30	0	0	32	93.7
BARR	0	0	0	1	1	20	0	22	90.9
WATR	0	0	0	0	0	0	16	16	100
Total	49	29	29	40	33	22	16	220	
Producer Accuracy (%)	93.8	93.4	89.6	82.5	90.9	90.9	100		
Overall Classification Accuracy = 90.1%									
Overall Kappa Statistics =0.88									

Appendix A. 3: Sediment reduction with filter strip simulation

Sub basin	Average annual sediment loading (ton/ha/year)		Reduction (%)
	Baseline	Filter strip (5m)	
9	73.84	23.9	67.6
12	21.03	11.6	44.8
13	18.9	9.9	47.6
14	27.30	15.4	43.6
18	27.24	15.8	42.0
20	31.94	16.7	47.7
21	36.6	18.2	50.3
22	33.37	17.3	48.2
27	44.93	20.4	54.6

Appendix A.4: Sediment reduction with the simulation of terracing

Sub basin	Average annual sediment loading (ton/ha/year)		Reduction (%)
	Baseline	Parallel Terracing	
9	73.84	26.9	63.6
12	21.03	14.6	30.6
13	18.9	12.9	31.7
14	27.30	18.4	32.6
18	27.24	18.8	31.0
20	31.94	19.7	38.3
21	36.6	21.2	42.1
22	33.37	20.3	39.2
27	44.93	23.4	47.9

Appendix A.5: Sediment reduction with the simulation of Reforestation

Sub basin	Average annual sediment loading (ton/ha/year)		Reduction (%)
	Baseline	Reforestation	
9	73.84	28.8	61.0
12	21.03	15.2	27.7
13	18.9	14.9	21.2
14	27.30	19.8	27.5
18	27.24	18.9	30.6
20	31.94	23.5	26.4
21	36.6	25.6	30.1
22	33.37	24.3	27.2
27	44.93	26.8	40.4

Appendix B.1: Double mass curve for six representative's meteorological stations

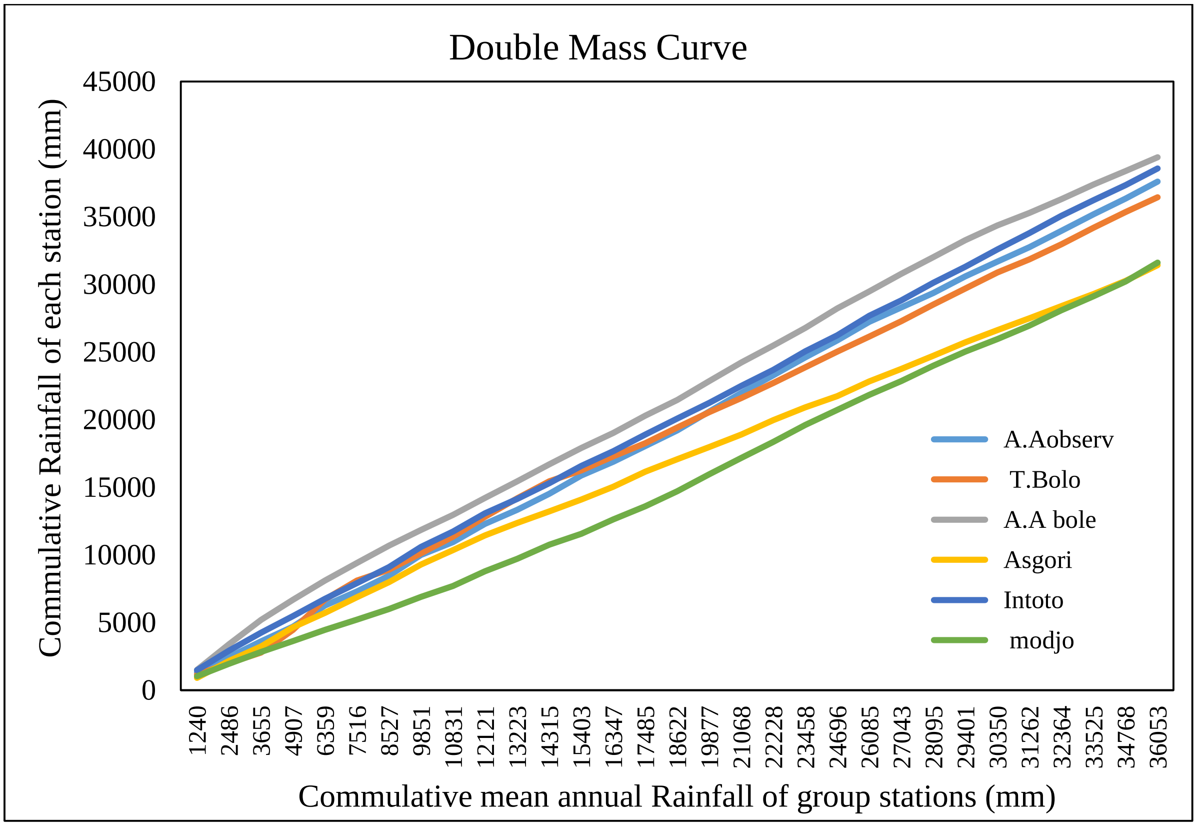

Appendix B.2: Cumulative deviation and Probability of rejecting homogeneity of annual dataset of meteorological station

i. A.A Observatory

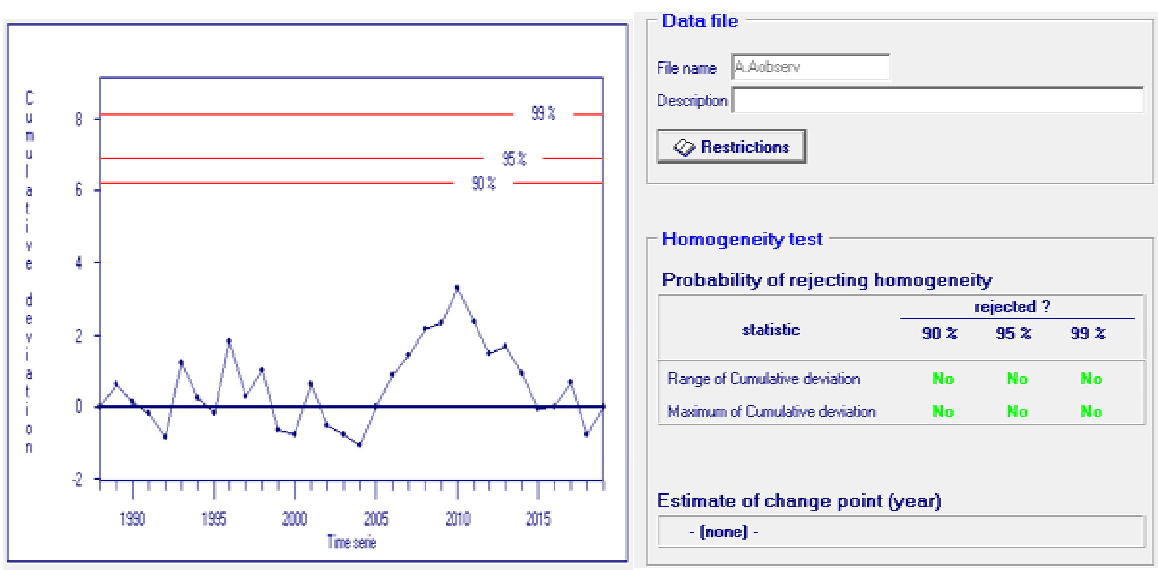

ii. Tulu Bolo

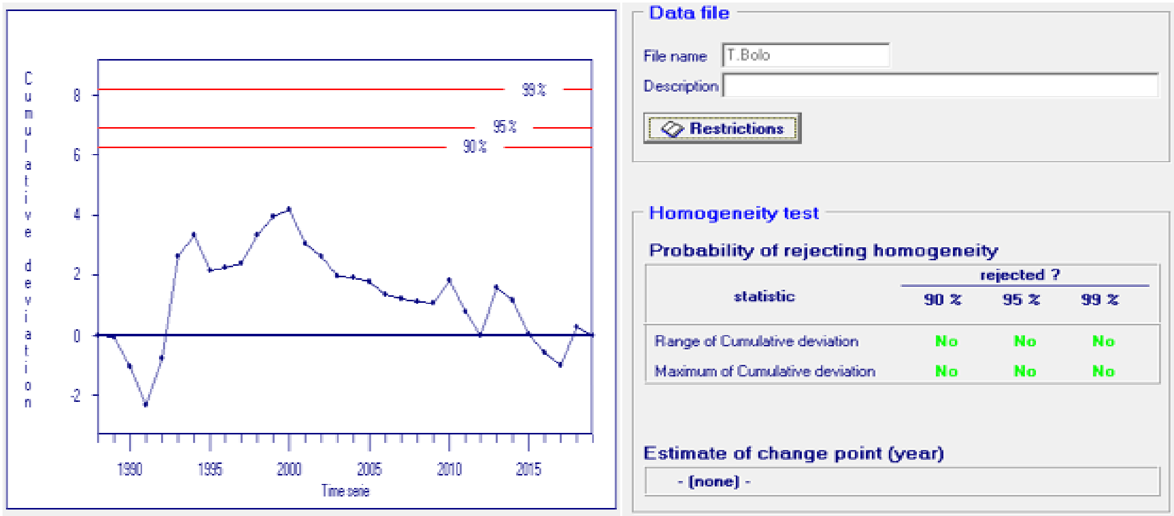

iii. Intoto

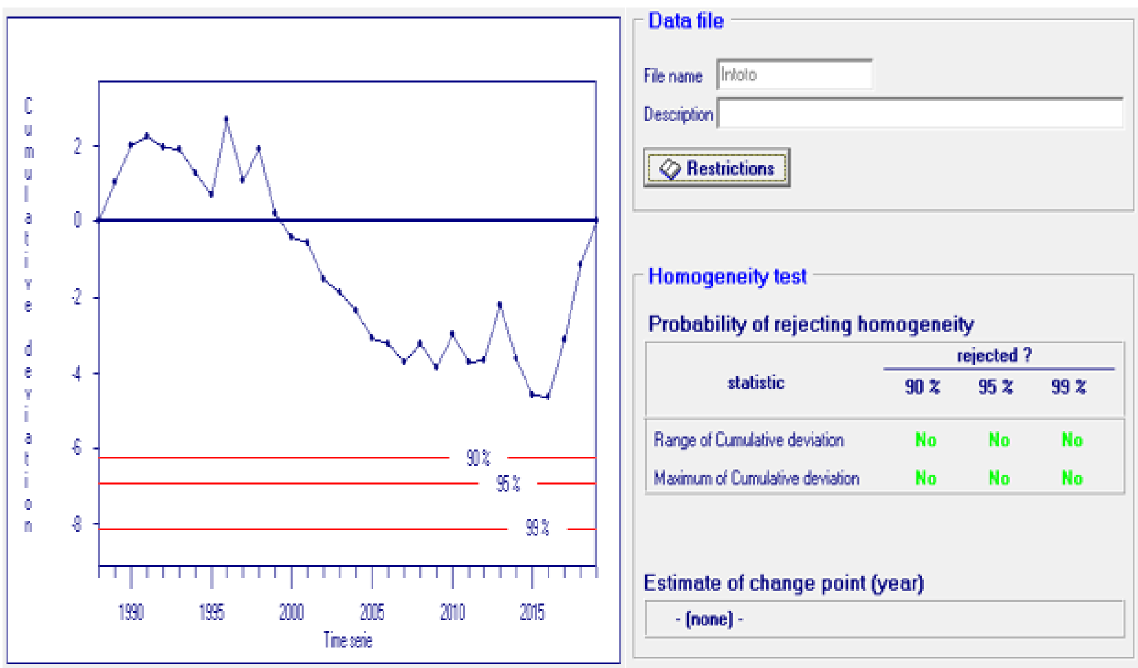

Appendix B.3: Annual trends of observed rainfall

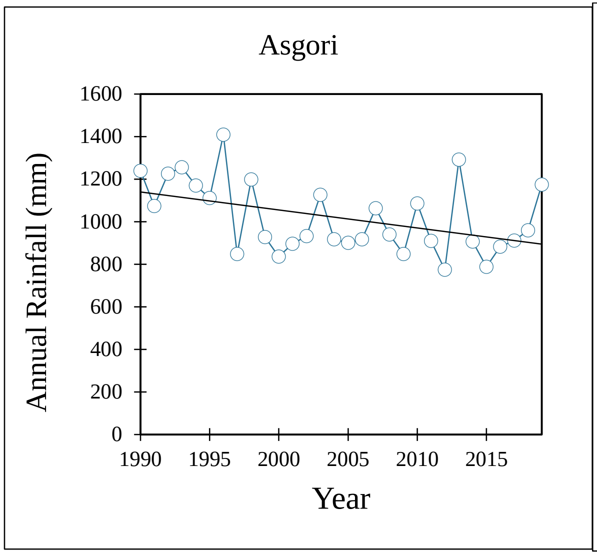

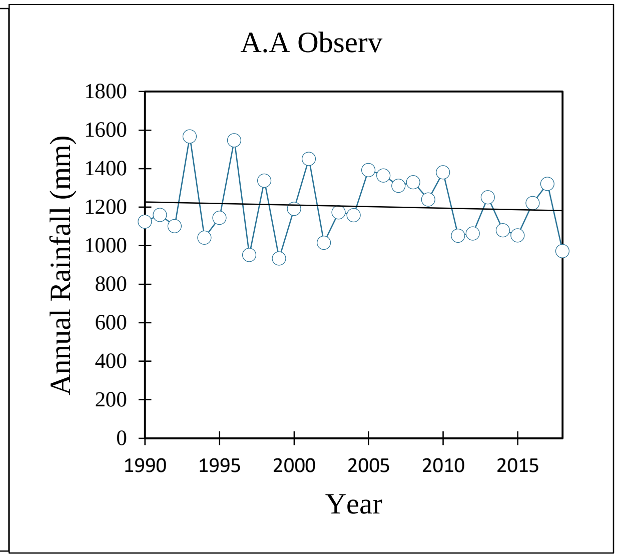

Appendix B.4:Annual trends of observed maximum temperature

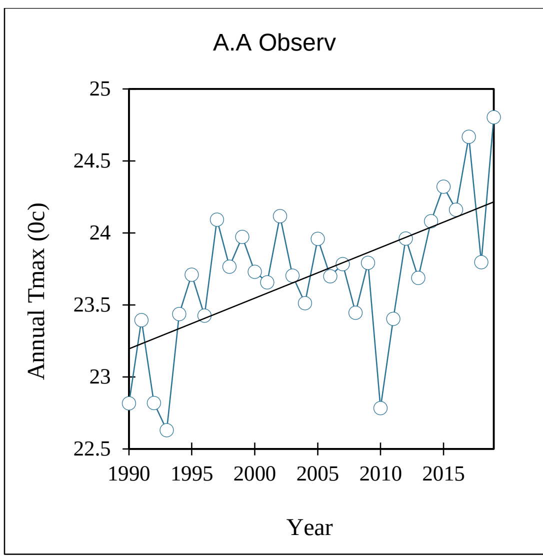

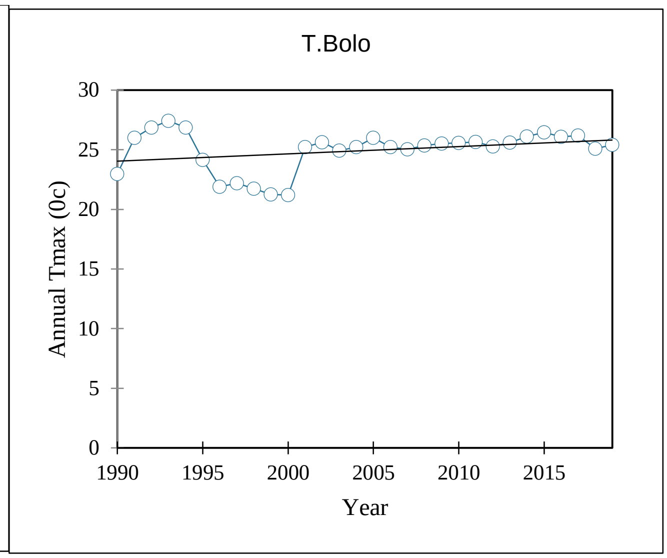

Appendix B.5: Annual trends of observed minimum temperature

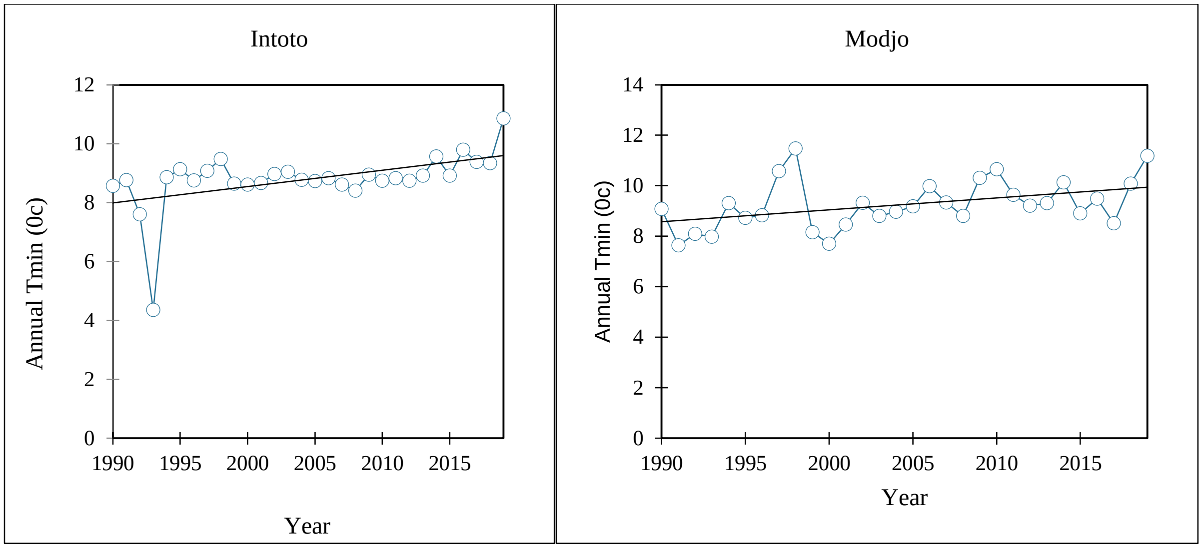

Appendix B.6: Simulated and observed average monthly flows during calibration

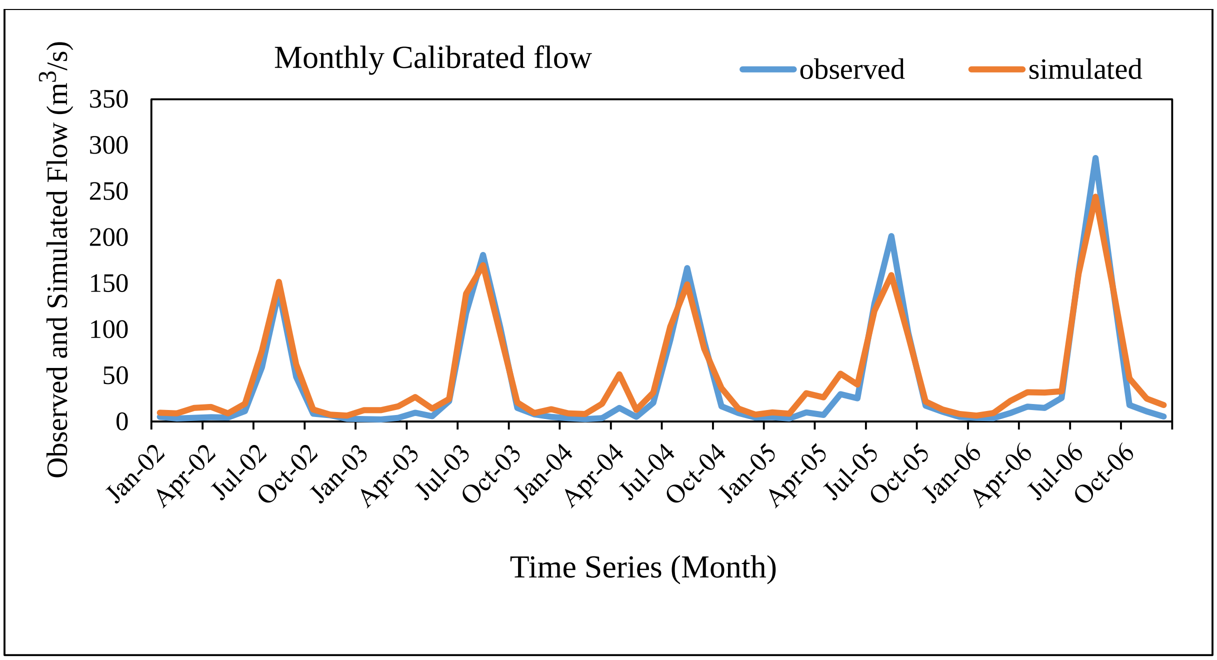

Appendix B.7: Simulated and observed average monthly flows during Validation

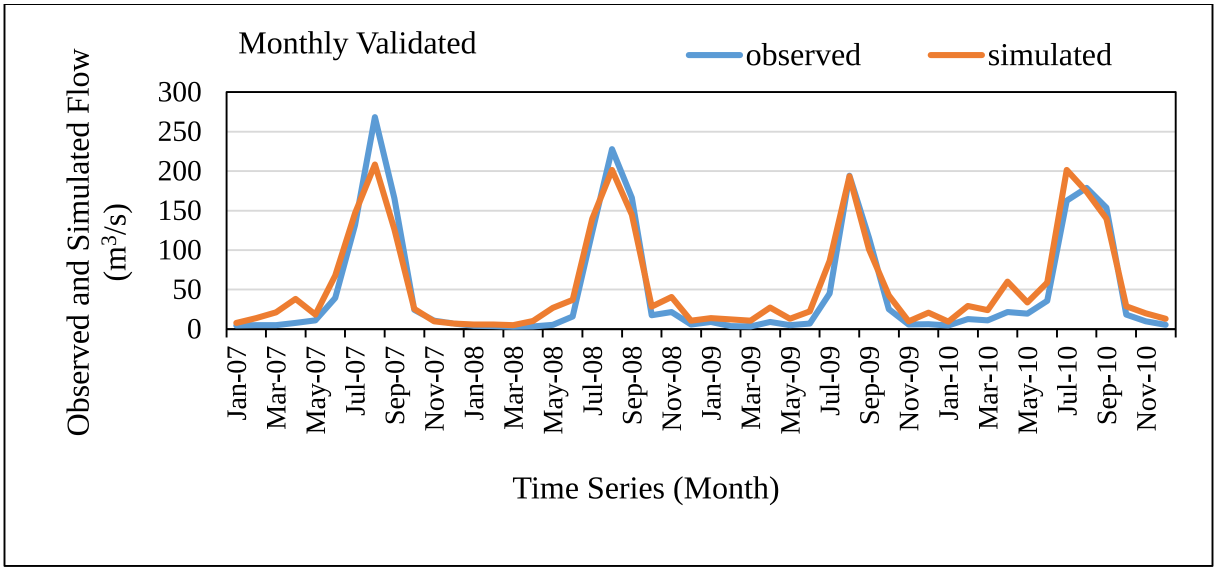

Appendix B. 8: Simulated and observed average monthly Sediments during calibration

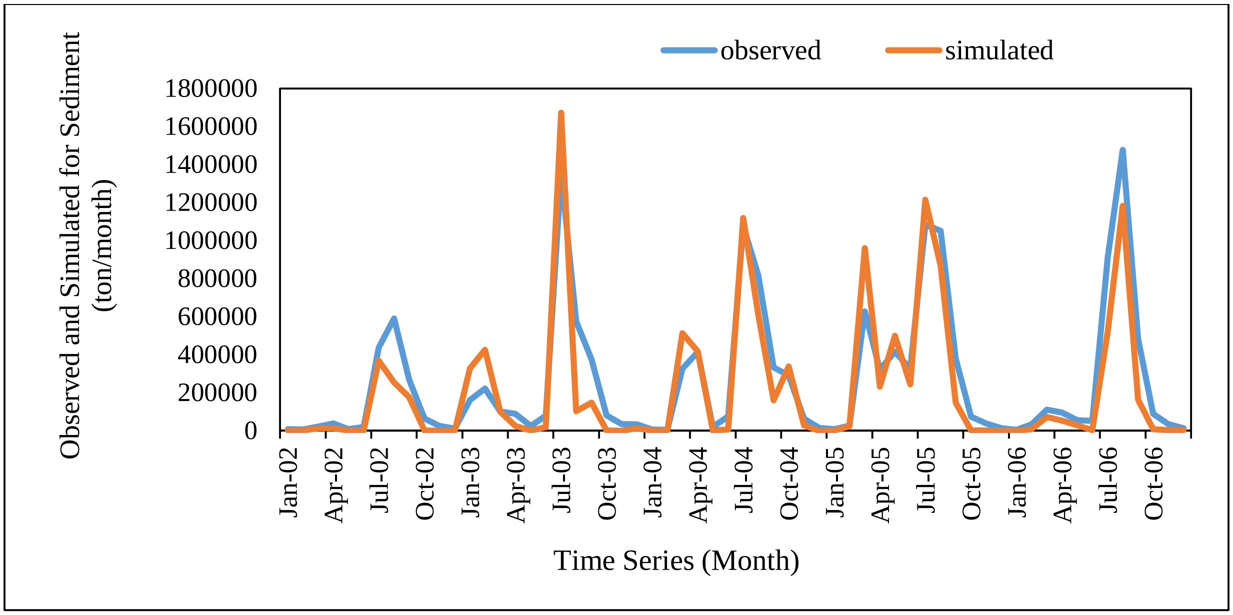

Appendix B. 9: Simulated and observed average monthly Sediments during Validation